THE PHYSICAL OCEANOGRAPHY OF BRITISH COLUMBIA'S INSIDE PASSAGE WITH RESPECT TO THE RETURN MIGRATION OF ONCORHYNCHUS NERKA

by
Bert Adrian terHart
B.Sc. (Physics and Physical Oceanography) Royal Roads Military College

A THESIS SUBMITTED IN PARTIAL FULFILLMENT OF THE REQUIREMENTS FOR THE DEGREE OF MASTER OF SCIENCE

in

THE FACULTY OF GRADUATE STUDIES
DEPARTMENT OF OCEANOGRAPHY

We accept this thesis as conforming
to the required standard

University of British Columbia
March 1990

In presenting this thesis in partial fulfilment of the requirements for an advanced degree at the University of British Columbia, I agree that the Library shall make it freely available for reference and study. I further agree that permission for extensive copying of this thesis for scholarly purposes may be granted by the head of my department or by his or her representatives. It is understood that copying or publication of this thesis for financial gain shall not be allowed without my written permission.

Department of OCEANOGRAPHY

The University of British Columbia
Vancouver, Canada

Date 26 APRIL 1990

DE-6 (2/88)

ABSTRACT

Data from five conductivity-temperature-depth (CTD) surveys collected during 1985 and 1986 in support of project MOIST –Meteorological and Oceanographic Influences on Sockeye Tracks– are used to describe the salient oceanographic features of the waters lying between Vancouver Island and the British Columbia mainland coast. Using these data, four oceanographic regimes are clearly defined on the basis of salinity structure. Temperature-Salinity diagrams are used to discuss water types and mixing ratios in these regimes. Vigorous tidal mixing over shallow sills and/or in narrow channels produces tidally mixed fronts that separate oceanographic regimes. The tidal evolution of two of these fronts located near Weynton Passage and Cape Mudge are discussed by means of 24-hour CTD stations. Seasonal variability of the residual estuarine circulation is examined and estimates of the seaward flow in the upper layer of a very simple two-layer geostrophic model were found to be in reasonable agreement with the few direct measurements made in this region. Seasonal variability of the general hydrography is described.

Ultrasonic telemetry provided horizontal and vertical distribution time series data for return migrating sockeye salmon (*Oncorhynchus nerka*). Concurrent high spatial resolution CTD data was used to specify the ambient temperature and salinity fields in the immediate vicinity of the tagged sockeye. Spectral analysis of the depth and ambient oceanographic data time series revealed periodic vertical movements at approximately 15 and 33 minutes per cycle for fish tracked in the slightly stratified regimes of Queen Charlotte Strait, western Johnstone Strait and the Strait of Georgia. High frequency large amplitude periodic vertical movements were characteristic of fish that did not make significant progress towards the Fraser

River: low frequency small amplitude vertical movements were characteristic of well oriented fish. Aspect ratio, defined as the horizontal distance travelled divided by the vertical distance travelled, gave an indication of the relative degree of homeward orientation. Vertical distribution and orientation were also related to the frequency and duration of successive vertical excursions. Fish depth and vertical swimming velocity were found to be positively correlated in regions of weak stratification and/or for well oriented fish. Ambient density gradients were not found to inhibit vertical movements as the rate of doing work against hydrodynamic drag was several orders of magnitude greater than that of doing work against a varying buoyancy force. In the presence of strong temperature and salinity gradients, tracked sockeye were most often observed at depths not associated with the maximum gradients. In stratification regimes where temperature and salinity gradients were nearly uniform with depth, tracked sockeye were observed at depths uniformally distributed throughout the thermo- and haloclines. Minimum vertical swimming velocities were generally associated with minimum vertical gradients. These observations suggest that the tracked sockeye frequently swam through but did not reside in the region of the maximum gradients. Dimensional analysis suggested that physical variables alone are insufficient to specify the vertical distribution of the tracked sockeye.

TABLE OF CONTENTS

LIST OF TABLES

LIST OF FIGURES

ACKNOWLEDGEMENTS

Funding for Project MOIST was provided by NSERC Strategic Grant G–1485 to Drs. L. Mysak, K. Hamilton and C. Groot and by the Department of Fisheries and Oceans of Canada. Funding was provided to the author in the form of an NSERC Postgraduate Scholarship and by research grants to Drs. L. Mysak and W.W. Hsieh.

The many animated and informative discussions with Drs. T.P. Quinn and K.A. Thomson are gratefully acknowledged as is the unfailing support of Dr. W.W. Hsieh, who became my supervisor upon the departure of Dr. Mysak from the University of British Columbia.

The generosity of A.T. and A.J. Weaver, and O. Walsh knows no bounds and is gratefully acknowledged. The many hours my sister, L. terHart, contributed in helping prepare the figures is gratefully acknowledged.

This thesis is dedicated to my wife, M.J. terHart, whose undying confidence was instrumental in seeing this work to its conclusion, and to my father, J.D. terHart, whose knowledge of the sea far exceeds that gained by academic experience alone.

CHAPTER 1

HYDROGRAPHY OF BRITISH COLUMBIA'S INSIDE PASSAGE

1.1: Introduction

An ambitious multi-disciplinary study was undertaken in the spring and summer of 1985 and 1985 to address the general relationships between an adult sockeye salmon's (*Oncorhynchus nerka*) immediate environment and its return migration route and timing. One aspect of this study was an intensive field program designed to combine high resolution data of the sockeye's vertical and horizontal movements with similar resolution physical oceanographic data. Thus, high resolution temperature (T), salinity (S) and depth data were obtained along the return migration route of ultrasonically tagged sockeye.

It became clear if the T and S data collected during tracking were to be used to relate the fish's immediate environment to its horizontal and vertical movements, then a detailed hydrography of the study area would be required. To this end, data collected from five conductivity-temperature-depth surveys conducted during the spring and summers of 1985 and 1986 in support of project MOIST–Meteorlogical and Oceanographic Influences on Sockeye Tracks– are used to describe the salient oceanographic features of the waters lying between Vancouver Island and the British Columbia mainland coast.

A total of 28 conductivity-temperature-depth (CTD) sections were completed and seven 24-hour stations occupied during the cruises of the research vessels CSS Vector (24–28 June 1985, 26–29 August 1985, 29 May 1986 and 23–25 June 1986)

and CSS Parizeau (3–6 September 1986). The study region was limited to those waters lying between Vancouver Island and the British Columbia (BC) mainland coast; an area known as the "inside passage". Special attention was given to those regions within the study area where strong tidally mixed and estuarine fronts were known to exist (Thomson *et al.*, 1985). The purpose of all the cruises was to provide baseline hydrographic data for the 1985 and 1986 sockeye tracking program of project MOIST (Quinn and terHart, 1987, Quinn *et al.*, 1989). To this end, the different stratification regimes and fronts that lay in the return migratory path of the sockeye salmon were examined.

The southern portion of the inside passage consists of Queen Charlotte Strait (QCST), Johnstone Strait (JS), Discovery Passage (DP) and the Strait of Georgia (SG). The general geographic region is illustrated in Figure 1. Table 1 summarizes the 28 CTD sections, Table 2 the observed fronts and Tables 3 and 4 the two sets of 24-hour stations in Weynton Passage and Discovery Passage, respectively.

Using these data, four oceanographic regimes are clearly defined on the basis of salinity structure. Temperature-salinity (TS) diagrams are used to discuss water types and mixing ratios in these regimes. Table 5 summarizes TS characteristics observed in this region. Vigorous tidal mixing over constricted sills produces tidally mixed fronts throughout the inside passage which serve to separate the oceanographic regimes. The isopleths of the observed fronts are substantially modified by the residual estuarine circulation and as such, the isopleth topology differs from that of a classically defined tidally mixed front. This different form of a tidally mixed front is defined as a hybrid tidally mixed front (Bowman and Essais, 1978). The tidal evolution of the fronts located near Weynton Passage (F7) and Cape

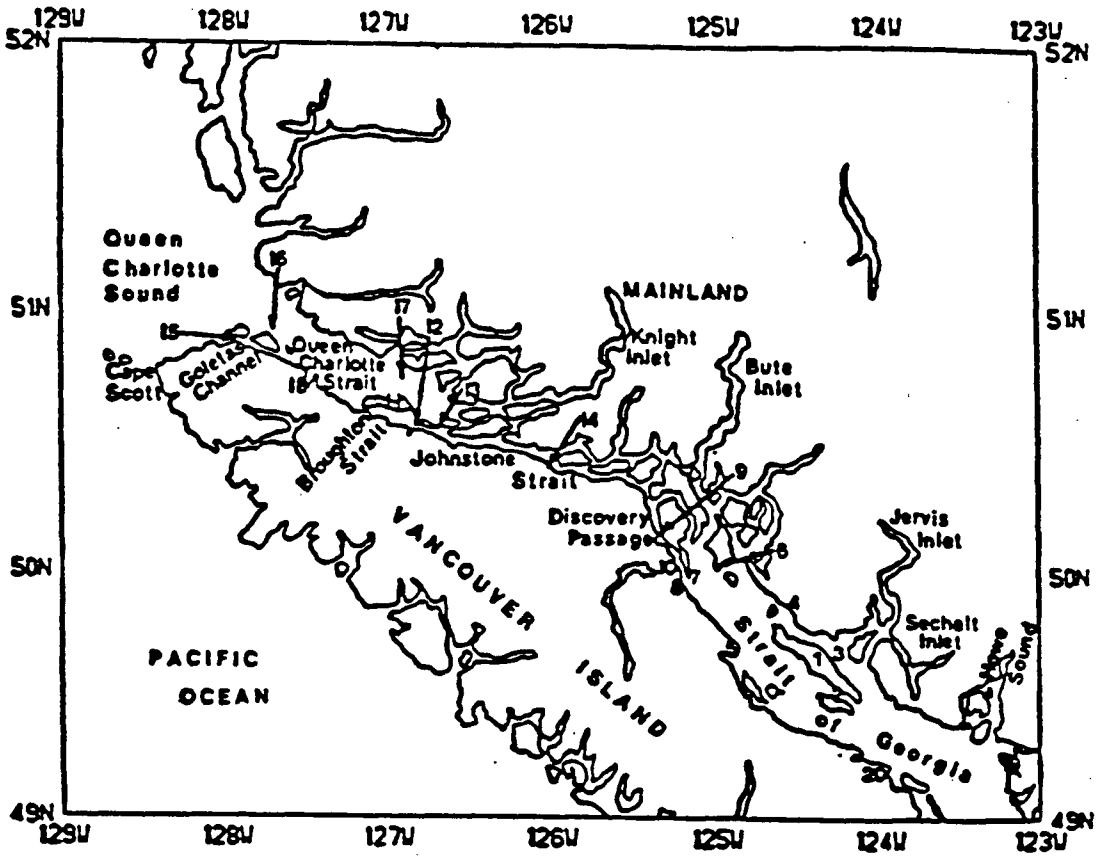

1. Texada Island
2. Sabine Channel
3. Malaspina Strait
4. Powell River
5. Cape Lazo
6. Cape Sutil
7. Cape Mudge
8. Willow Point
9. Seymour Narrows
10. Campell River
11. Malcolm Island
12. Weynton Passage
13. Blackney Passage
14. Kelsey Bay
15. Nahiwitti Bar
16. Gordon Channel
17. Salmon Passage
18. Port Hardy
19. UBC
20. PBS

Figure 1 . Map of Vancouver Island and the B.C. mainland coast. Locations referred to in the text are shown as well as important land masses and waterways.

Mudge (F1) are described by means of twenty-four hour stations. Figure 2 gives the locations of the 7 sets of 24-hour stations. A description is given of the seasonal changes in the general hydrography where applicable.

Thomson *et al.* (1985) and terHart (1988) contain the complete set of T, S and sigma-t (σ_t) sections for each of the 28 sections, the 7 24-hour stations and plots of all 393 CTD profiles. These surveys provide the greatest spatial resolution of the hydrography of this region to date. Detailed examinations of the physical oceanography of the region may be found in Waldichuck (1957) and in the excellent reviews of Thomson (1981) and LeBlond (1983).

1.2: Data Collection and Processing

The research vessels CSS Vector and CSS Parizeau of the Institute of Ocean Sciences, BC were used to collect 393 CTD profiles. With the exception of the 24–28 June 1985 cruise of the CSS Vector and the 3–6 September 1986 cruise of the CSS Parizeau, ship time aboard the CSS Vector was shared with other investigators. At the request of the author, the data collected on 29 May 1986 presented herein was acquired while the CSS Vector was transitting the study area.

A Guildline Instruments Model 8705 Digital CTD Probe and a Model 87102 Control Unit were used in conjunction with a Hewlett Packard (HP) 93101 personal computer and plotter. The manufacturer's reported accuracies are $\pm 0.005°C$, $\pm$ 0.01 parts per thousand (ppt) and $\pm$ 0.15% full scale pressure. The use of the 1000 and 1500 db pressure transducer resulted in depth accuracies of ± 1.50 and ± 2.25 m respectively. This system transmitted a triplet of data to the control unit at 40 ms intervals that was recorded on a stereo casette tape recorder. Data were recorded

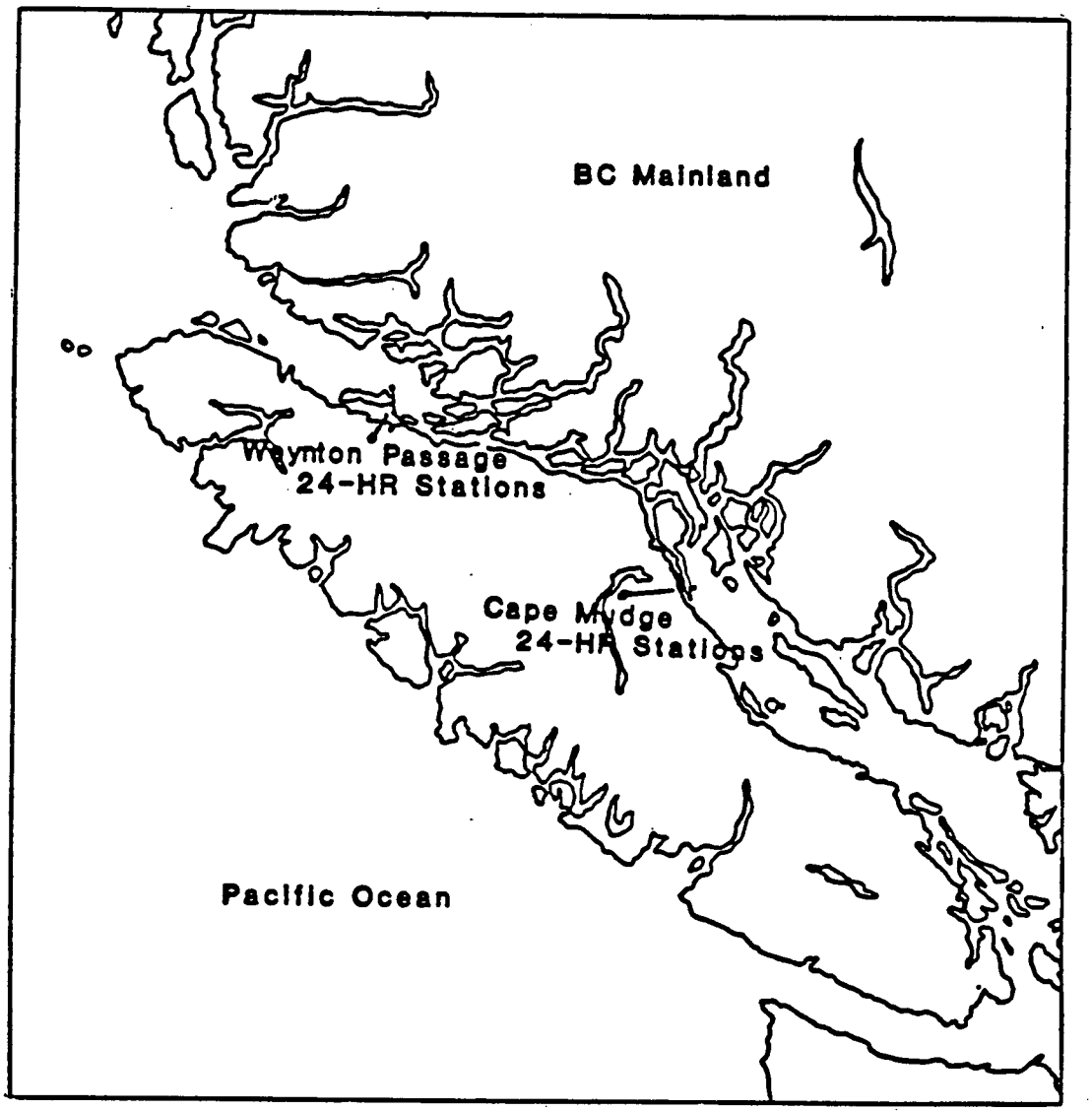

Figure 2 . Map showing the location of the two sets of 24 hour stations. Stations in the vicinity of Weynton Passage were conducted 28–19 August 1985 and those in the vicinity of Cape Mudge were conducted 24–15 June 1986.

only on the downcasts. A rate of descent of 0.5–1.0 m/s generated 12 to 25 triplets of data per meter of depth. Conductivity and pressure were converted to salinity and depth respectively by the HP and plotted in real time at .5 m intervals. The 87102 control unit was later used to play back the stereo cassette tape to a 9-track magnetic tape for processing on UBC's Amdahl computer.

The data were despiked and averaged over one meter depth intervals and σ_t calculated using the International Equation of State, 1980 (Pond and Pickard, 1983). Header data for each cast was added consisting of cruise designation number, consecutive CTD cast number for a particular cruise, time (PDT), date and position to one one-hundredth of a minute. All graphical output was produced on UBC's QMS Lazergrafix 1200 laser printer.

An intermittant electronics failure within the CTD probe itself probe produced an intermittant positive spike in the T readings. This fault occurred generally at depths greater than 70 m and only during the initial cruise of the CSS Vector (24–28 June 1985). This was not considered a catastrophic problem and rather than smooth the CTD casts affected, the bad data were liberally removed from the affected profiles.

1.3: Discussion

The inside passage (Figure 1) consists of two large basins (QCST in the north and the SG in the south) connected by a narrow, sinuous channel (JS and DP). Sections obtained during this multi-year survey include sixteen along-channel and twelve across-channel transects. The seven 24-hour stations consist of data obtained from a set of three stations in Weynton Passage and four in the vicinity of Cape

Mudge (Figure 2). It should be noted that more effort was expended in areas of more physical oceanographic interest. The following discussion will be formatted as follows: an examination of the along-channel sections through the entire inside passage, of the along and across-channel sections and 24-hour stations obtained in QCSD and QCST and finally, of the along and across-channel sections and 24-hour stations obtained in the SG. Table 1 summarizes all sections for the 5 surveys.

1.3.1: The Inside Passage

Two continuous along-channel sections were conducted throughout the inside passage during 24–25 June 1985 and 26–27 August 1985 (sections 1 and 2 – Figures 3 and 4– respectively).

The general physical oceanographic characteristics of the inside passage result from the intrusion, at depth, of relatively cold, salty Pacific Ocean water through QCSD and QCST, the relatively warm, brackish water of the SG moving seaward on the surface and the vigorous tidal mixing in the constricted channels of JS and DP (Thomson, 1981; Thomson *et al.*, 1985; terHart, 1988).

Four distinct oceanographic regimes can be identified in section 1 (Figure 5): the slightly stratified vertical structures of the SG, JS and QCST with surface to bottom salinity differences of 3 ppt, .5 ppt, and 1.5 ppt respectively and the vertically well-mixed waters of DP.

The slightly stratified vertical salinity structure of the SG , with surface waters of over 12°C and less than 29 ppt, is largely due to the fresh water run-off of the Fraser River. Run-off from several large inlets, most notably Bute and Toba in northern SG and Howe Sound in the south, amounts to only a fraction of that of the

Table 1
Details of the CTD sections. Figures 2–6 show the cruise tracks of the research ships and section numbers. Sections and 24-hour stations are grouped geographically and are summarized in terms of the number and station spacing.

Section	Region	No. of CTD's	Stn. spacing
1	Central SG to QCSD (25–26 June 1985)	46	3–20 km
2	Central SG to QCST (26–27 Aug 1985)	30	4–20 km
3	QCSD to JS (26 June 1985)	24	3–10 km
4	Western JS to QCSD (3 Sep 1986)	14	7.5–25 km
5	Goletas Channel (3 Sep 1986)	7	7.5–14 km
6	Meridional section of QCSD (25 June 1985)	5	7 km
7	Meridional section of QCSD (3 September 1986)	5	7–10 km
8	Broughton Strait (26 June 1985)	9	3–8 km
9	Western JS to QCST (29 May 1986)	7	4–9 km
10	Weynton Passage (3 September 1986)	3	5.5–8 km
11	Transverse section of northern QCST (26 June 1985)	7	3 km
12	Transverse section of northern QCST (3 September 1986)	7	2–3 km
13	Transverse section of central QCST (27 August 1985)	9	3 km
14	Transverse section of south QCST 26 June 1985	5	3 km
15	Transverse section of southern QCST (3 September 1986)	5	2–3 km
16	SG (23–24 June 1986)	15	7.5–14 km

Table 1 (Cont.)
Details of the CTD sections. Figures 2–6 show the cruise tracks of the research ships and section numbers. Sections and 24-hour stations are grouped geographically and are summarized in terms of the number and station spacing.

Section	Region	No. of CTD's	Stn. spacing
17	Central SG (4 Sep 1986)	8	15 km
18	Malaspina Strait (27–28 June 1985)	6	13 km
19	Malaspina Strait 5 September 1986	5	7–15 km
20	DP to Cape Lazo (flood) (27 June 1985)	14	3 km
21	DP to Cape Lazo (ebb) (27 June 1985)	17	3 km
22	Cape Mudge to Cape Lazo (4 September 1986)	5	7.5 km
23	Transverse section of northern SG (4 Sep 1986)	5	2.5–3.5 km
24	Cape Lazo to Cape Sutil (27 Jun 1985)	10	3–5 km
25	Cape Sutil to Willow Point (27 June 1985)	7	3 km
26	Transverse section of central SG (4 Sep 1986)	8	4 km
27	Cape Lazo to Powell River (27 Jun 1985)	10	3 km
28	Transverse section of southern SG (4 Sep 1986)	7	4–6 km

Fraser River and as such, accounts for little of the observed salinity structure. The vertically well-mixed waters of DP are produced by rigorous tidal agitation through Seymour Narrows. To the east of Kelsey Bay, the relatively shallow and slightly stratified waters of JS have temperatures and salinities that vary only slightly from

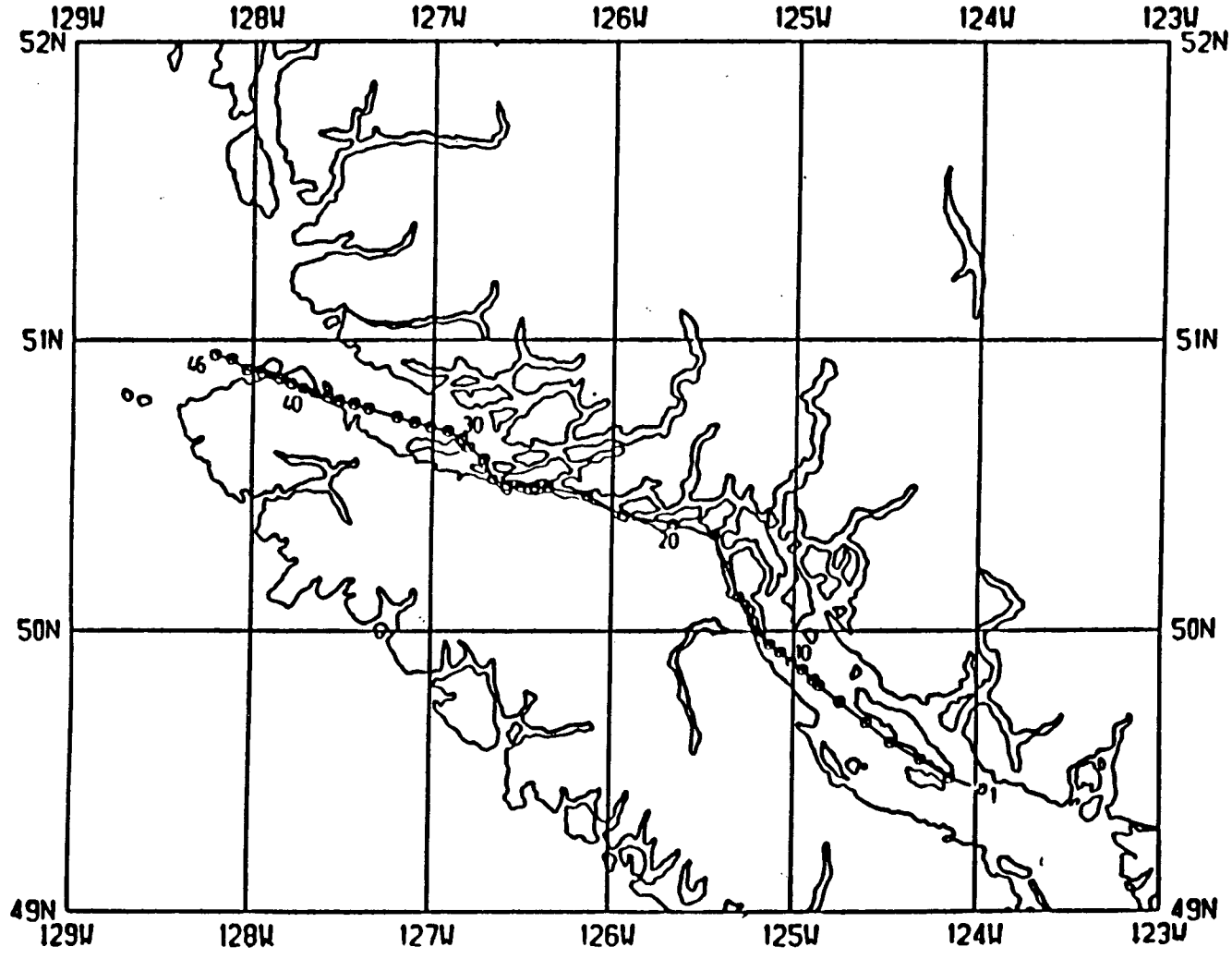

Figure 3. Cruise track of the research vessel CSS Vector (section 1: 24–25 June 1985). Station locations and selected station numbers are superimposed over the vessel's track.

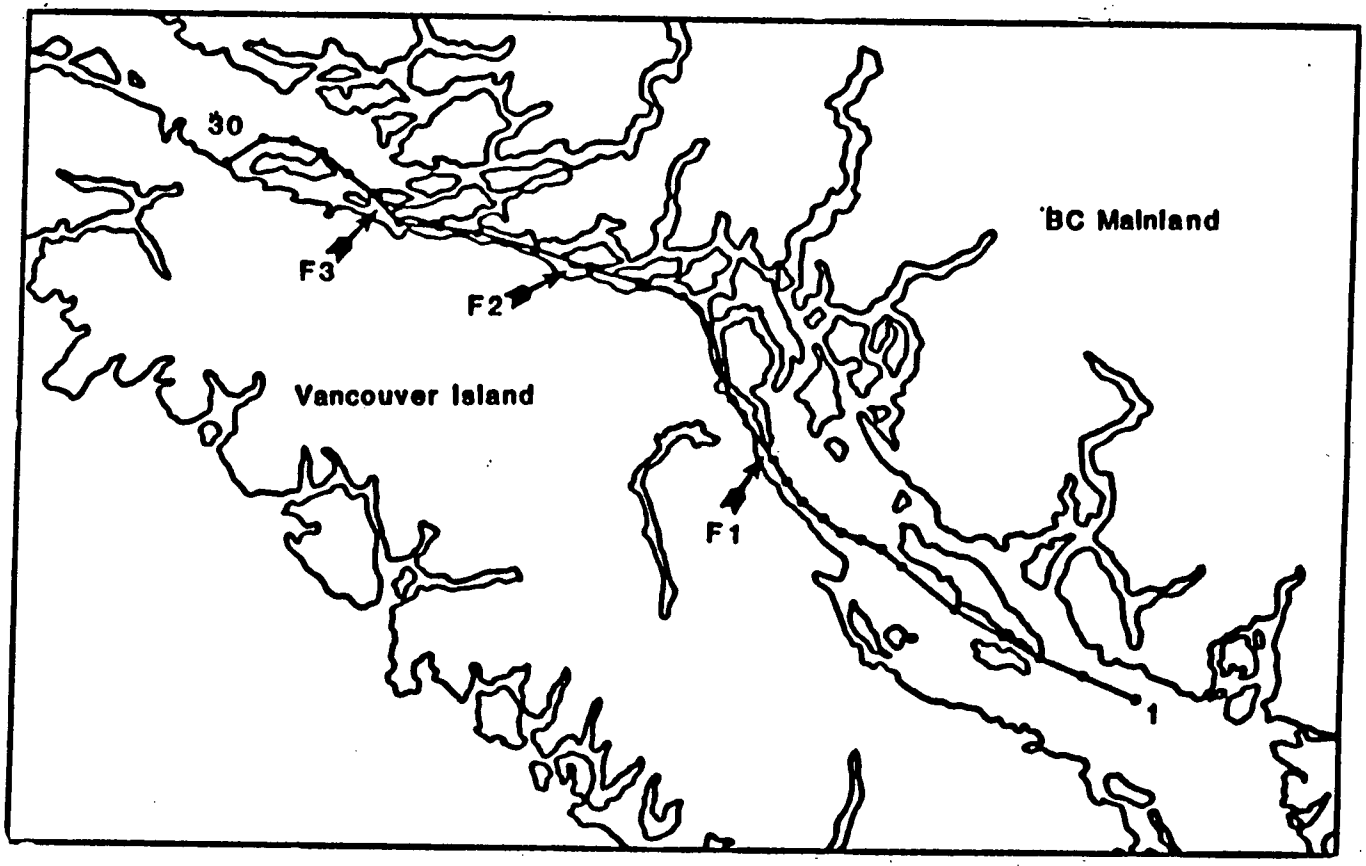

Figure 4. Cruise track of the research vessel CSS Vector (section 2: 25-26 August 1985). Station locations and selected station numbers are superimposed over the vessel's track.

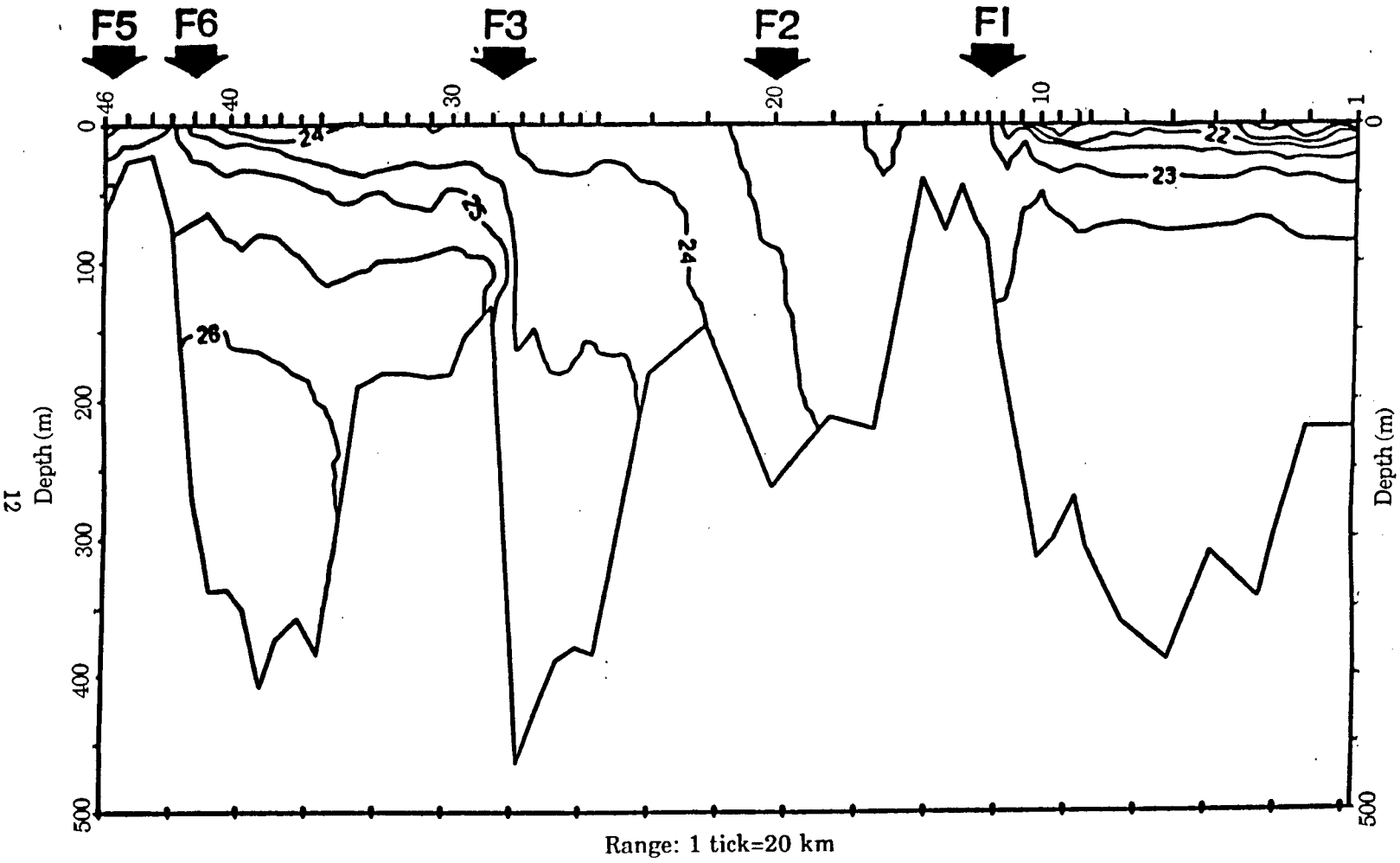

Figure 5. Vertical section of σ_t for section 1. Stations extend from central SG to QCSD (right to left) and were occupied during the period 25–26 June 1985. Station locations are shown in Figure 2. Contouring interval is 0.5 σ_t.

10°C and 30 ppt. West of Kelsey Bay, the slightly stratified but relatively deep waters of this portion of JS have values of T and S in the range of 9–10°C and 31–32 ppt respectively. The greater degreee of stratification in the deep western portion of JS is a result of the intrusion of cold, salty Pacific Ocean water via QCST and QCSD. Lastly, the slightly stratified waters of QCST show bottom waters of Pacific Ocean origin with temperatures near 7°C and salinities greater than 33 ppt. Surface temperatures are near 10°C and surface salinities are less than 30 ppt.

Tidal forcing provides the kinetic energy necessary to mix and in extreme cases, homogenize the water column over shallow sills and in constricted channels (Farmer and Freeland, 1983). Indeed, the general estuarine (gravitational) circulation is greatly dependent on the rate at which mixing occurs and its spatial extent within these topographic features (Geyer and Cannon, 1982). Thus, the four oceanographic regimes are separated by three tidally mixed fronts (see Figures 5 and 6): a subsurface/surface front at the southern entrance to DP (F1), a surface front at Kelsey Bay (F2) and subsurface fronts at the western entrance to JS in Blackney Pass (F3) and Weynton Passage (F7: Figure 8). Table 2 summarizes all fronts observed in the study area.

The strongest and most dynamically significant feature anywhere in the study area is surface/subsurface front (F1) near Cape Mudge where the vertically well-mixed waters of DP debouch into the SG to meet a buoyancy layer formed by fresh water run-off and solar heating. This surface layer is less than 30 m deep and is bounded by the 10.5°C isotherm, the 29.5 ppt isohaline or the 22.5 σ_t isopycnal. Surface gradients in the region of the front are 4°C and 1.5 ppt per 10 km. The surface front at Kelsey Bay (F2) separates the vertically well-mixed waters of DP

Table 2
Details of the observed fronts. The fronts are numbered in order of their first mention in the text. Summary includes location, Sections observed in, type of front ('sfc' implies surface, 'ssfc' subsurface, MT mixed tidal and E estuarine), horizontal gradients and the state of the tide.

Designation	Location	Section	Type	Hor. Grad. °C/10 km	ppt/10 km
F1 (Ebb)	Cape Mudge	1	sfc/ssfc, MT	2.7	1.0
F1 (Flood)	Cape Mudge	20	sfc/ssfc, MT	12.5	3.3
F1 (Ebb)	Cape Mudge	21	sfc/ssfc, MT	1.4	1.2
F1 (Ebb)	Cape Mudge	2	sfc/ssfc, MT	4.0	1.5
F1 (Ebb)	Cape Mudge	22	sfc/ssfc MT	2.5	1.0
F2 (Ebb)	Kelsey Bay	1	sfc/ssfc, MT	.1/.2	.1/.3
F2 (Ebb)	Kelsey Bay	2	sfc, MT	0.3	0.5
F3 (Flood)	Blackney Pass	1	ssfc, MT	1.5	0.8
F3 (Slack)	Blackney Pass	2	sfc, MT	1.5	1.0
F3 (Ebb)	Blackney Pass	4	sfc, MT	1.0	1.0
F4 (Flood)	QCST	4	sfc, E	1.0	0.3
F5 (Flood)	Nahwitti Bar (west)	1	sfc MT	0.8	0.7
F5 (Ebb)	Nahwitti Bar (west)	5	sfc, MT	3.0	1.0
F6 (Flood)	Nahwitti Bar (east)	1	sfc, MT	1.5	0.8
F6 (Ebb)	Nahwitti Bar (east)	5	sfc, MT	1.0	1.0
F7 (Flood)	Weynton Passage	3	ssfc, MT	1.0	0.5
F7 (Flood)	Weynton Passage	9	sfc/ssfc, MT	.4/.2	.8/.8
F7 (Flood)	Weynton Passage	10	sfc/ssfc M	1.0	0.4
F8 (Ebb)	Broughton Strait	8	ssfc, MT	1.9	1.1
F9 (Ebb)	Malaspina Strait	26	sfc, E	0.3	1.9

and eastern JS from the slightly stratified waters of western JS. Surface gradients associated with F2 are .3°C and .5 ppt per 10 km. There is a subsurface front (F3) in Blackney Pass where the intrusion of dense Pacific water into the deep basin of JS is evidenced by waters less than 9°C and greater than 32 ppt. The intrusion is deeper than 25 m and its upper extent is delineated by the 9°C isotherm, the 32 ppt isohaline or the 25 σ_t isopycnal. Subsurface gradients are 1.5°C and 1.0 ppt per 10 km. There is a minimal surface signature. Tidal agitation over the relatively long shallow sill at the seaward entrance to Goletas Channel produces the hybrid tidally mixed fronts F5 and F6 at the western and eastern extremities, respectively,

of the sill.

The major difference between sections 1 and 2 (Figure 6) is the presence of a warmer, more buoyant surface layer in the SG during the latter part of the summer. Differences in σ_t within the surface layer ($\leq .5$) were largely due to increased solar radiation. Increased surface salinities within the central SG were not evident despite significantly less freshwater input from the Fraser River during late summer. Royer and Emery (1982) discuss the response of the Fraser River plume to discharge of the river itself and to wind and tidal forcing. Their results show that the northern portion of the central SG is not as strongly influenced by the plume as the southern portion. Observations made during this study support Royer and Emery's (1982) conclusions.

1.3.2: Queen Charlotte Sound

Data collected in QCSD was logistically limited to the area to the immediate north of the northernmost tip of Vancouver Island. The general physical oceanography is characterized by the outflow of surface waters and the inflow of dense Pacific Ocean waters caused partially by continuity constraints and by the wind-induced upwelling of deep waters in QCSD and offshore (Dodimead, 1980; Daniel, 1985).

Three along-channel sections (Figures 8–10) and two meridional section (Figures 11 and 12) were made during the CSS Vector and Parizeau cruises of 25–28 June 1985 and 3–6 September 1986 respectively. Locations for sections 4 and 5 are shown in Figure 7.

Sections 3 and 4 (Figures 8 and 9), from the western entrance of JS through Blackney Pass or Weynton Passage and into QCST and the open waters of QCSD

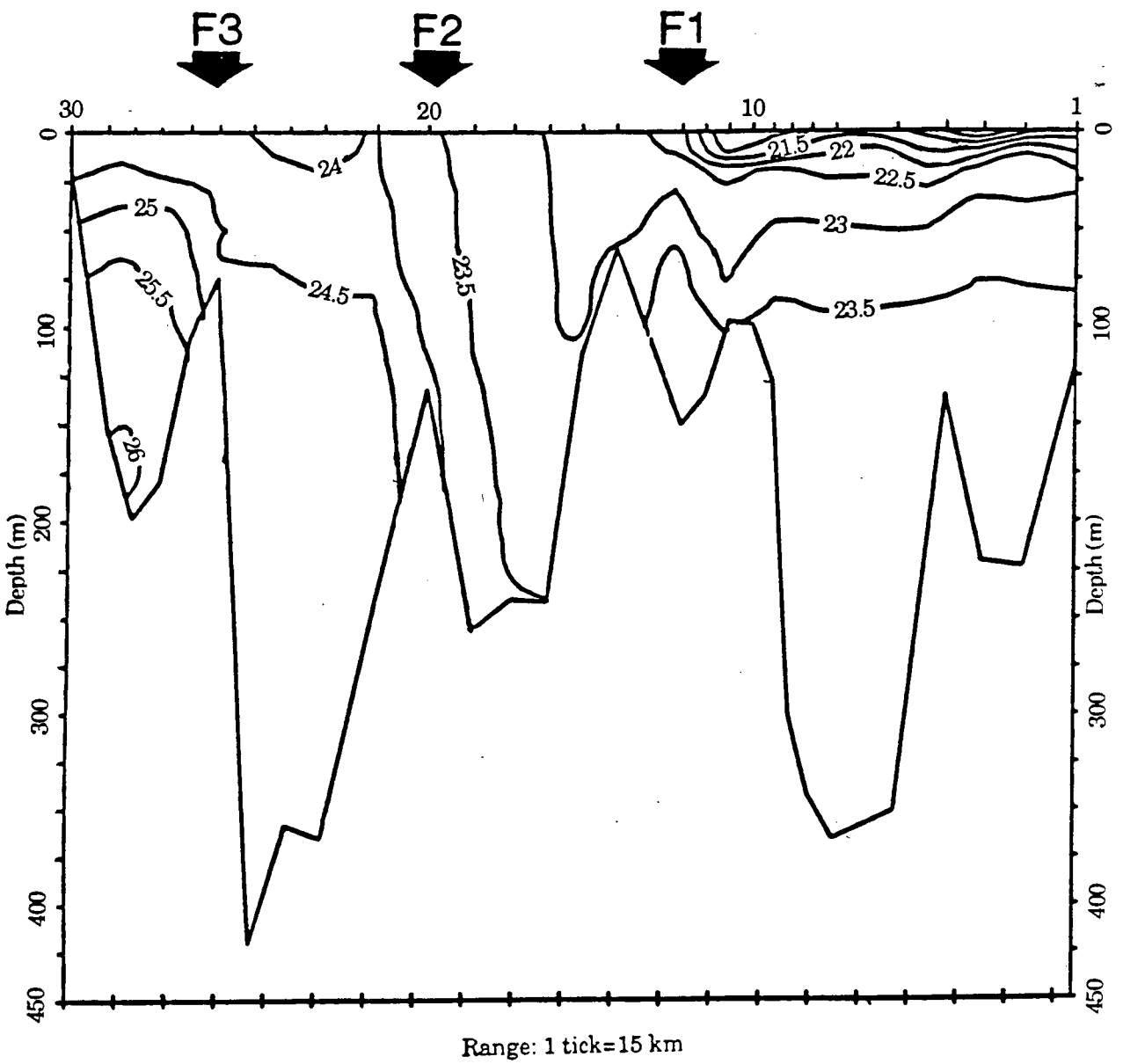

Figure 6 . Vertical section of σ_t for section 2. Stations extend from central SG to QCST and were occupied during the period 26–27 August 1985. Station locations are shown in Figure 3. Contouring interval is 0.5 σ_t.

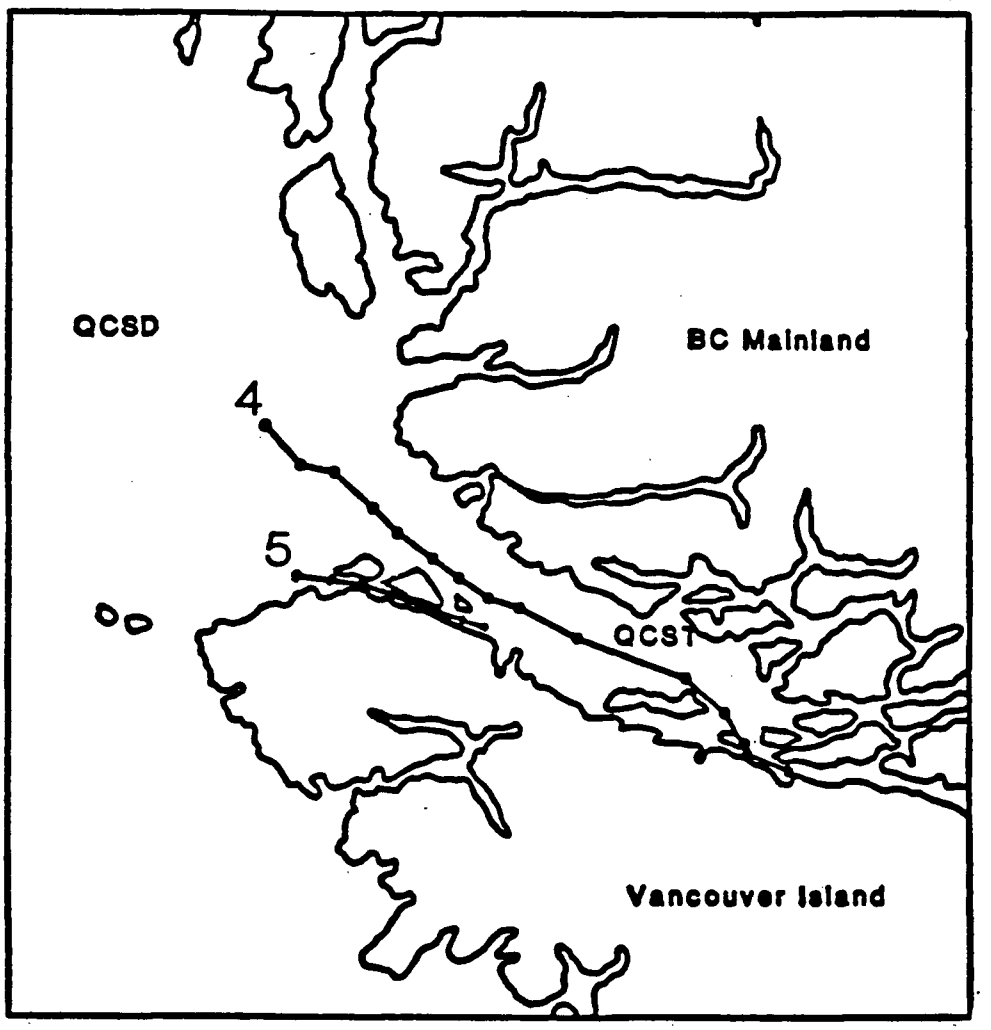

Figure 7 . Cruise track of the research vessel CSS Parizeau (sections 4 and 5: 3 September 1986). Station locations are superimposed over their respective tracks. Section numbers are shown adjacent to their respective tracks.

show the subsurface tidally mixed fronts (F3 and F7), in Blackney Pass and Weynton Passage respectively, and the progressively more saline water column as the section progresses seaward. Subsurface gradients are slightly greater than 1.5°C and 0.8 ppt per 10 km at 100 m (F3) and 1.0°C and 0.5 ppt per 10 km at 100 m (F7). A weaker front (F4), delineated by the surfacing of the 24.5 σ_t isopycnal, separating the greater degree of stratification in QCSD from that of the weaker stratified waters of QCST is apparent in both sections in the region north of Hope and Nigel Islands. Surface gradients associated with F4 are slightly greater than 1.0°C and .3 ppt per 10 km. Section 3 (26 June 1985) has a cooler (1°C) less saline (1 ppt) surface layer in QCSD than section 4 (3 September 1986). Surface layer variability in sections 3 and 4 (Figures 8 and 9) is caused by increased solar heating and much reduced freshwater input.

Section 5 (Figure 10), from QCSD to QCST via Goletas Channel, shows the strong tidally mixed fronts (F5 and F6, fig 10) produced by tidal flow over Nahwitti Bar (see Figure 1 for location). Gradients are 3.0°C and 1.0 ppt and 1.0°C and 1.0 ppt for F5 and F6 respectively.

The meridional sections 6 and 7, Figures 11 and 12, made in the open waters of QCSD shows the Pacific Ocean waters outside of QCST. Most of the water column deeper than 20 m is relatively cold ($\leq$ 8.5°C) and saline ($\geq$ 32.5 ppt). As opposed to Figure 12 (section 7), subsurface isopycnals are clearly sloped down to the north in Figure 11 (section 6).† Southward sloping subsurface isopycnals on

† Given that the Rossby internal deformation radius is less than the channel width, sloping isopycnals may, but are not necesssarily indicative of rotational effects (LeBlond and Mysak, 1982). The applicability of simple geostrophy to these data

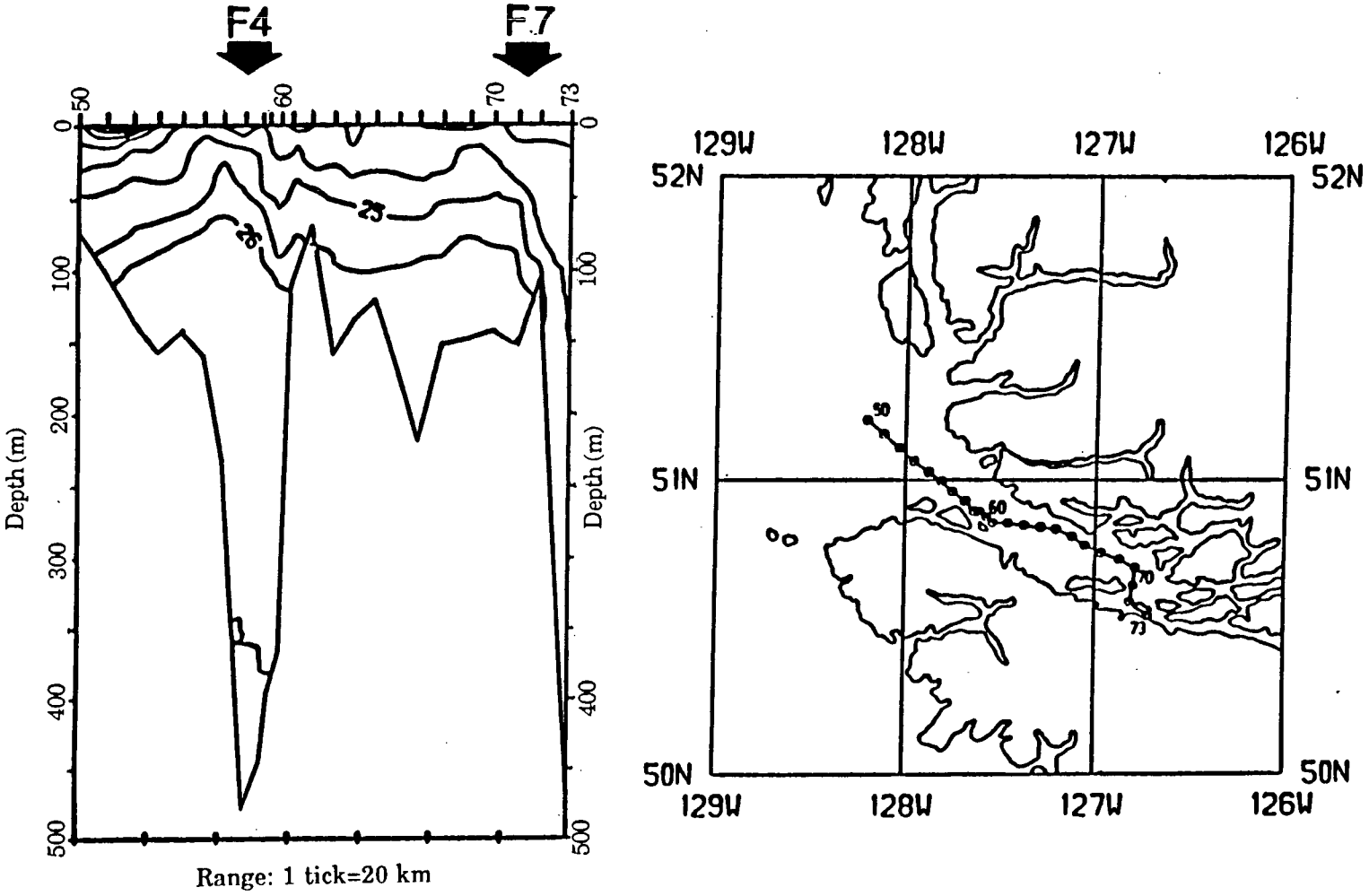

Figure 8. Vertical section of σ_t for section 3. Stations extend from QCSD to JS and were occupied during 26 June 1985. Contouring interval is 0.5 σ_t.

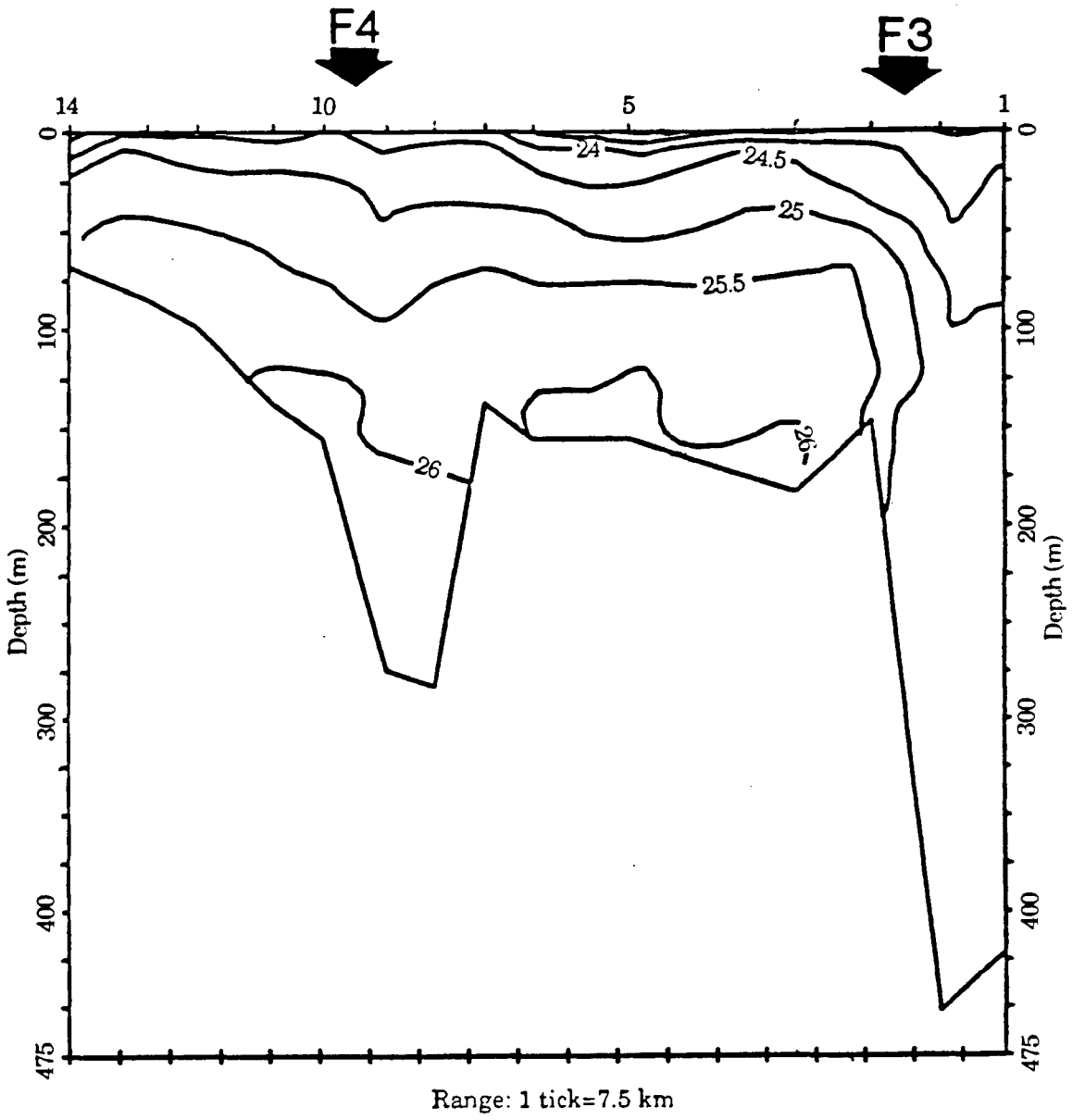

Figure 9 . Vertical section of σ_t for section 4. Stations locations (shown in Figure 4) extend from western JS to QCSD and were occupied during 3 September 1986. Contouring interval is 0.5 σ_t.

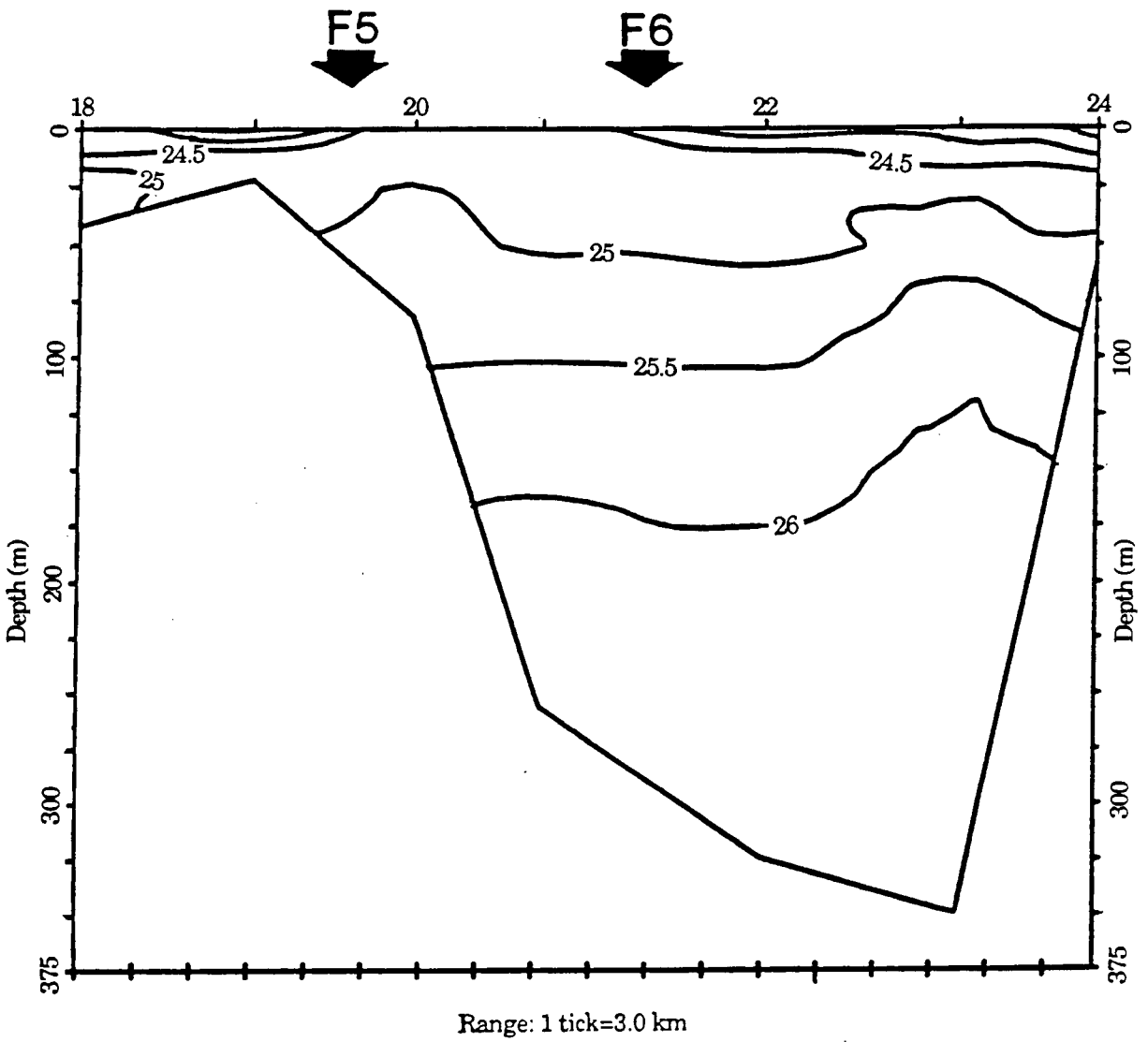

Figure 10 . Vertical section of σ_t for section 5. Stations locations (shown in Figure 4) extend west to east through Goletas Channel and were occupied 3 September 1986. Contouring interval is 0.5 σ_t.

the Vancouver Island side of Figure 12 (section 7) indicate a relatively strong influx of cold ($\leq$ 8°C), saline ($\geq$ 33 ppt) Pacific Ocean water into QCST via Goletas Channel. The weakening of the residual seaward flowing current velocities in the upper layer, as evidenced by the change in the across-channel slopes of subsurface isopycnals in Figures 11 and 12, is largely due to decreased freshwater input during summer months. The influx of cold, saline Pacific Ocean water at depth during the summer is mainly due to increased wind-induced upwelling in QCSD (Pickard, 1975; Thomson, 1981)

1.3.3: Queen Charlotte Strait

Data from five across-channel sections, three along-channel sections and a set of three 24-hour stations were collected during the early and late summer of 1985 and the late spring and summer of 1986. The across-channel sections conducted in the northern, central and southern regions of QCST (26 June 1985, 27 August 1985 and 3 September 1986) were made to determine the across-channel structure of QCST. Two along-channel sections through Weynton Passage (29 May 1986 and 4 September 1986) were made to observe the intrannual variability of the subsurface tidally mixed front (F7) in this region. A single section through Broughton Passage (26 June 1985) was conducted to observe the tidal mixing that occurs over the shallow sill ($\leq$ 50 m) separating QCST from western JS and the resultant tidally mixed front (F8). Three 24-hour stations were occupied during 28–29 August 1985 to observe the strength of the tidal signal within Weynton Passage.

The across and along-channel structures of QCST are similar in that there is generally weak vertical stratification and significant seasonal variability. Section 9

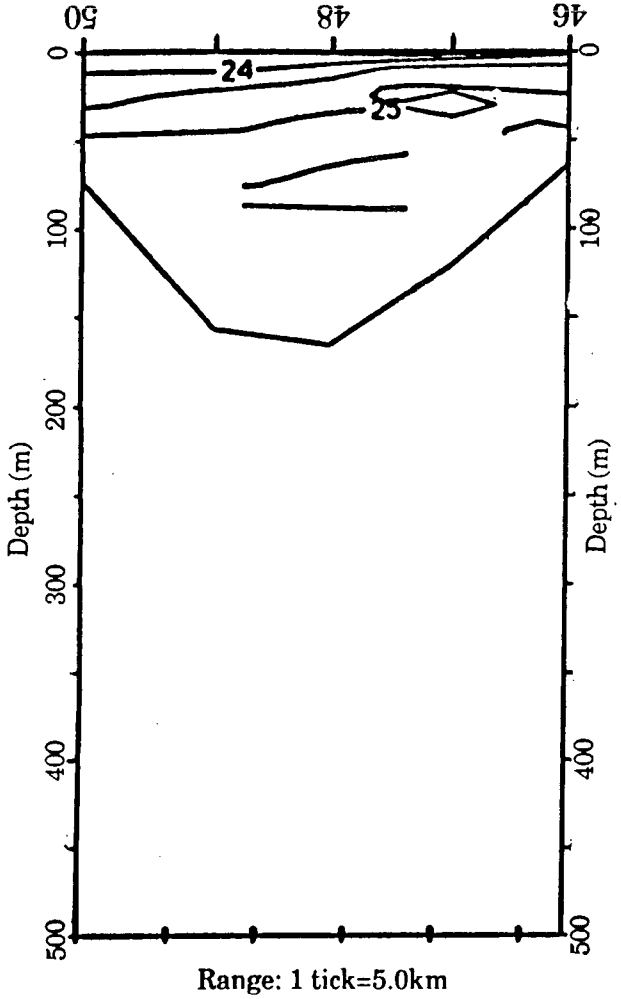

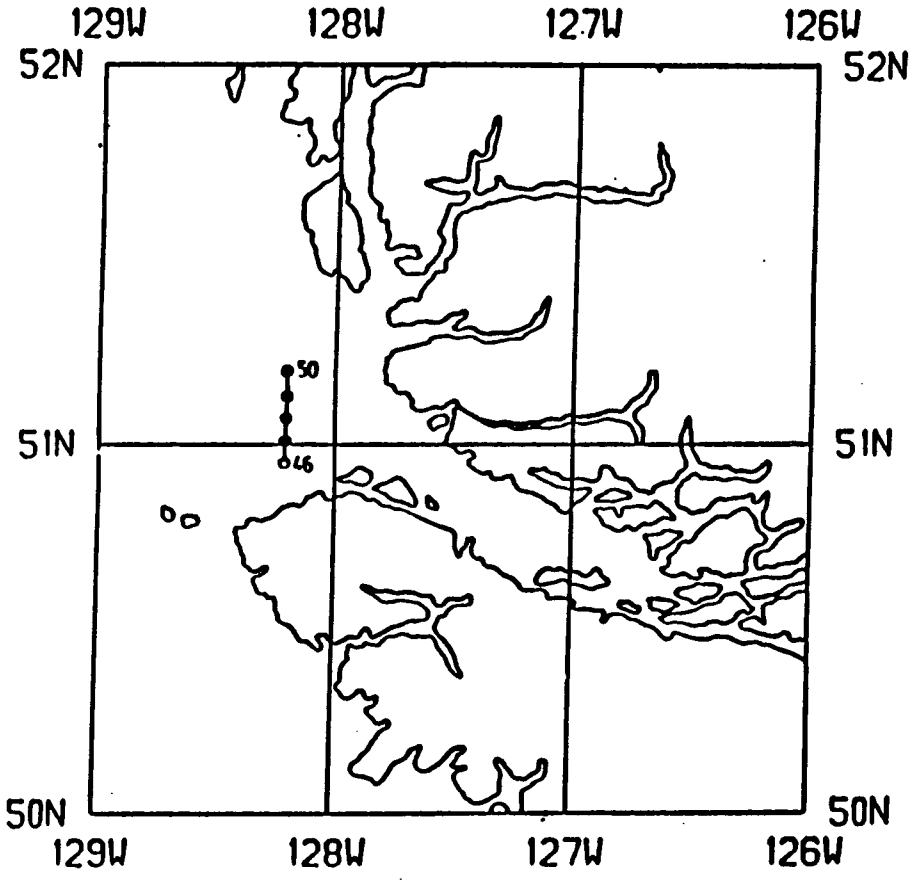

Figure 11. Vertical section of σ_t for section 6. Stations extend meridionally in QCSD and were occupied during 25 June 1985. Contouring interval is 0.5 σ_t.

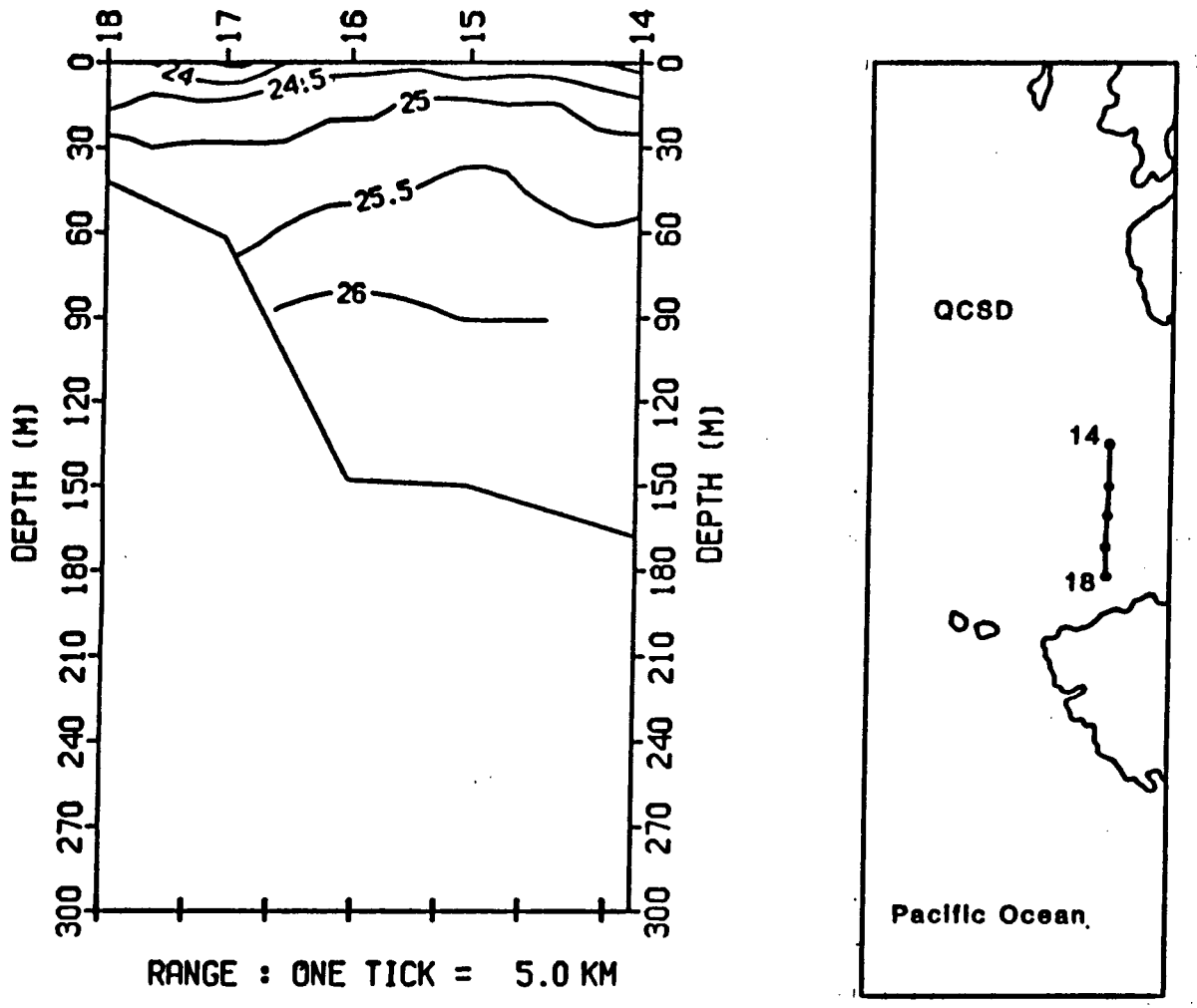

Figure 12. Vertical section of σ_t for section 7. Stations extend meridionally in QCSD and were occupied during 3 September 1986. Contouring interval is 0.5 σ_t.

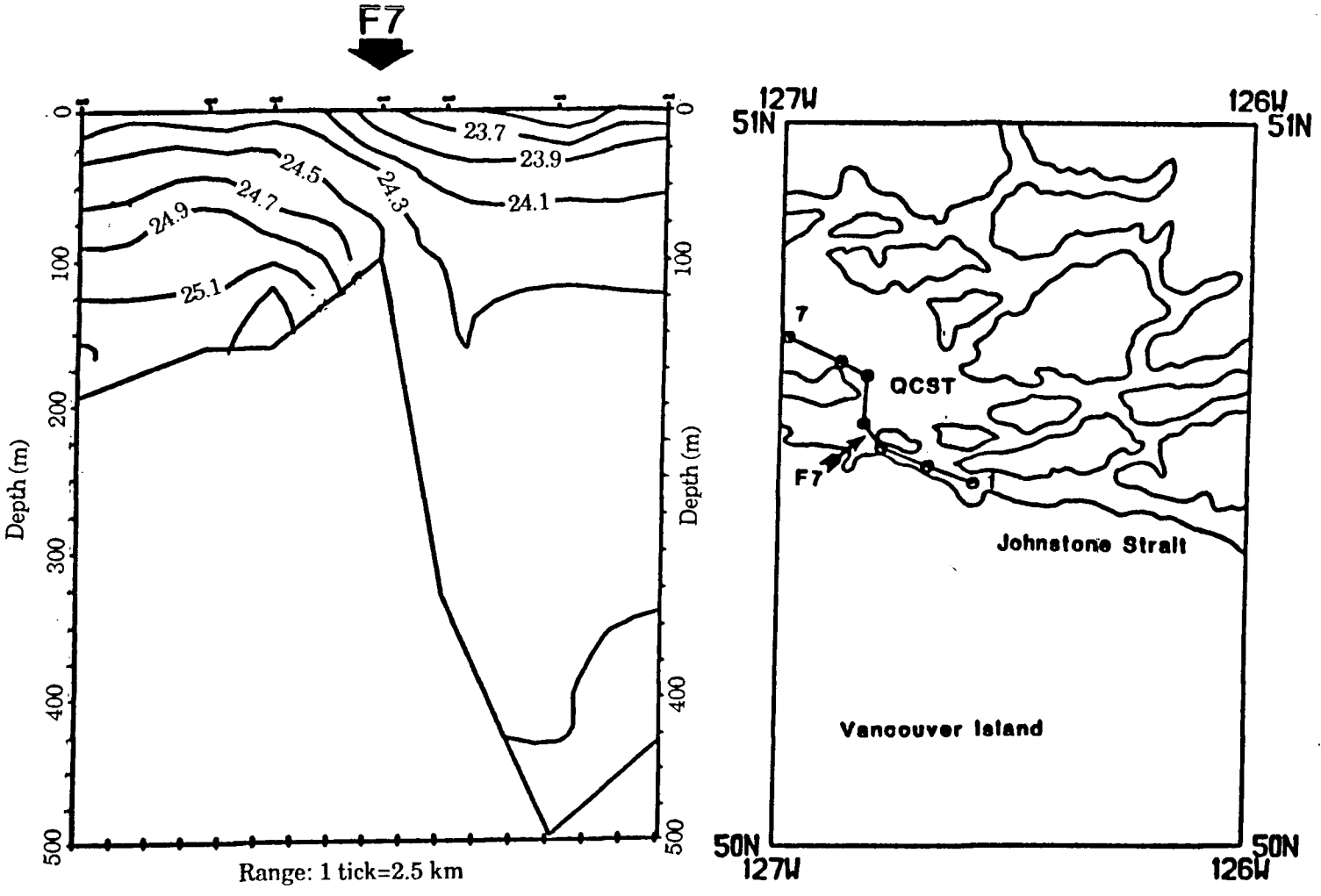

Figure 13. Vertical section of σ_t for section 9. Stations extend from western JS to QCST and were occupied 29 May 1986. Contouring interval is 0.2 σ_t.

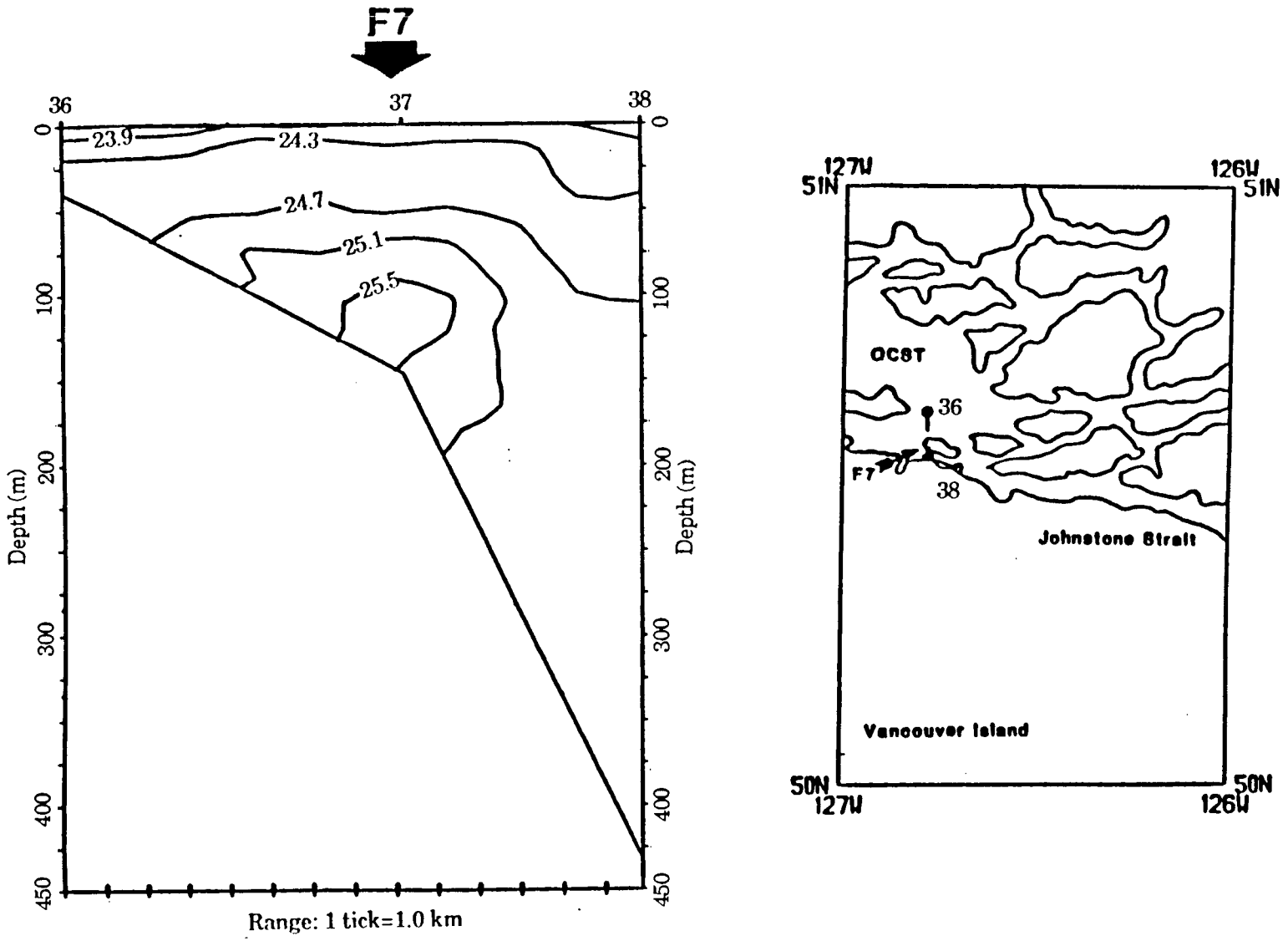

Figure 14. Vertical section of σ_t for section 10. Stations extend north to south through Weynton Passage and were occupied 3 September 1986. Contouring interval is 0.4 σ_t.

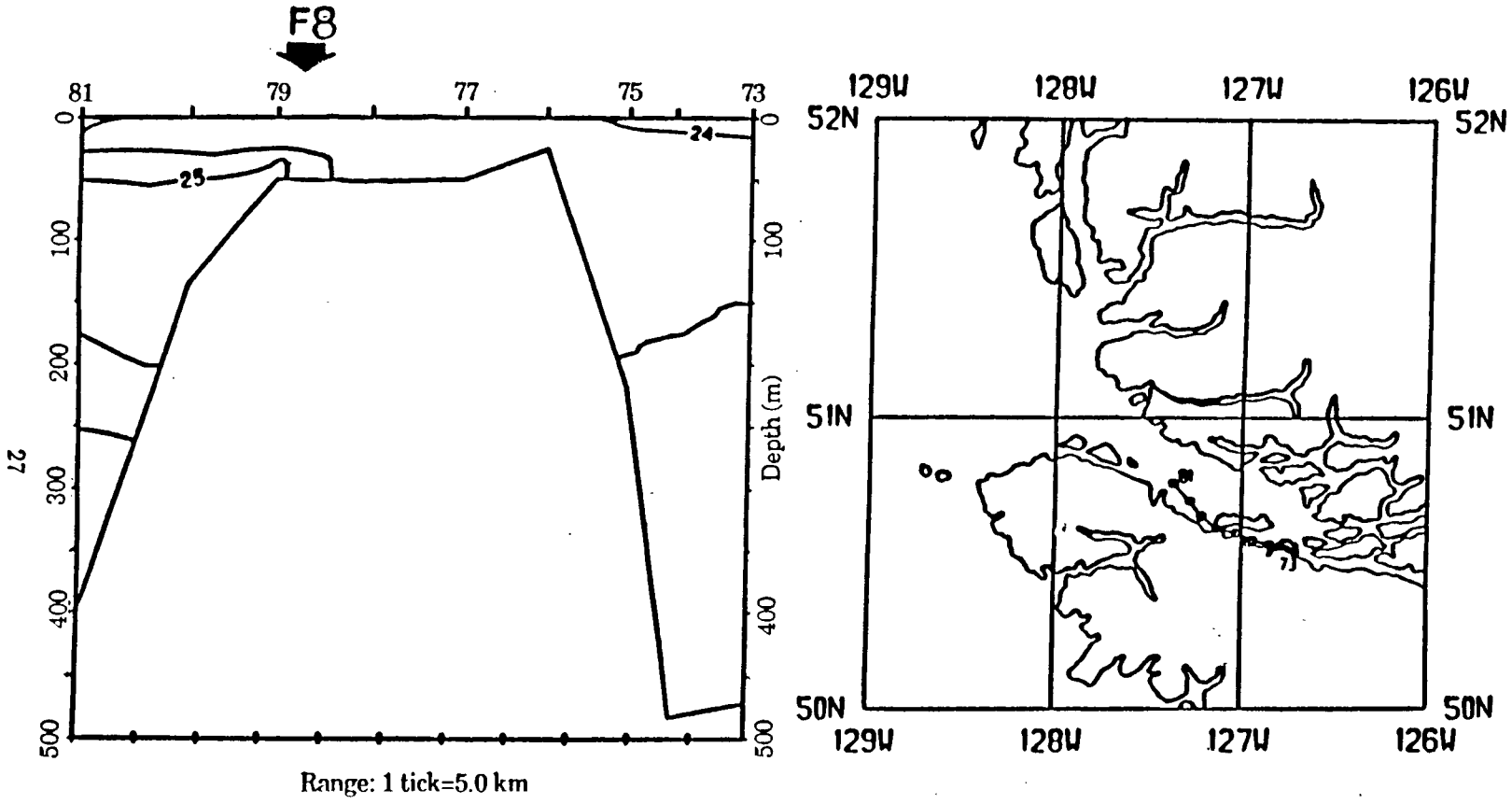

Figure 15. Vertical section of σ_t for section 8. Stations extend east to west Broughton Channel and were occupied 26 June 1985. Contouring interval is 0.5 σ_t.

(Figure 13) made during 29 May 1986 contrasts with Section 10 (Figure 14) made during 4 September 1986. Data from section 9 show colder surface waters ($\leq 9.0^{o}$C) in the upper buoyancy layer owing to relatively weak solar insolation in early summer. Increased freshwater run-off accounts for decreased surface salinities (≤ 30.5 ppt) in Section 9 as compared to Section 10. Additionally, the tidally mixed front (F7) associated with the intrusion of waters of Pacific Ocean origin into JS in Section 9 (Figure 13) shows a significant surface signature in sharp contrast to the same feature in Section 10 (Figure 14). Surface gradients in Section 9 associated with F7 are .4°C and .8 ppt per 10 km; subsurface gradients are .2°C and .8 ppt per 10 km at 100 m. The upper limit of the dense intruding waters is denoted by the 7.9°C isotherm, the 31.3 ppt isohaline or the 24.3 σ_t isopycnal (Figure 13). Subsurface gradients for this same feature (F7) in Section 9 are 1.0°C and .4 ppt per 10 km at 100 m. Section 8 (Figure 15), conducted on 26 June 1985 form JS to QCST , clearly shows the presence at depth of cold, saline waters originating in the Pacific. Tidal mixing over the shallow sill in Broughton Passage results in the formation of the tidally mixed front F8 and the production of relatively dense ($\sigma_t \geq 25.0$) water that eventually spills into the deep trough in western JS (Figure 15). In fact, seasonal changes in water properties in both the upper and lower layers are communicated to varying depths via this mechanism (LeBlond, 1983). It should be noted that the horizontal extent of the sill significantly affects the manner in which tidal energy is propagated into the basin beyond the sill itself (Farmer and Freeland, 1983). Sills in Weynton Passage and Blackney Pass play significantly different dynamical roles in redistributing tidal energies. During summer, when lower layer salinities are at a maximum (Thomson, 1981), the negatively buoyant plume produced by tidal agi-

tation may penetrate the complete water column, enhancing vertical structure and abyssal dissolved O_2.

The along-channel two layer, weakly stratified structure of QCST was observed to vary seasonally as was the across-channel structure. The depth of this layer is fairly uniform along-channel due to tidal mixing in the north over shoals and through narrow channels in the south. Along-channel variations in the depth of the buoyancy layer may be caused by entrainment of dense, off-shore waters, especially in summer when wind-induced upwelling is at a seasonal maximum. This effect, however, was not obvious in the sections obtained during the summer months and is likely obscured by the tidal mixing in the north and the south extremeties of QCST. As expected, the across-channel structure is stongly affected by varying freshwater input albeit freshwater sources are significantly less in QCST than in the SG.

A transverse section made in northern QCST during 26 June 1985 shows sloping subsurface isopycnals throughout most of the water column (section 11, Figure 16). These slopes are indicative of a relatively strong seaward flow in the upper layer. In sharp contrast to this section is section 12, obtained on virtually the same transect during 3 September 1986, which shows a nearly uniform across-channel structure. Surface temperatures and salinities are $\geq 11°C$ and ≤ 30.5 ppt. respectively. Cold (7.0°C) and saline (33.0 ppt) Pacific Ocean water is present in the deep basin near the Vancouver Island coast. Figure 17 shows the isopycnals gently sloping down to the north on the mainland side of the channel indicating a weak geostrophic flow to the NW at section 12. In addition, isopycnals (≥ 25.5) slope down to the south on the Vancouver Island side of the channel indicating a

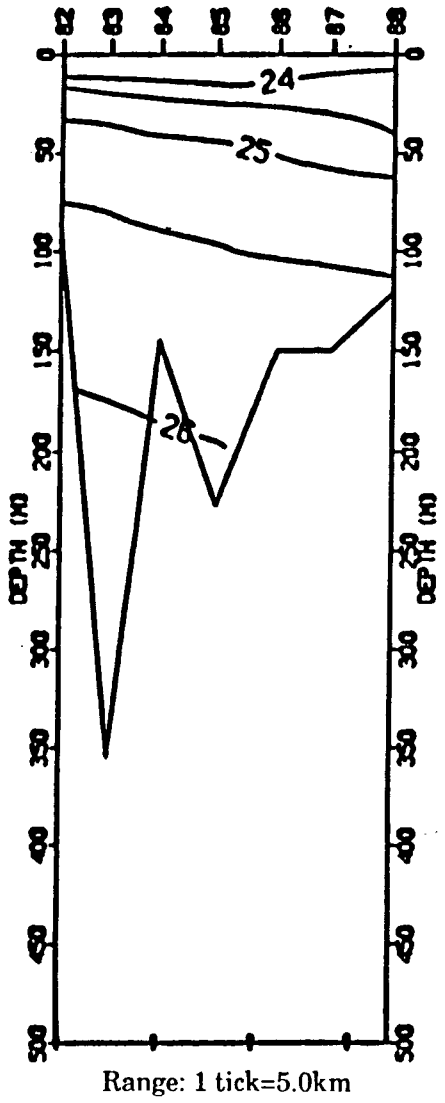

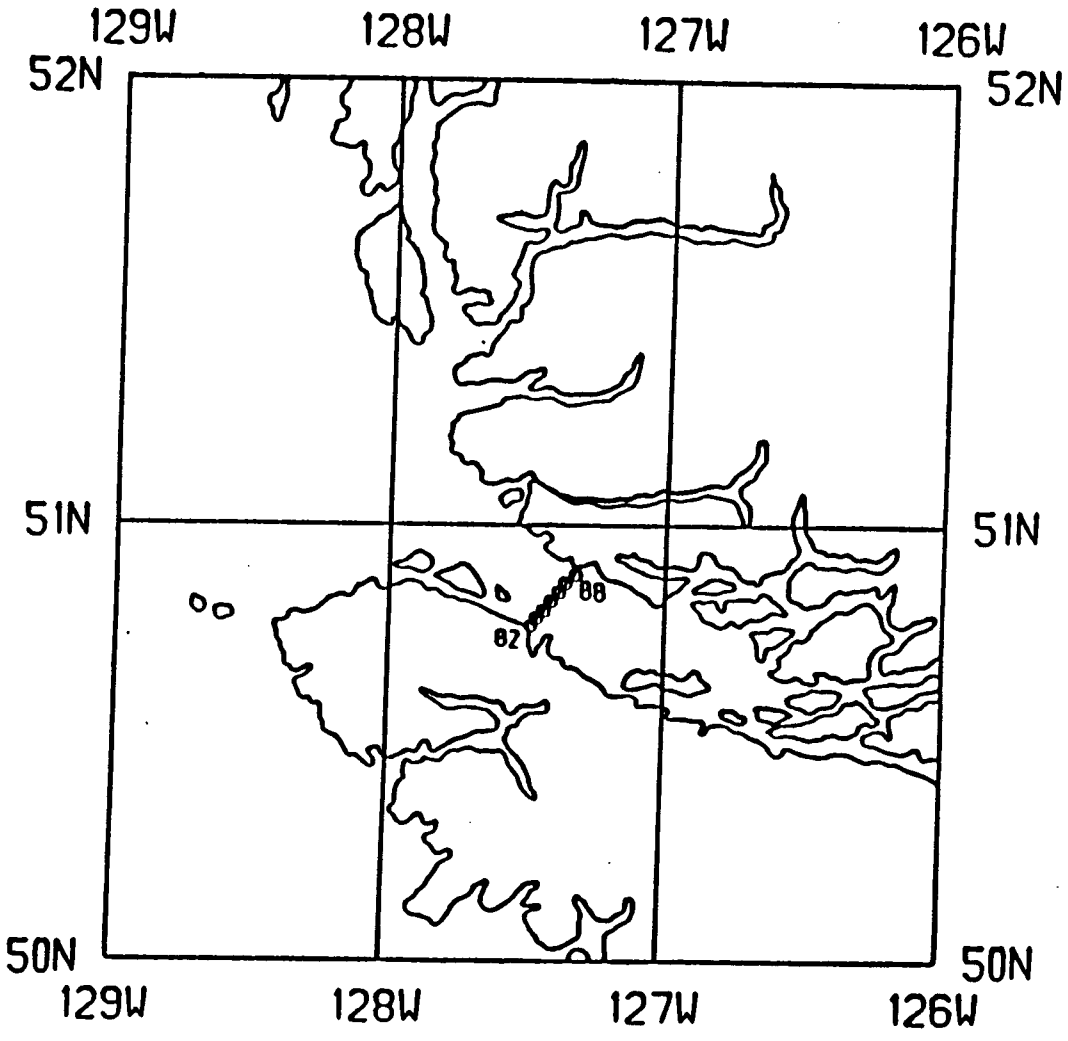

Figure 16. Vertical section of σ_t for section 11. Stations extend across-channel in northern QCST and were occupied 26 June 1985. Contouring interval is 0.5 σ_t.

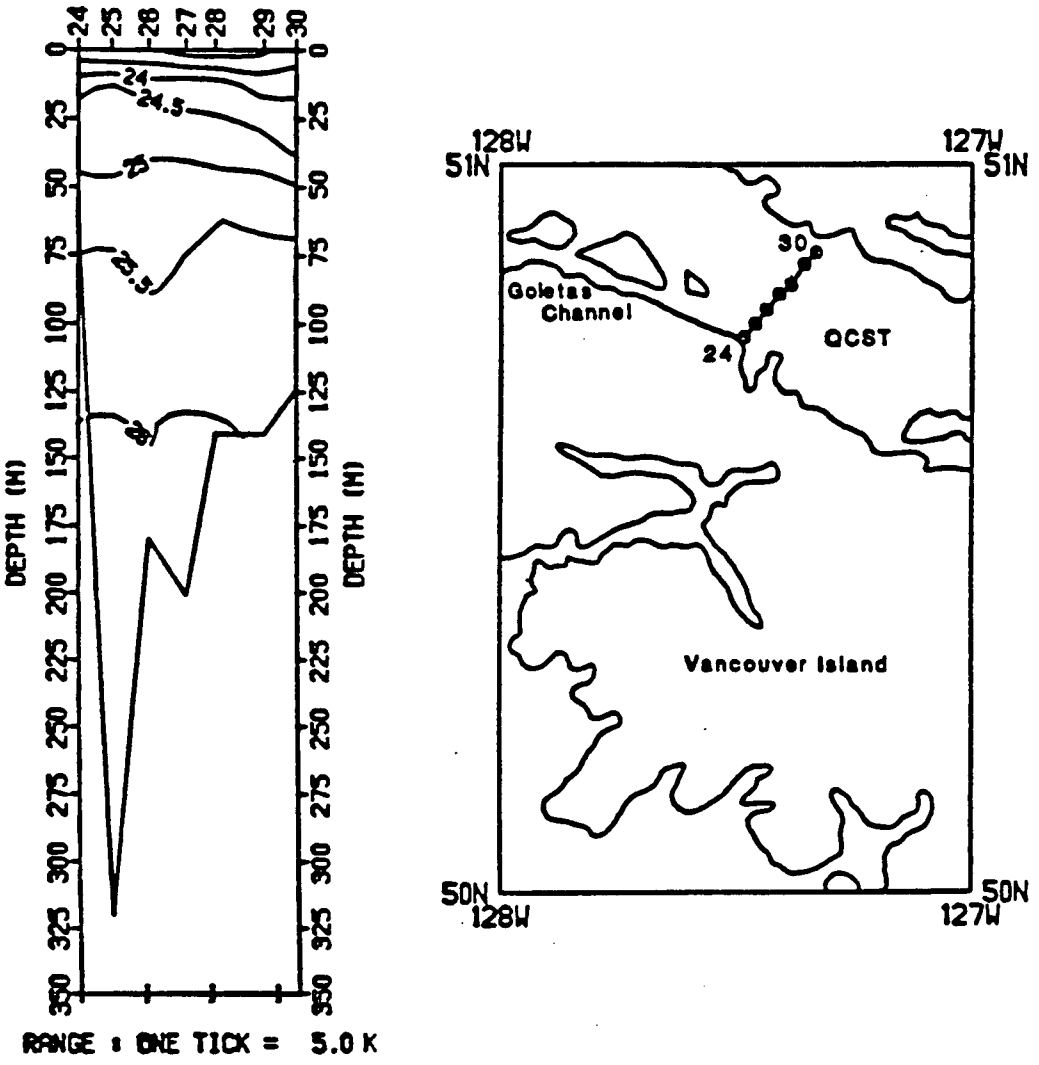

Figure 17 . Vertical section of σ_t for section 12. Stations extend across-channel in northern QCST and were occupied 3 September 1986. Contouring interval is 0.5 σ_t.

weak geostrophic flow into QCST. Section 13 (Figure 18) reveals the across channel structure of central QCST. There is somewhat less vertical stratification present in the central strait than in the northern portions. There is a broad thermocline and halocline and cold ($\leq 8.5°C$) and saline (≥ 32.5 ppt) Pacific Ocean water is present in the deep portion of the basin. Surface temperatures and salinities are approximately 9.5°C and 31.5 ppt respectively. The isopycnals slope down to the north, indicative of a geostrophic flow out of QCST to the northwest. Similar transverse sections of the southern entrance to QCST, made during 26 June 1985 (section 14, Figure 19) and 3 September 1986 (section 15, Figure 20) show little difference in temperature, salinity or σ_t values. There is, however, less slope to the subsurface isopycnals in section 15 (September 1986) due to much reduced freshwater input during the summer months. Consequently, the upper layer estuarine flow out of QCST to the northwest (seaward) diminishes. Table 6 presents geostrophic calculations based on a simple two layer model as well as summarizing the transverse sections made in QCST.

Stations north of Malcolm Island (Station WI), in Weynton Passage (Station WP) and off of Blinkhorn Light (Station BL) were sampled recursively during the period 28–29 August 1985. Table 3 provides details on this set of 24-hour stations.

The location of Station WP and the times of higher-high water (HHW) and lower-low water (LLW) during the period when this station was occupied are shown in Figure 21.

Data obtained from Station MI (north of Weynton Passage) shows highly correlated vertical excursions of isotherms, isohalines and isopycnals of approximately 20 m below 15 m indicating the intrusion of cold ($\leq 9.0°C$), saline (≥ 32.0 ppt) rel-

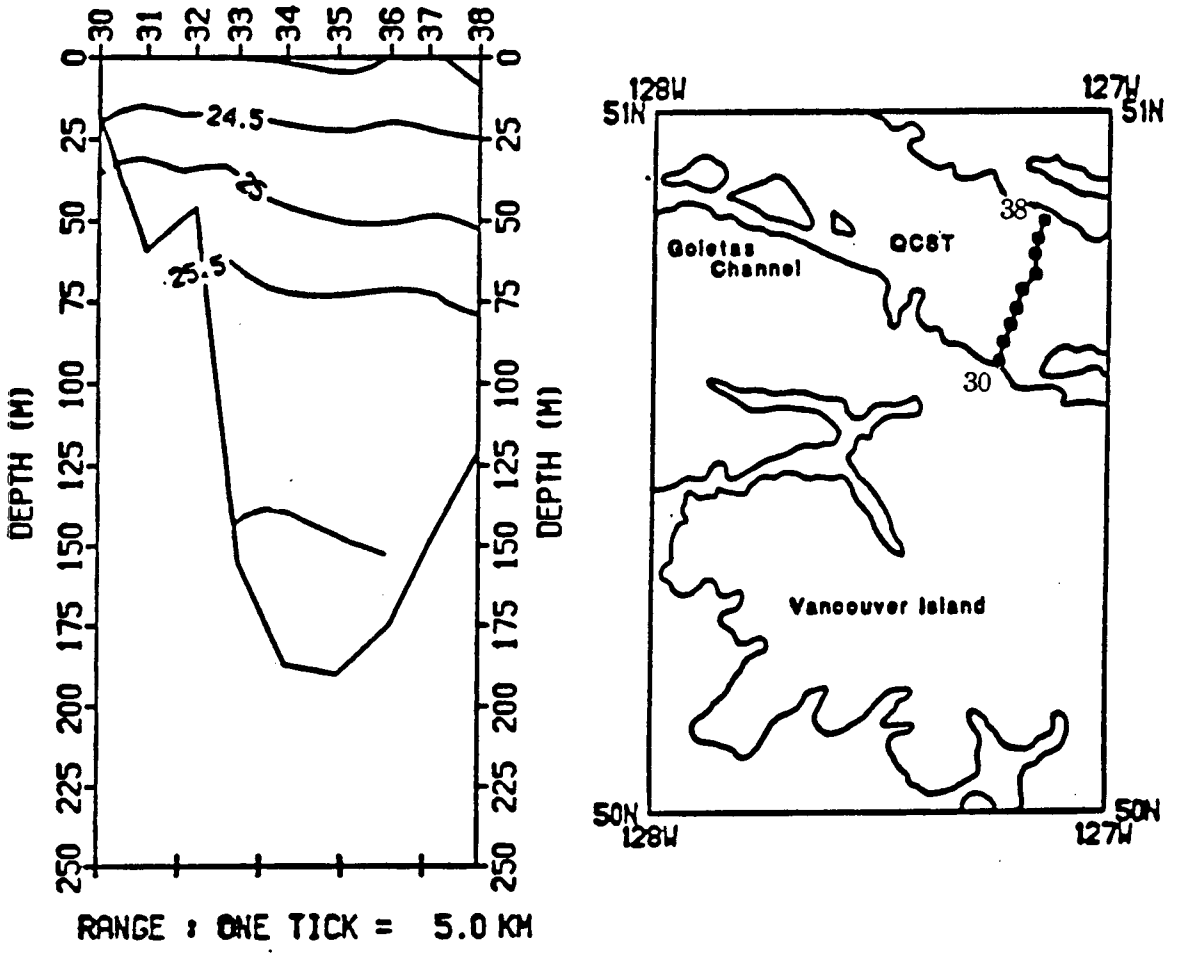

Figure 18 . Vertical section of σ_t for section 13. Stations extend across-channel in central QCST and were occupied 27 August 1985. Contouring interval is 0.5 σ_t.

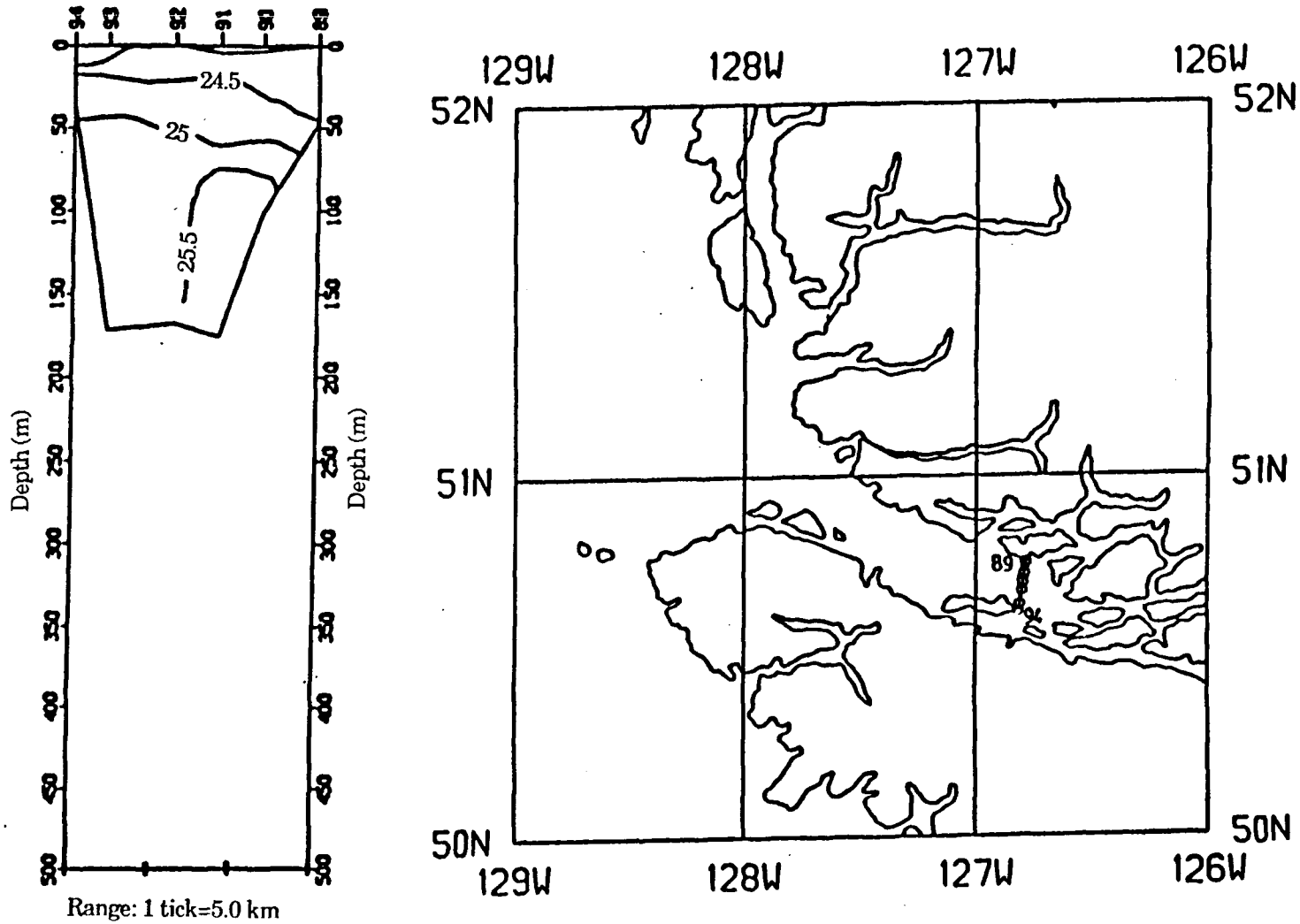

Figure 19. Vertical section of σ_t for section 14. Stations extend across-channel in southern QCST and were occupied 26 June 1985. Contouring interval is 0.5 σ_t.

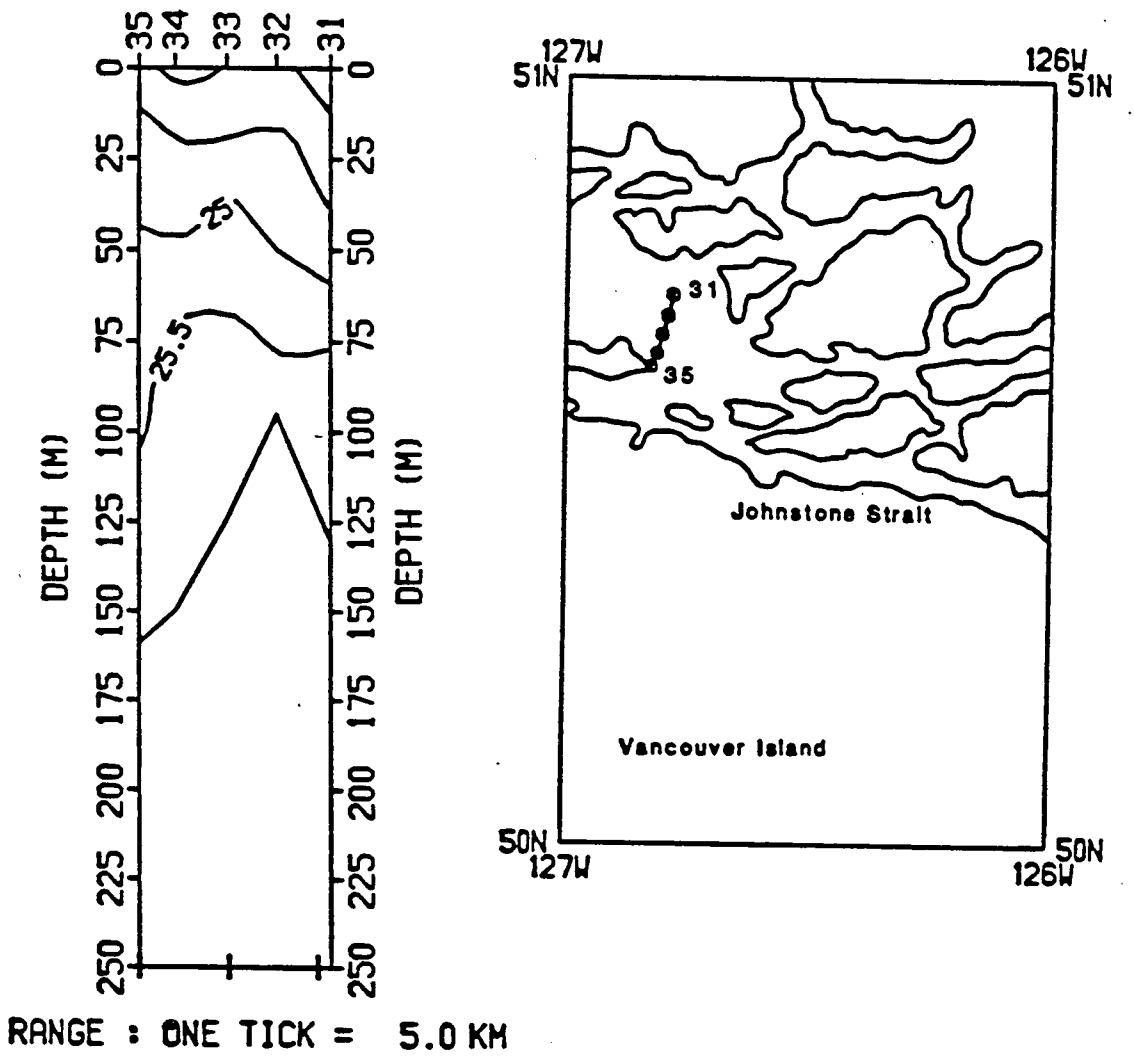

Figure 20 . Vertical profile of σ_t for section 15. Stations extend across-channel in southern QCST and were occupied 3 September 1986. Contouring interval is 0.5 σ_t.

Table 3
Details of the set of 24-hour stations that were conducted in the vicinity of Weynton Passage. The summarized data includes station location, the number of CTD casts, the spacing–in hours–between the casts and the CTD cast numbers. Note that the CTD cast numbers are not sequential.

Station location	No. of CTD's	CTD spacing	CTD cast no.'s
Malcolm Island (Station MI)	12	2 hr	010056–089
Weynton Passage (Station WP)	12	2 hr	010057–090
Blinkhorn Light (Station BL)	12	2 hr	010058–091

atively dense ($\geq 25.0\ \sigma_t$) water into Weynton Passage. At Station WP in Weynton Passage itself, this same water mass is seen to advance and retreat with the flood and ebb tide. Figure 21 shows the core of this dense tongue of water ($\geq 25.5\ \sigma_t$) to completely appear and disappear indicating the strength and variability of the tidal forcing. The strength of the tidal signal, that is to say the volume of water entering JS, is evidenced by the depression of the 9.0°C isotherm by approximately 100 m at Station BL, located to the south and east of Weynton Passage. The surface waters at Station BL, delineated by the 9.5°C, the 32.5 ppt isohaline or the 24.0 σ_t isopycnal remained relatively undisturbed during the one tidal cycle observed. The depression of the isopleths is also evidence of the rapid sinking of the negatively buoyant plume debouching into JS from Weynton Passage.

The net result of these tidal motions is the formation of strong subsurface hybrid tidally mixed front (F7, Figures 8, 13 and 14) and a negatively buoyant plume. The plume is pulsed over the sill in Weynton Pass and flows down-slope into the deep basin in western JS. Thomson (1981) describes current measurements made in the deep portion of western JS that indicate dense waters formed and forced into JS

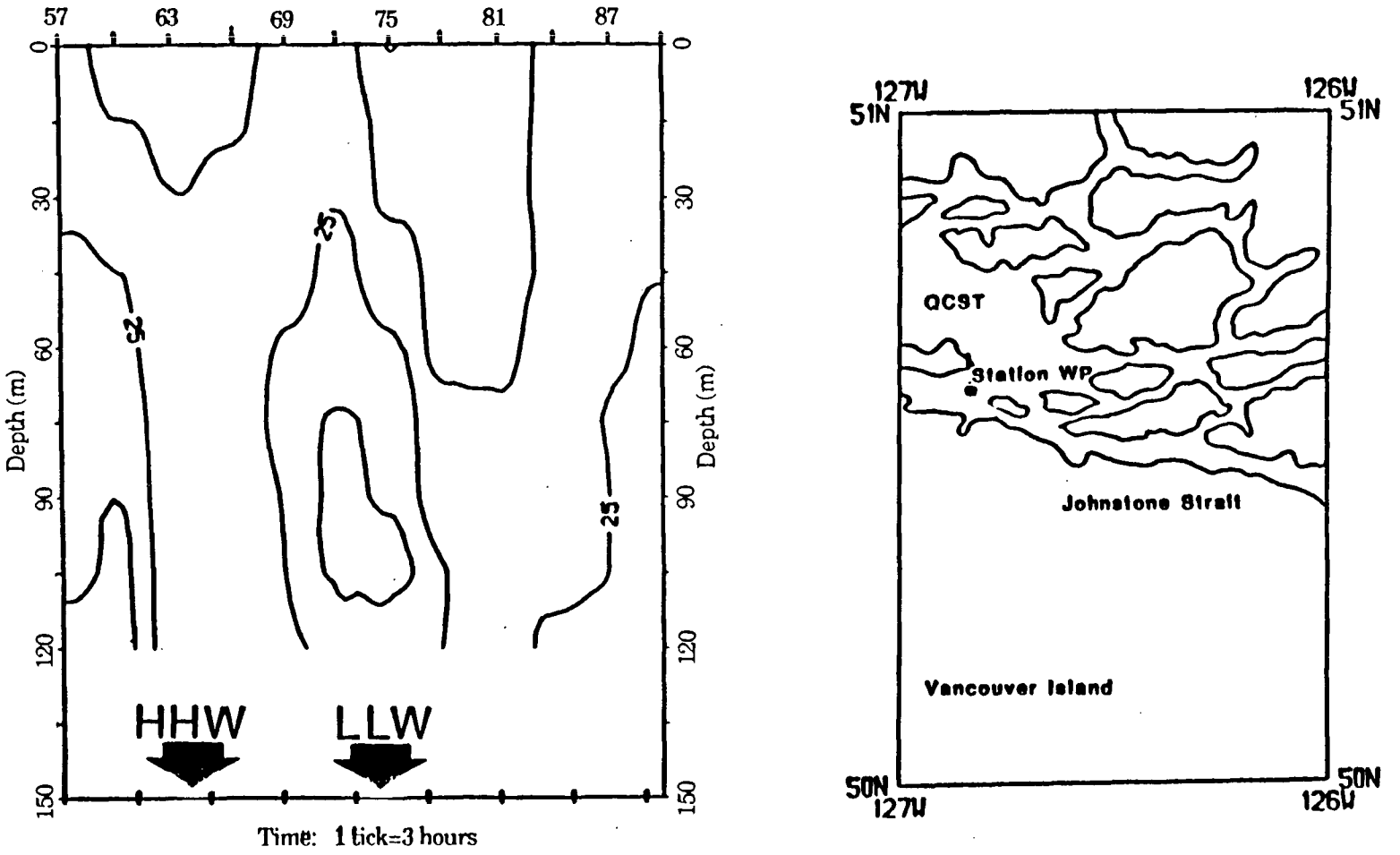

Figure 21. Time-depth contour plot of σ_t for Station WP located in Weynton Passage. This station was sampled recursively over the 24 hour period 28-29 August 1985. Contouring interval is 0.5 σ_t. The occurence of Higher high water (HHW) and lower low water (LLW) is shown from which the general duration of the flood and ebb tides may be inferred.

through Weynton Pass result in a strong bottom jet that sweeps up-channel (eastward) at maximum velocities in excess of 150 cm/s. Similar deep water formation occurs through Blackney Passage and to a lesser extent, Broughton Passage where the horizontal exent of the sill serves to appreciably alter the dynamics (Geyer and Cannon, 1982; Farmer and Freeland, 1983).

1.3.4: Strait of Georgia

During the 25–27 June 1985 and the 23–26 June 1986 cruises of the CSS Vector and the 3–5 September cruise of the CSS Parizeau, eight along-channel and five across-channel sections and four 24-hour stations were conducted within the central and northern portion of the SG. Particular attention was paid to the hybrid tidal mixing front (F1) observed in sections 1 and 2, (Figures 5 and 6). Locations for sections 16–19 are shown in Figure 22.

Section 16, taken along-channel from central SG to just south of Cape Mudge (see Figure 22 for section and station location), shows the early summer vertical structure of the SG. Surface temperatures observed were in excess of 16°C in the south decreasing to less than 12°C in the north while surface salinities increased from $\leq$ 16 ppt in the south to $\geq$ 26 ppt in the north. There is no surface mixed layer owing to weak and variable winds during summer and a brackish, buoyant layer bounded by the 20 σ_t isopycnal (Figure 23) caused by solar heating and run-off. In contrast to section 2, Figure 6, early summer conditions in the central SG show a pronounced decrease in surface salinities (16 ppt as compared to 28.5 ppt) and similar surface temperatures of $\approx$ 15°C.

Section 17 (Figure 24), taken on 4 September 1986 from Active pass to Sabine

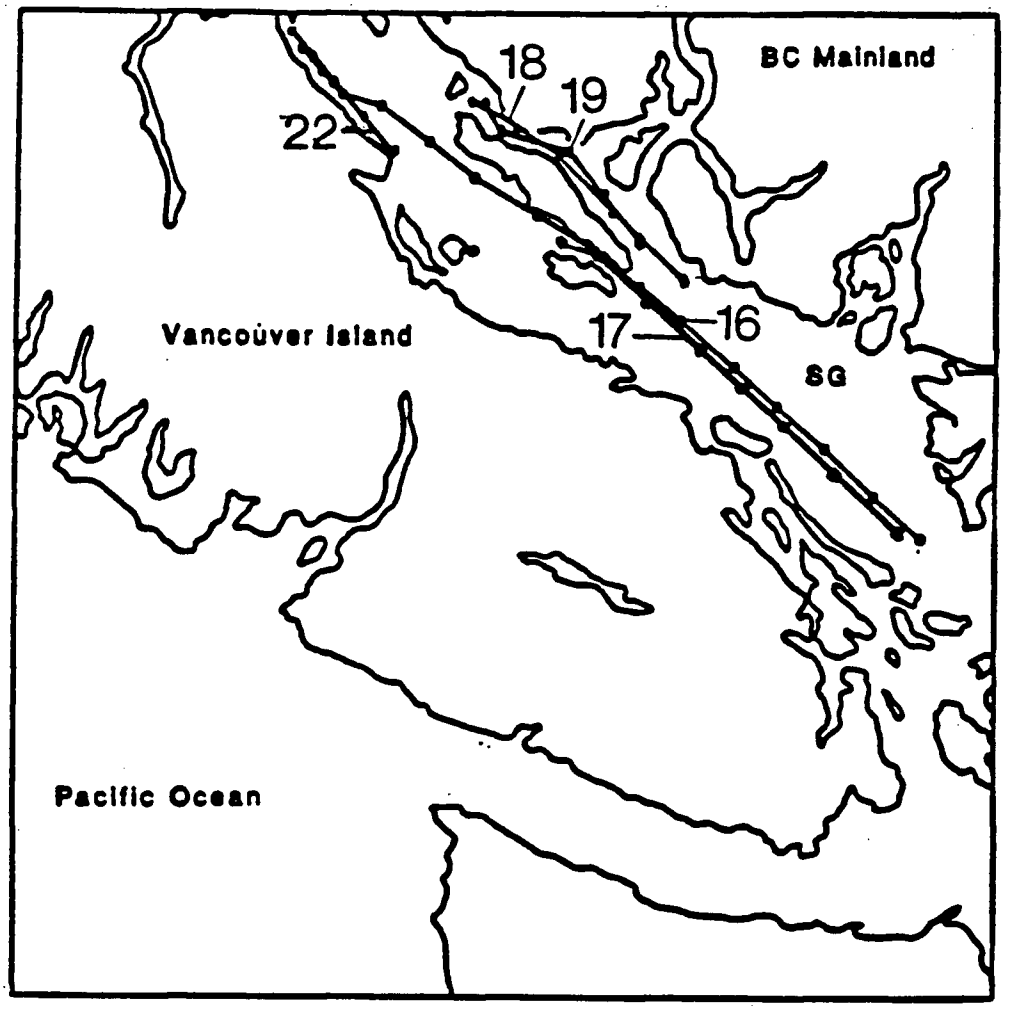

Figure 22 . Cruise tracks of the research vessels CSS Vector (section 16: 23–24 June 1986 and section 18: 27–28 Jun. 1985) and CSS Parizeau (sections 17, 19 and 22: 5–6 September 1986) Station locations are superimposed over their respective tracks. Section numbers are shown adjacent to their respective tracks.

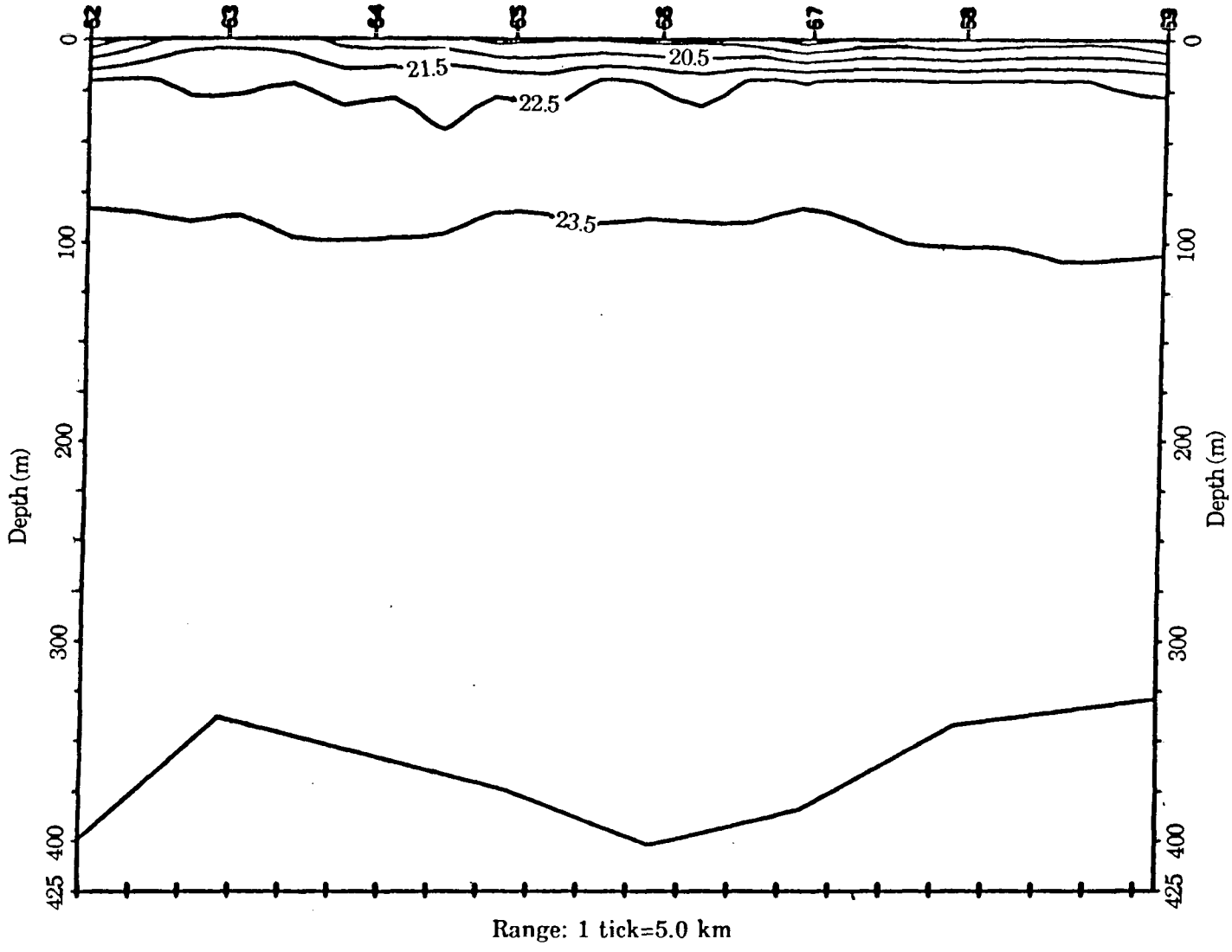

Figure 23. Vertical section of σ_t for section 16. Station locations (shown in Figure 5) extend axially in the SG and were occupied 23–24 June 1986. Contouring interval is 1.0 σ_t.

Channel, again contrasts section 16 and may also be compared to section 2, conducted approximately one year earlier. In Section 17, a warm brackish buoyancy layer, bounded by the 22.5 σ_t isopycnal near 25 m is present (Figure 24). Surface temperatures of $16 - 18^0$C are generally $2 - 3^0$C greater in September 1986 as compared to June 85, but surface salinities are 1.0–1.5 ppt less. In contrast to the early summer conditions (Section 16, Figure 23) of the same year, Section 17 shows a much warmer, much more saline and less buoyant surface layer. The southern SG is more strongly stratified, in terms of salinity and density structure, in early summer due to increased run-off from the Fraser River. Temperature stratification increases as increased solar heating, reduced cloud cover and weak wind-induced mixing combine to heat the surface layer as summer wears on. However, in temperate regions, density is much more strongly influenced by changes in salinity than changes in temperature. Thus the density stratification decreases, despite increased surface layer temperatures, due to the increased surface layer salinities.

Sections 18 and 19 (Figures 25 and 26), conducted during 27–28 June 1985 and 4 September 1986, clearly show the effects of variable fresh-water input and heating. In general, waters in Malaspina Strait are very similar in vertical structure to those in the central portion of the SG. However, residence times of brackish waters originating in Howe Sound and near the mouth of the Fraser River that are advected into Malaspina Strait are prolonged by generally weak, variable tidal currents and winds. Hence, the effects of surface heating and dilution are magnified in Malaspina Strait. In early summer, surface T and S ranged from 10–16.5°C and the surface buoyancy layer was bounded by the 22.5 σ_t isopycnal at 20 m.

Section 19 (Figure 26), conducted during 4 September 1986, shows a simi-

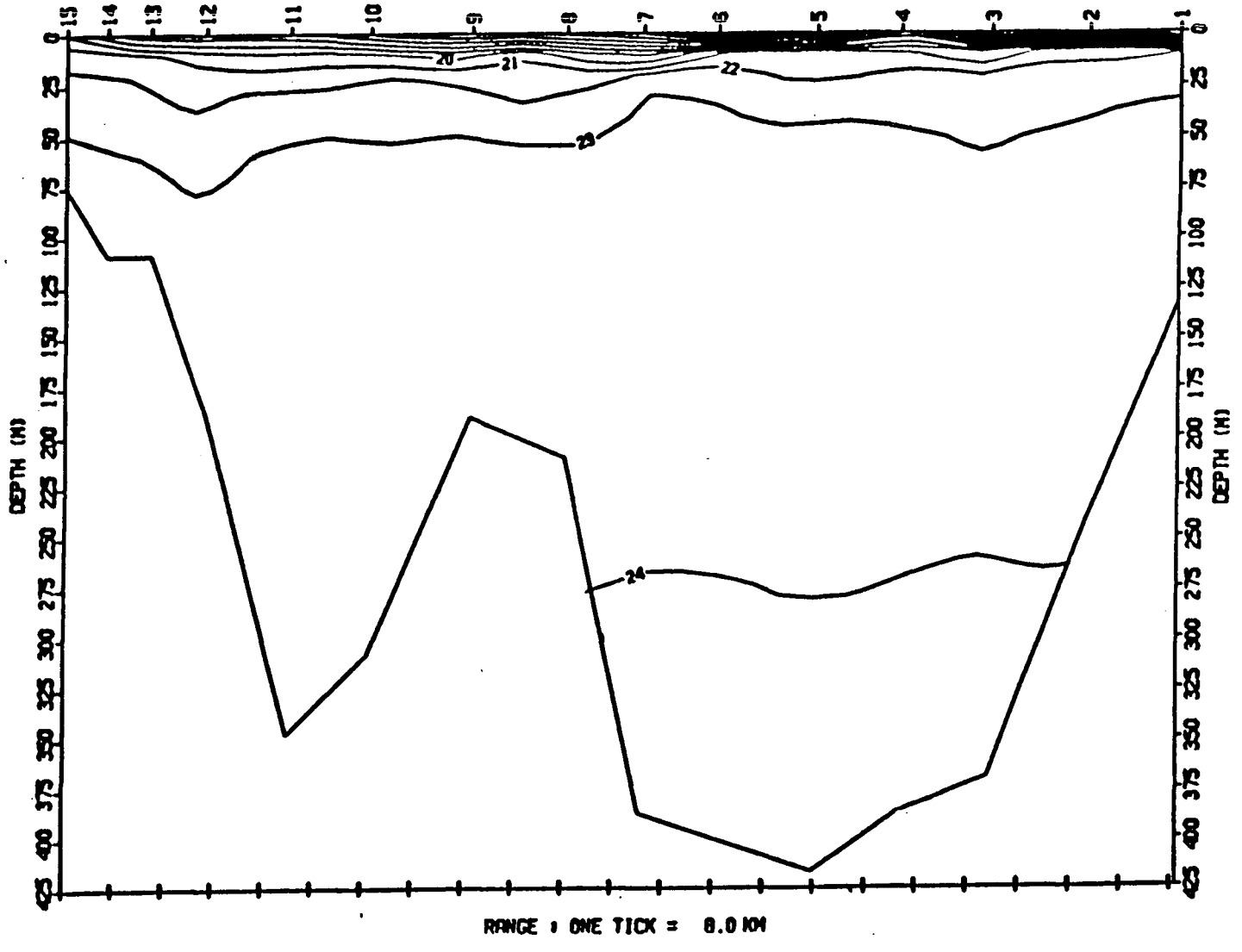

Figure 24. Vertical section of σ_t for section 17. Station locations (shown in Figure 5) extend north from central SG to DP and were occupied 4 September 1986. Contouring interval is 1.0 σ_t.

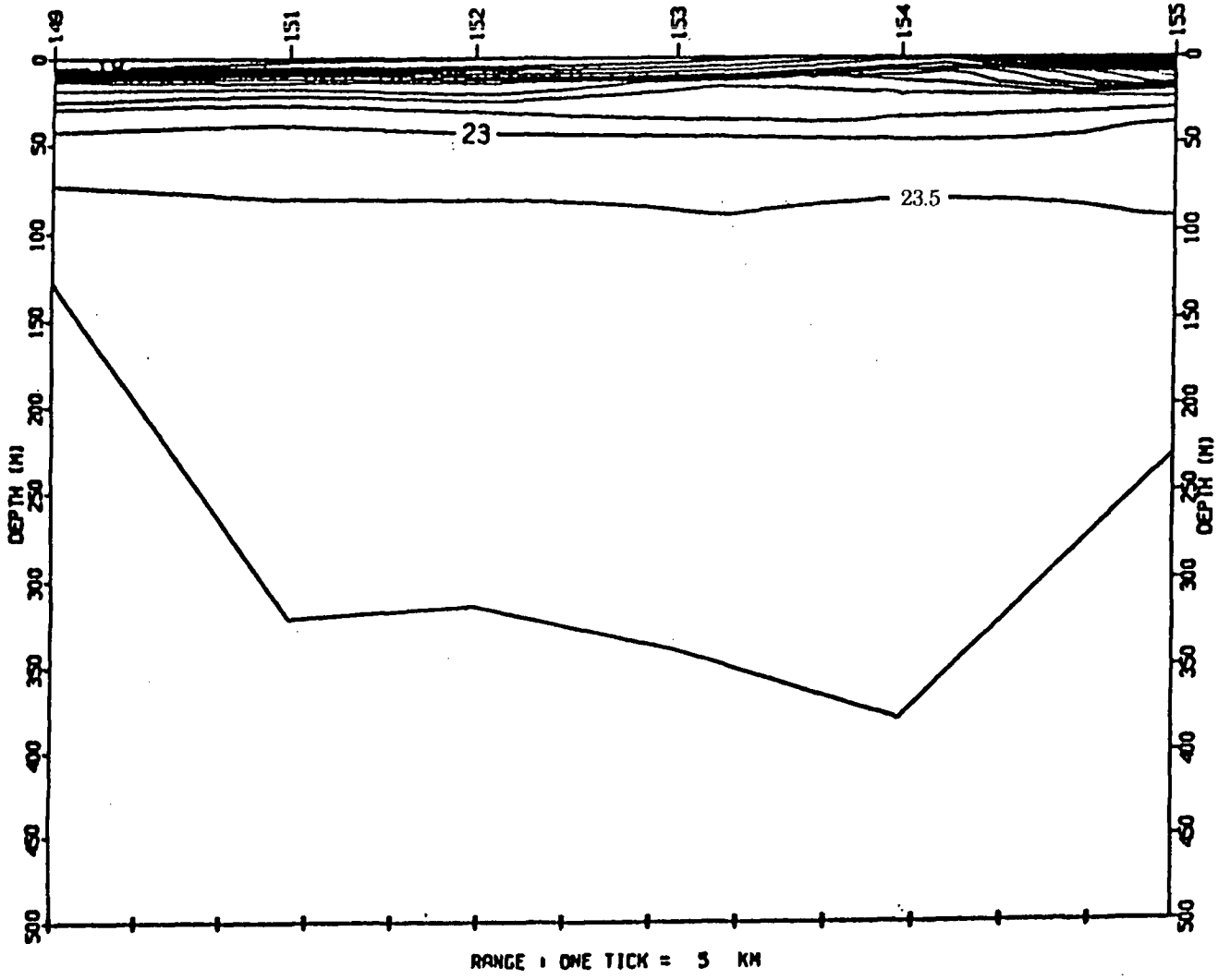

Figure 25. Vertical section of σ_t for section 18. Station locations (shown in Figure 5) extend north to south in Malaspina Strait and were occupied 27–28 June 1985. Contouring interval is 0.5 σ_t.

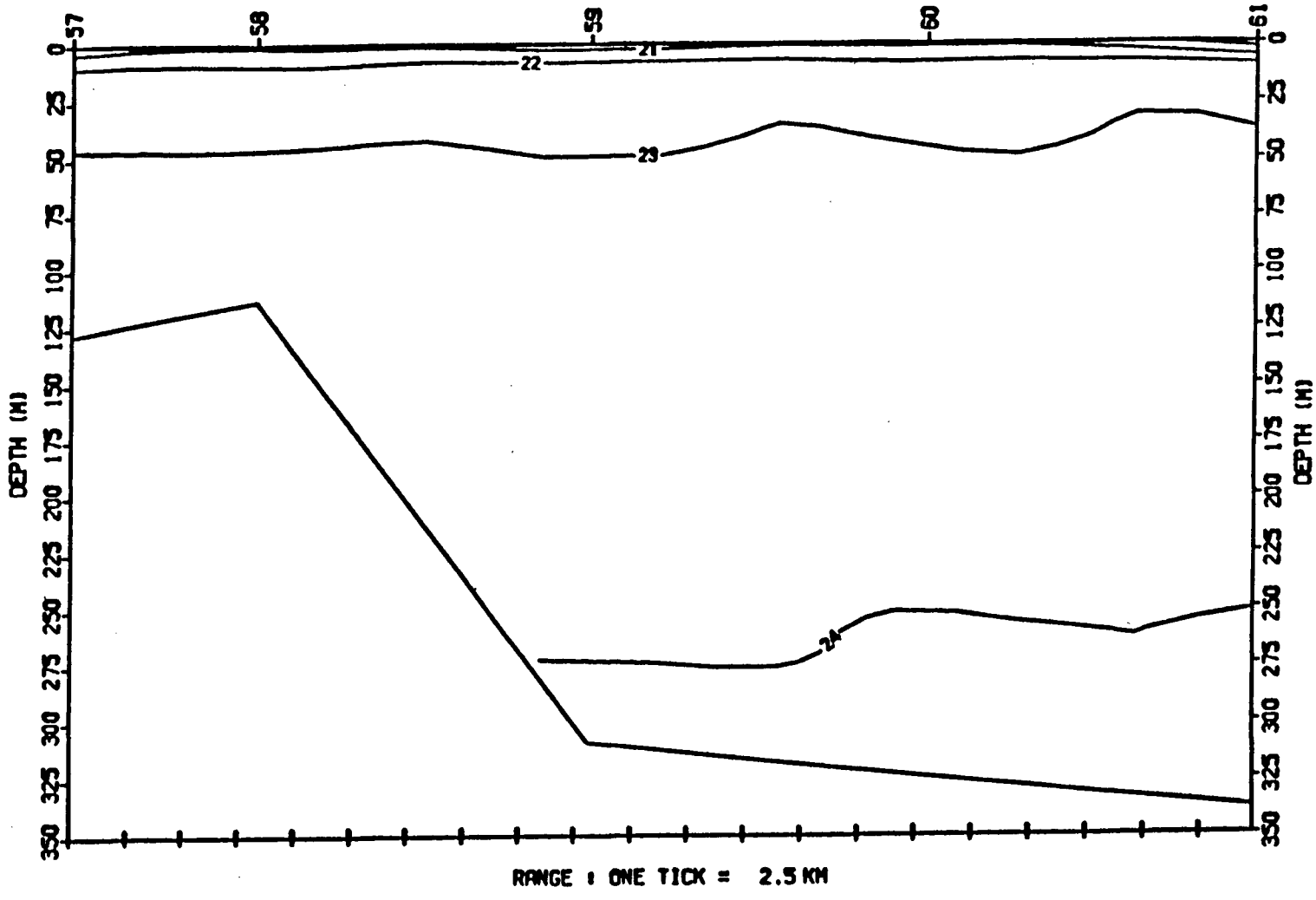

Figure 26. Vertical section of σ_t for section 19. Station locations (shown in Figure 5) extend north to south in Malaspina Strait and were occupied 5 September 1986. Contouring interval is 1.0 σ_t.

larily stratified water column to that of Figure 25. There is a strong buoyancy layer in both sections and a marked decrease in surfacce salinites. Surface layer temperatures and salinities of 10–15.5°C and 29–28 ppt bounded at 20 m by the 22.5 σ_t isopycnal were observed. There is no surface mixed layer. A general trend to warmer (16°C) and less saline (27 ppt) waters towards the southern entrance to Malaspina Strait is evidence in both sections of the presence of brackish waters originating in the central portions of the SG. The strength of the tidal signal near the southern entrance to Malaspina Strait may be examined by considering two CTD casts made at different times at the same location. Figure 27 shows surface layer T and S to be 12.8°C and 27 ppt respectively one hour into a strong ebb after a weak flood. Data from the same location but collected at the end of a relatively strong flood, shows surface layer T and S to be 16.8°C and 23 ppt.

Three sections were made along the axis of the tidal jet exiting DP in the vicinity of Cape Mudge in the northern SG. Sections 20 and 21 (Figures 28 and 29) were made during 27 June 1985 on the flood and ebb respectively; section 22 (Figure 30) was made during 4 September 1986 on the ebb tide (the location for this section is shown in Figure 22). The surface hybrid tidally mixed front is strongest on the flood with surface gradients of 12.5°C, 3.3 ppt and 1.5 σ_t units per 10 km (Figure 28).

Section 21 shows surface layer temperatures to increase southward from 10.0–16.4°C and surface layer salinities to decrease southward from 29.5–28.0 ppt. During flood tides, waters at the entrance to DP may be expected to be vertically homogeneous. Section 21, conducted on 27 June 1985 during an ebb tide, shows surface gradients of 1.4°C, 1.2 ppt and 0.5 σ_t units per 10 km (Figure 29) and surface T(S)

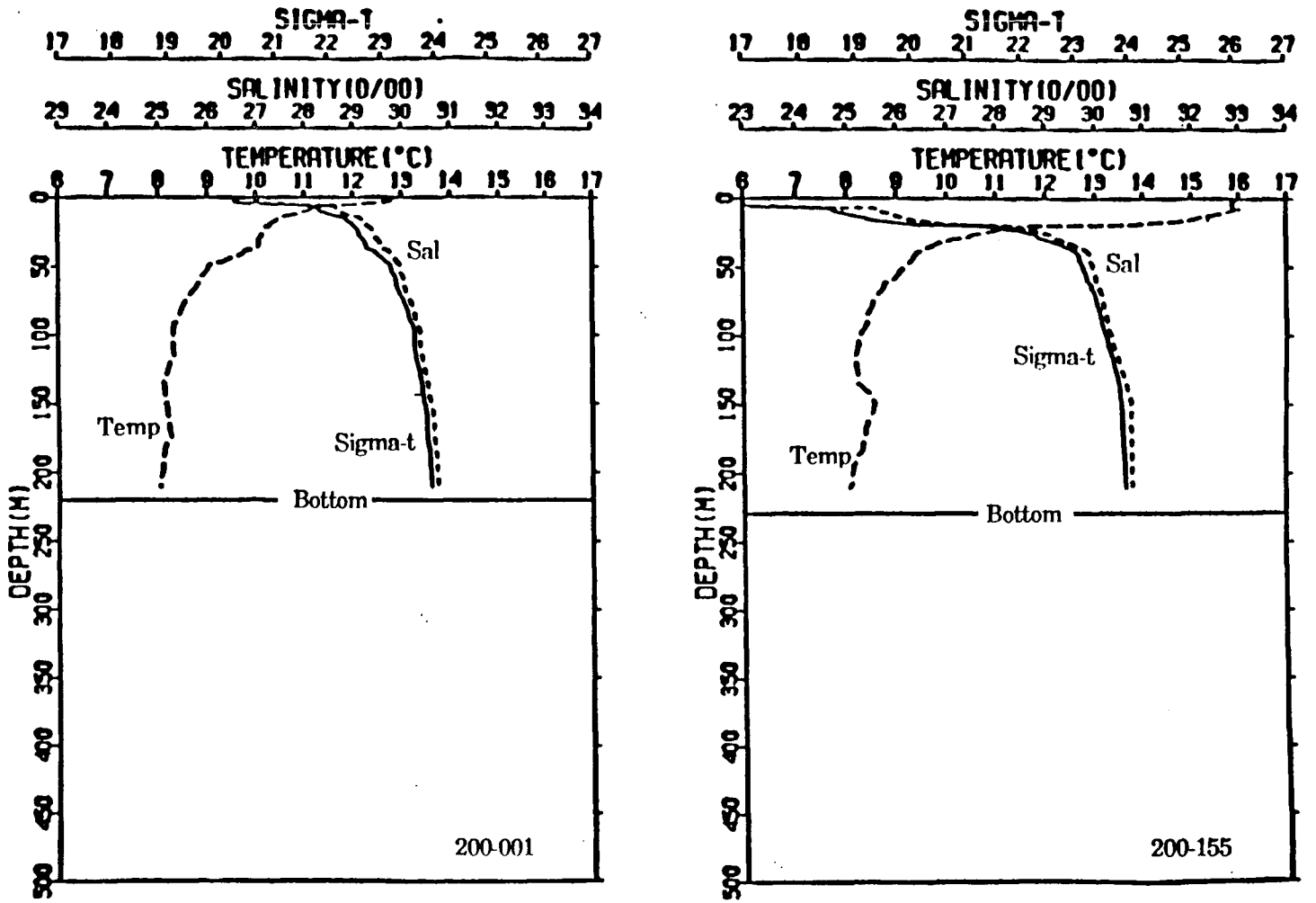

Figure 27. Vertical profiles of T, S and σ_t for CTD 200-001 and 200-155 taken in central SG (sections 1 and 18, Figures 2 and 5 respectively). Station positions are identical but were occupied during different phases of the tide.

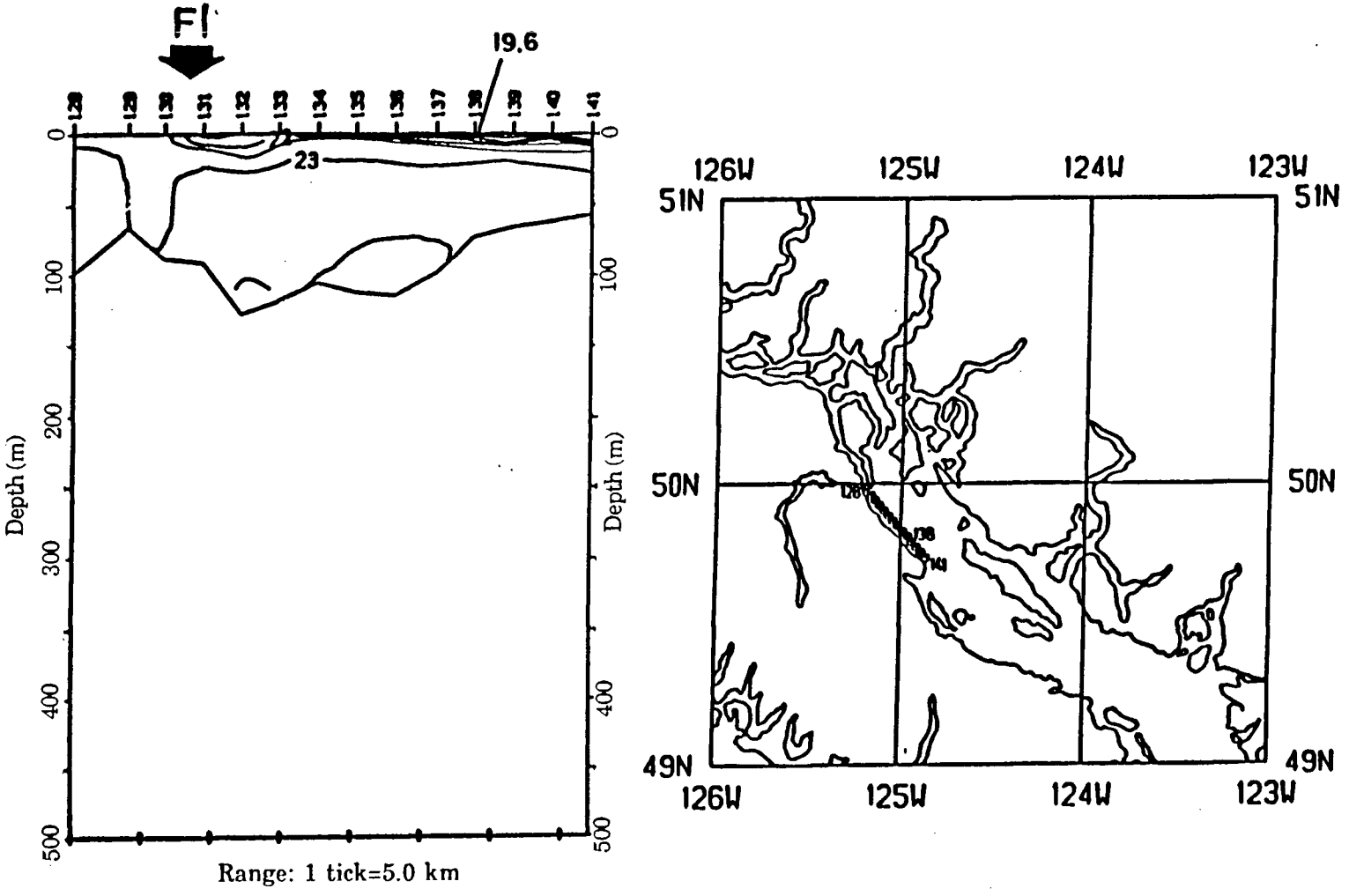

Figure 28. Vertical section of σ_t for section 20. Stations extend north to south from DP to Cape Lazo and were occupied 27 June 1985. Tides at Campbell River were flooding. Contouring interval is 0.5 σ_t.

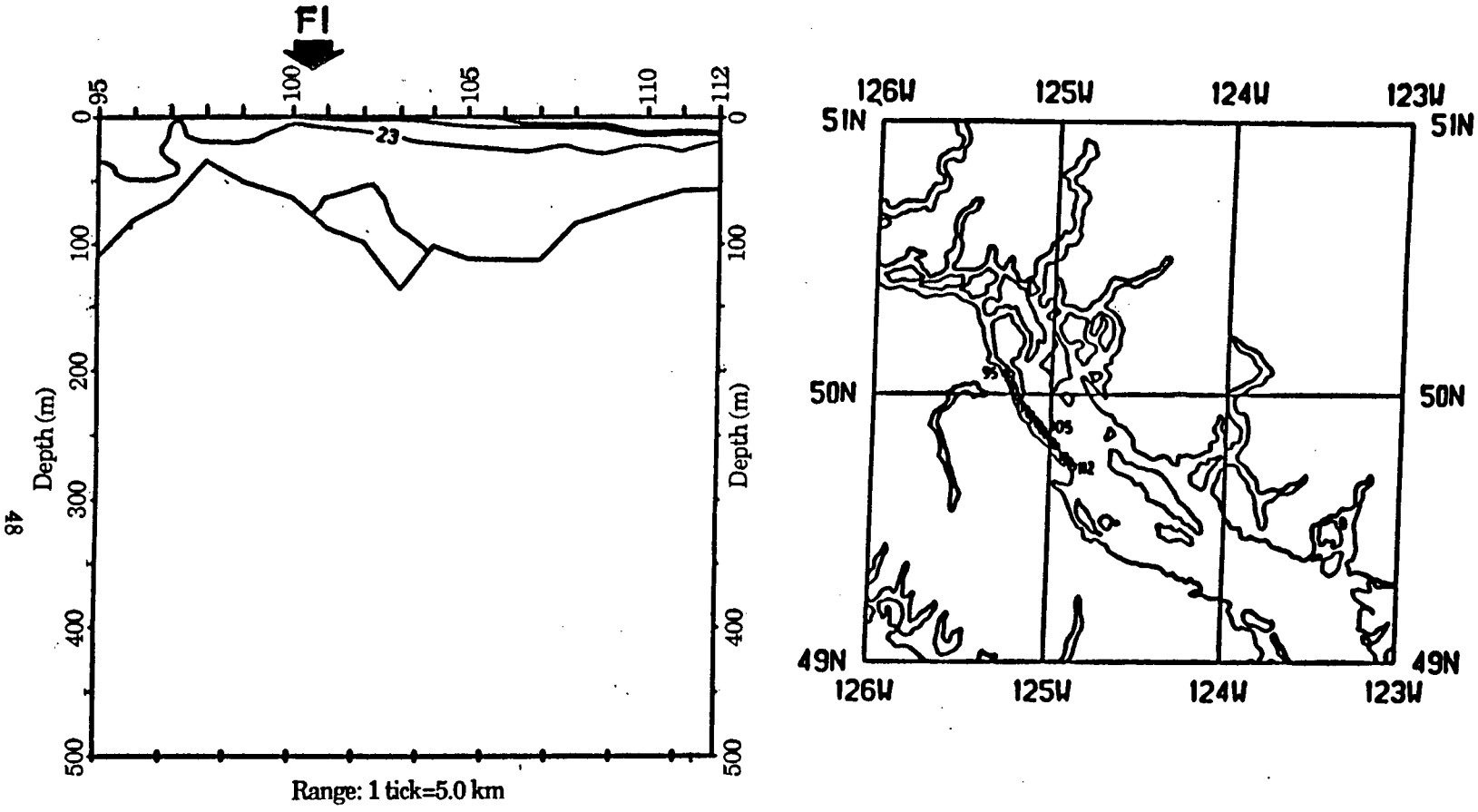

Figure 29. Vertical section of σ_t for section 21. Stations extend north to south from DP to Cape Lazo and were occupied 27 June 1985. Tides at Campbell River were ebbing. Contouring interval is 0.5 σ_t.

increase(decrease) southward from 10.0–12.5°C(29.5–28.0 ppt). Section 22, conducted on 4 September 1986 during an ebb tide shows a marked increase(decrease) in surface T(S) from $\leq$ 10.5°C($\geq$ 28.5 ppt) at the entrance to DP to $\geq$ 16°C($\leq$ 27 ppt) off Cape Lazo. Surface gradients are of the order 2.5°C, 1.0 ppt and 1.0 σ_t units per 10 km (Figure 30).

During ebb tides, the surface T and S gradients are significantly weaker as the buoyancy layer is pulled back into the SG and DP by the southward and northward retreating tides respectively (LeBlond, 1983). Hence, the ebb tides lead to a rarifaction of isopleths and, consequently, weaker horizontal gradients. Considering the 22.5 σ_t isopycnal to be the leading edge of the buoyancy layer, Figures 28 and 29 show the surface front to be 7 km closer to DP on the flood than on the ebb.

Section 23 (27 June 1985) from Cape Lazo to Cape Sutil is roughly perpendicular to the horizontal gradients in the northern SG. Thus, there are no apparent horizontal gradients (Figure 31).

Five across-channel sections were obtained to help specify the across-channel structure of the majority of the SG. Sections 24–28 (Figures 32–36) reveal the cross channel structure of the entire SG to be similar: there is a relatively shallow, strong buoyancy layer on the surface with no surface mixed layer and very sharp, coincidental thermo-, halo- and pycnoclines. The bottom boundary of this layer, taken as the depth of the 22 σ_t isopycnal increases southward from $\leq$ 15 m in the north and central SG to approximately 20 m in the south. In the extreme northern portion of the SG, section 24 (27 June 1985, Figure 32) shows the influence of the dense well-mixed water tidally pumped into the SG. Surface T(S) increases(decreases) eastward from 10.0–13.0°C(29.5–28.9 ppt). Figure 32 shows the subsurface isopycnals to slope

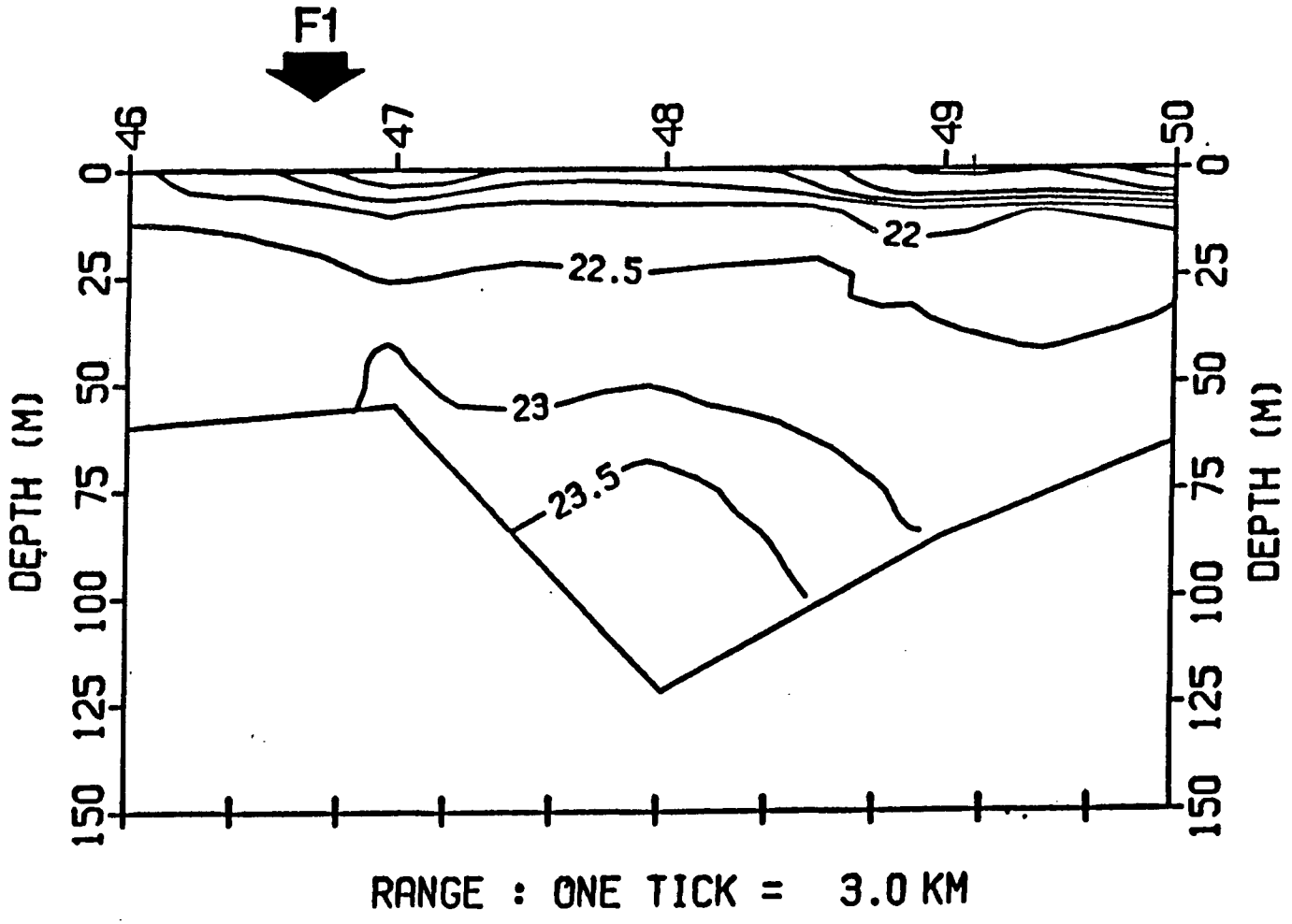

Figure 30. Vertical section of σ_t for section 22. Station locations (shown in Figure 5) extend north to south from Cape Mudge to Cape Lazo and were occupied 5 September 1986. Tides at Campbell River wer flooding. Contouring interval is 0.5 σ_t.

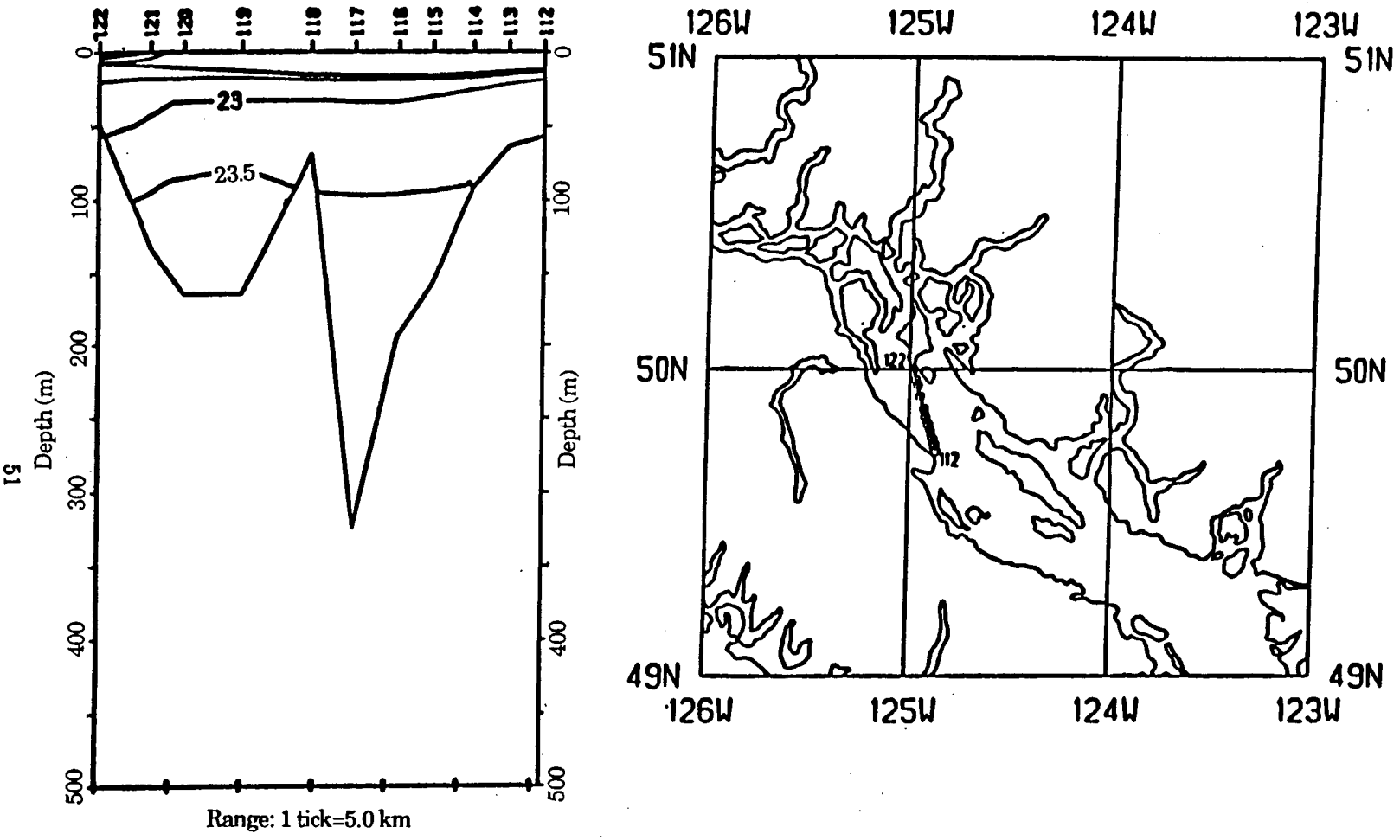

Figure 31. Vertical section of σ_t for section 23. Stations extend south to north from Cape Lazo to Cape Sutil and were occupied 27 June 1985. Contouring interval is 0.5 σ_t.

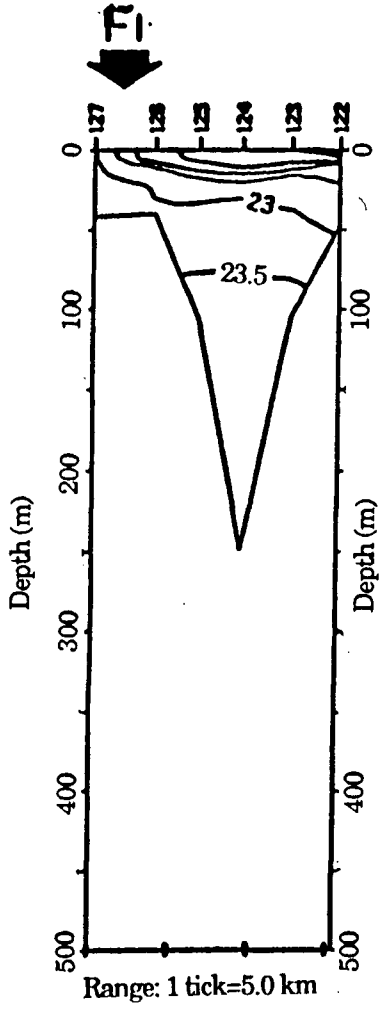

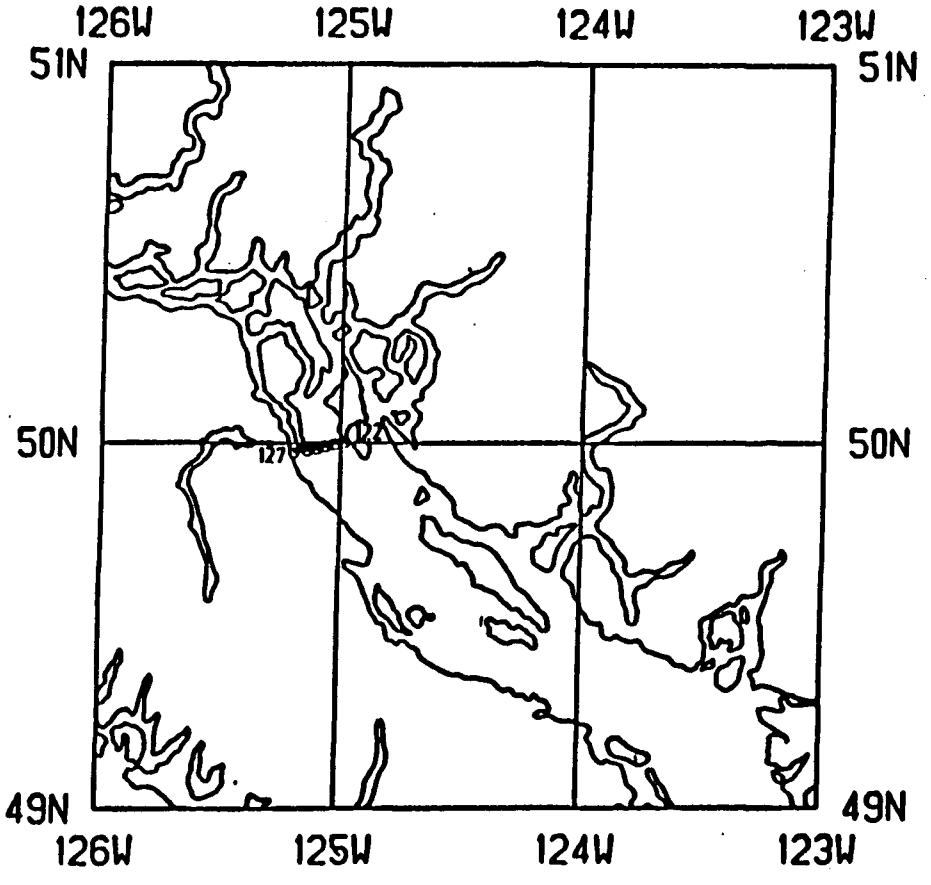

Figure 32. Vertical section of σ_t for section 24. Stations extend across-channel in northern SG and were occupied 27 June 1985. Contouring interval is 0.5 σ_t.

steeply down to the north signifying a strong residual flow out of the SG in the upper layer. Section 25 (4 September 1986, Figure 33) is very similar to section 24 made one year earlier during early summer. Surface temperatures increase and surface salinities decrease westward ($\leq$ 11.5 – 13.5°C and 28.5 – 27.5 ppt). Decreased across-channel subsurface isopycnal slopes are evidence of a weaker residual outflow in Figure 33 (September 1986) than in Figure 32 (June 1985).

In the central SG, Section 26 and 27 (27 June 1985, Figure 34, and 4 September 1986, Figure 35) are essentially the same. Temperature data from sections 26 and 27 (Thomson *et al.*, 1985; terHart, 1988) both show generally warm water in the western portion of the section. The presence of this water is likely due to the summer warming of the shallow waters contained in Comox Bay and on the banks off Cape Lazo and the subsequent tidal flushing of these waters into the SG. Temperatures decrease eastwards from approximately 17°C in the west to 14°C in the east. Surface salinities similarily increase eastwards from $\leq$ 27 ppt to $\geq$ 28 ppt. Section 26 (Figure 34) does show surface σ_t values to be $\leq$ 19.0) near the mainland. Again, this is due to run-off maxima in early summer. A surface estuarine front exists where the buoyancy layer formed in Malaspina Strait meets the surface waters of the SG proper (F9: Figure 34). The surface salinity gradient associated with this feature is 1.9 ppt per 10 km. There is a minimal surface temperature gradient. In Figure 34 there is an obvious sloping of the subsurface isopycnals down to the north indicative of a geostrophic flow out of the channel to the northwest. The downward northerly sloping isopycnals are not evident in Figure 35 (section 27). Once again, a decrease across-channel isopycnal slopes are likely caused by reduced run-off during late summer. Both sections, however, display a broadening of the

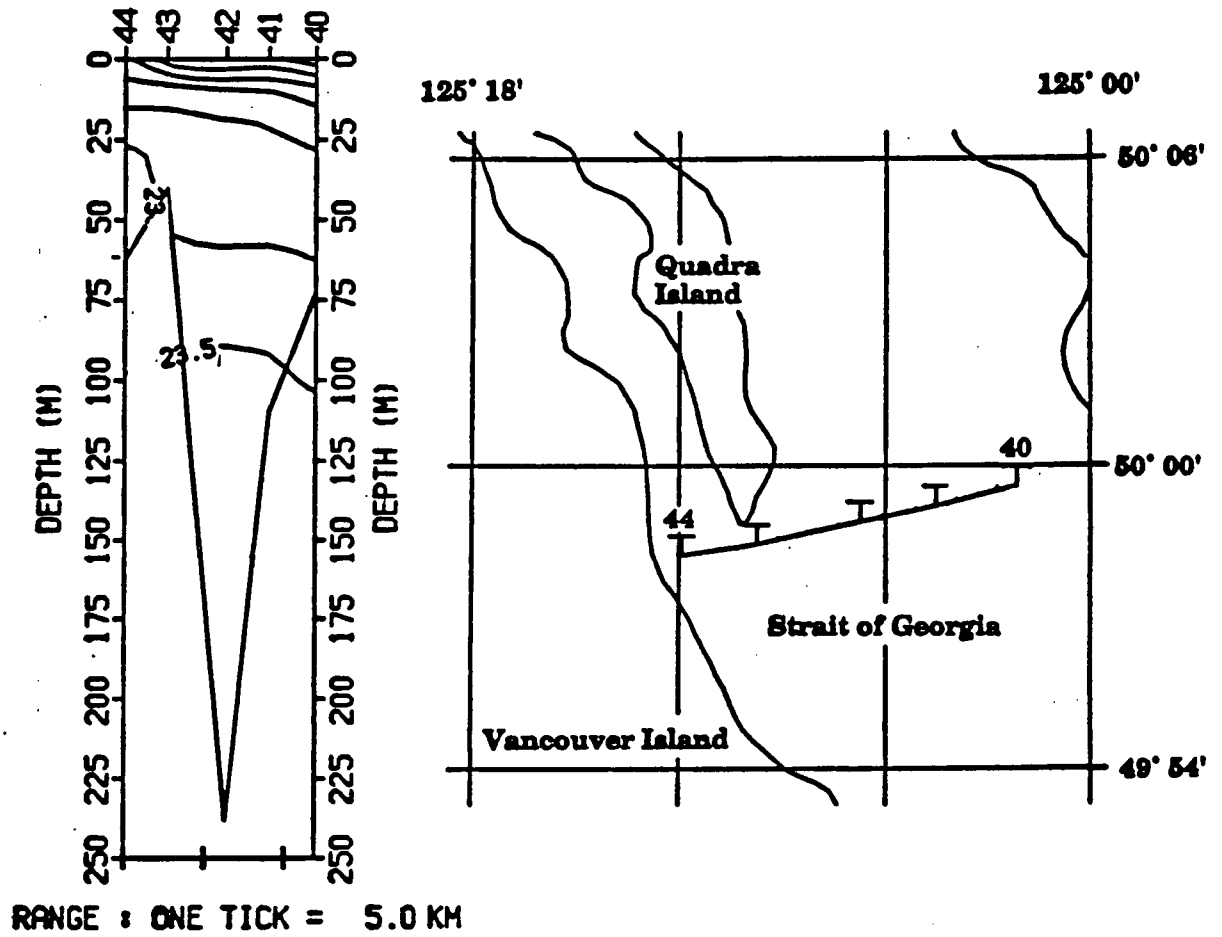

Figure 33 . Vertical section of σ_t for section 25. Stations extend across-channel in northern SG and were occupied 5 September 1986. Contouring interval is 0.5 σ_t.

9.0–10.0°C isotherm and 29.5–30.0 ppt isohaline on the western (Vancouver Island) side of the transect. This feature is the result of the southern subsurface movement of a cold, saline negatively buoyant created by tidal mixing in DP. Figure 34 shows the deep isopycnals sloping down to the west on the island side of the SG indicating a deep geostrophic flow into the SG. This feature is not observed in section 27.

Surface temperatures in the south (section 28) are approximately ≥ 15°C and fairly uniform across the Strait. Surface salinities, however, are directly affected by freshwater input from the Fraser River and they decrease from 20.5 ppt near the eastern shore to 25.5 ppt near the western shore. However, the depth of the buoyancy layer, bounded by the 22.5 σ_t isopycnal, is uniform across the channel (Figure 36) despite the significant across-channel variations in the upper layer itself.

The set of four 24-hour stations conducted in the vicinity of Cape Mudge Shoals (Figure 2) depicts the strength and horizontal variability of the tidal jet exiting Discovery Passage. Table 4 provides the details on this set of 24-hour stations.

Table 4
Details of the set of 24-hour stations that were conducted in the vicintity of Cape Mudge Shoals. The summarized data includes station location, the number of CTD casts, the spacing–in hours–between the casts and the CTD cast numbers. Note that the CTD cast numbers are not sequential.

Station location	No. of CTD's	CTD spacing	CTD cast no.'s
Discovery Passage (Station DP)	13	2 hr	100101–113
Willow Point (Station WPT)	25	1 hr	100201–225
Oyster Bay (Station OB)	13	2 hr	100301–313
Cape Mudge Shoals (Station CMS)	12	2 hr	100401–412

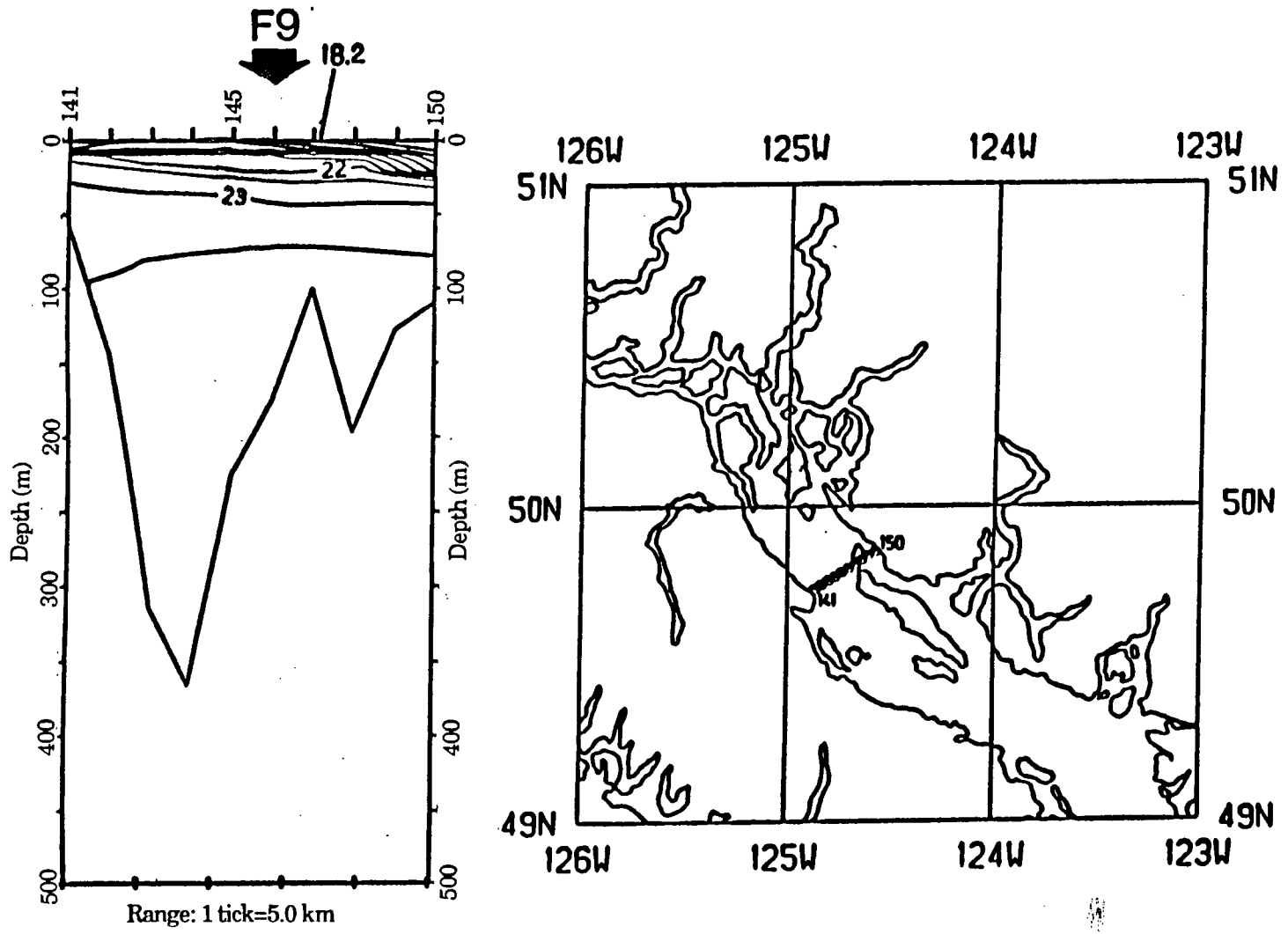

Figure 34. Vertical section of σ_t for section 26. Stations extend across-channel in central SG (Cape Lazo to Powell River) and were occupied 27 June 1985. Contouring interval is 0.5 σ_t.

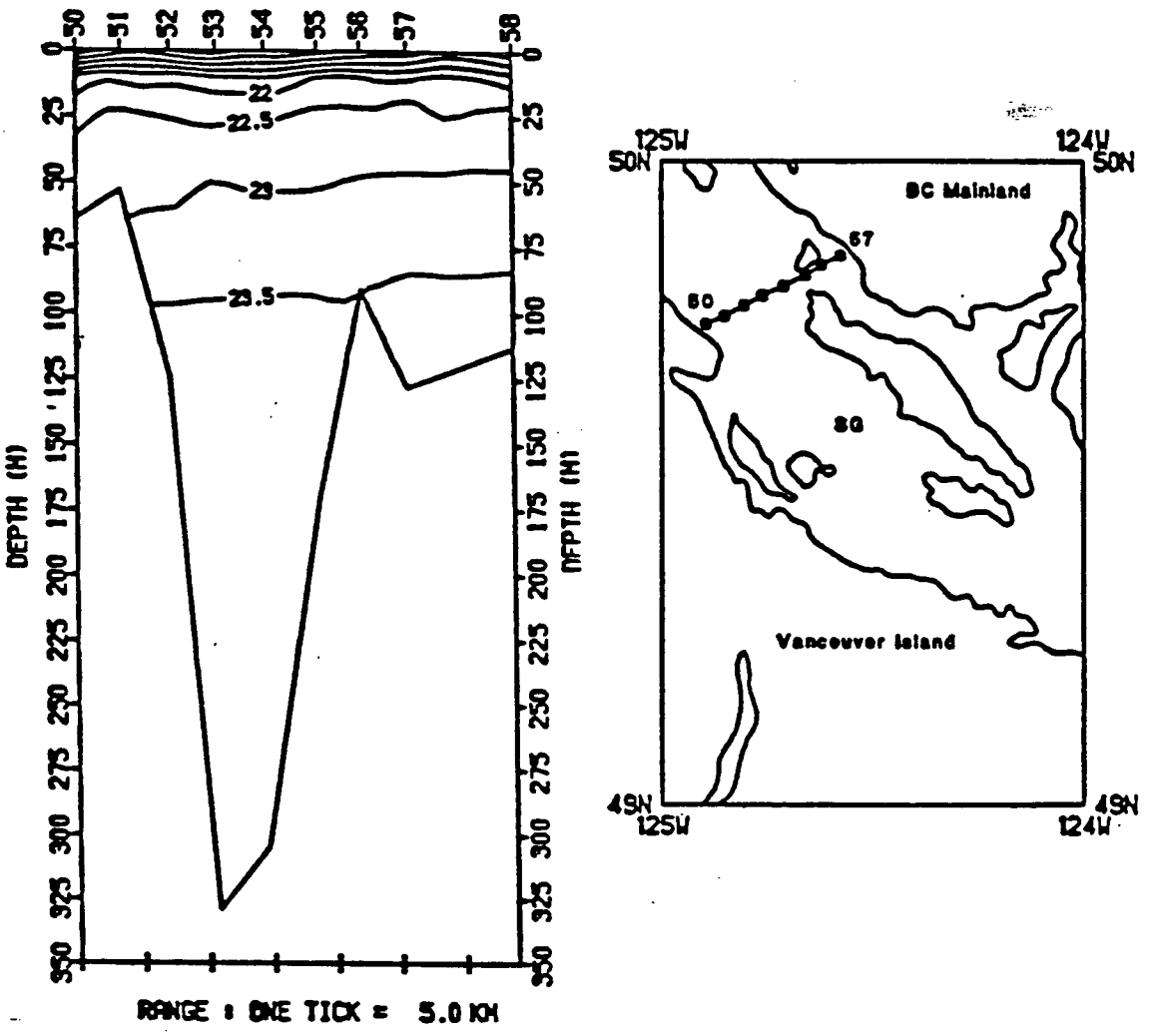

Figure 35 . Vertical section of σ_t for section 27. Stations extend across-channel in central SG (Cape Lazo to Powell River) and were occupied 5 September 1986. Contouring interval is 0.5 σ_t.

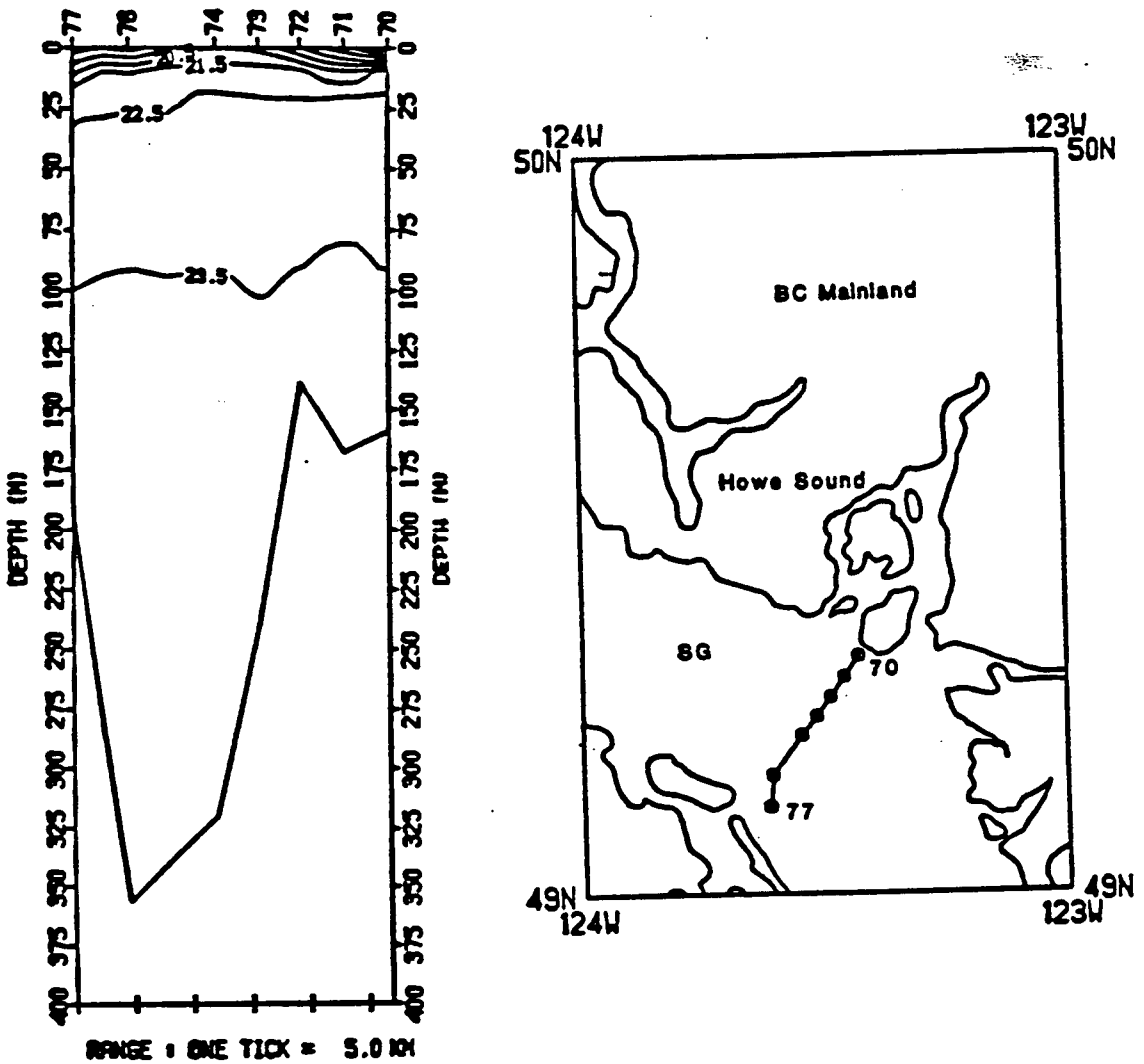

Figure 36 . Vertical section of σ_t for section 28. Stations extend east to west across-channel in southern SG and were occupied 5 September 1986. Contouring interval is 1.0 σ_t.

Station DP (Figure 37), occupied at the extreme southern entrance to DP clearly shows the vertically well-mixed waters produced by tidal flows through Seymour Narrows being pumped past the station location as the tide floods and ebbs (Figure 37). Of further interest is the presence of cold (8.5°C), saline (30 ppt), dense (23.5 σ_t) waters underlying a warm (13.5°C), brackish (25.5 ppt) buoyancy layer ($\leq$ 19.0 σ_t) between the periods when homogeneous water occupies the station site. These observations indicate a cold, saline negatively buoyant plume of water of intermediate density debouching into the SG on the flood tide. These dense waters flowing into the SG represent the formation of a density current that may play a significant role in the formation of intermediate and deep water in the northern SG (Waldichuck, 1957; Thomson, 1981; LeBlond, 1983). These same features were in data collected during the same 24-hour period at Station WPT (CTD 100201–225), just offshore of Willow Point and further south, at Station OB (CTD 100301–313). The negatively buoyant plume is obvious, but becomes slightly warmer (9°C as opposed to 8.5°C) and less saline (29.5 ppt as opposed to 30.0 ppt) due to entrainment of upper layer fluid and mixing. It is interesting to note that the appearance of the most dense bottom water occurs when surface stratification is strongest (Figure 37).

It appears, then, that there was a tidally modulated inflow of this negatively buoyant plume over this one tidal period and that the greatest propagation speed of the gravity current thus formed (Benjamin, 1968) will occursduring the minimum in tidal flow. Geyer and Cannon (1982) report a similar result for a gravity current in Puget Sound where "the nature of tidal forcing is curious in that the low frequency circulation is maximized during minimum tidal flow.". These conclusions were at least partially substantiated by conductivity-temperature-depth-velocity (CTDV)

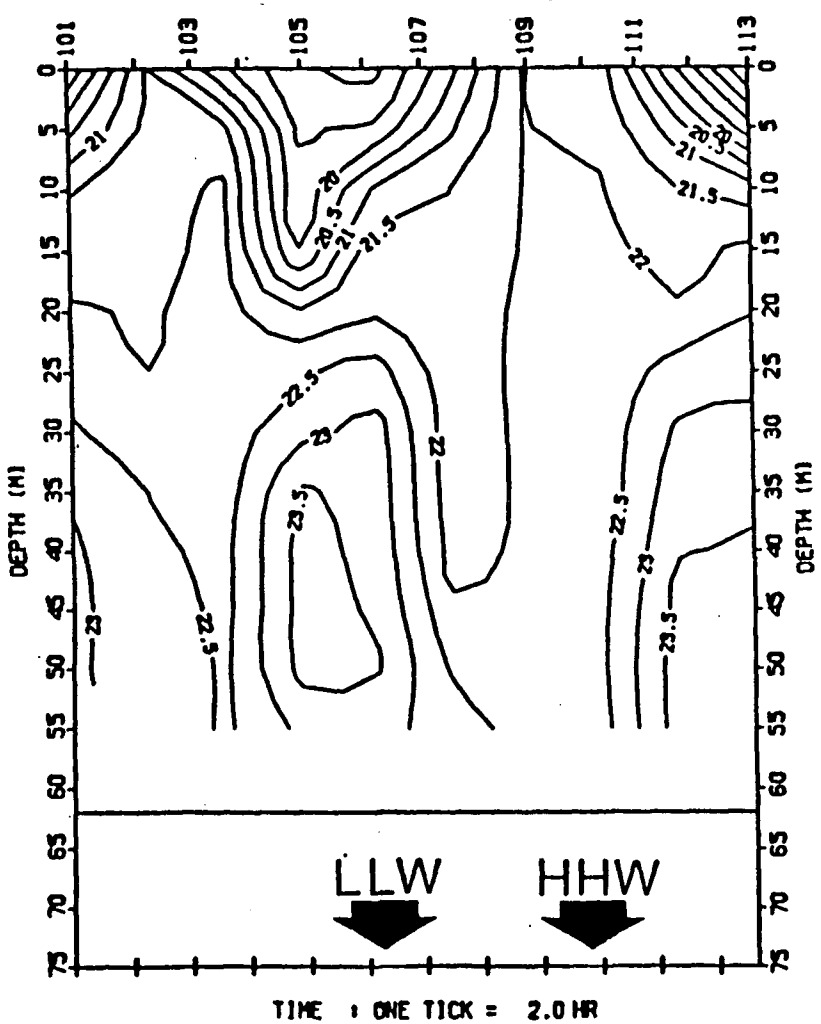

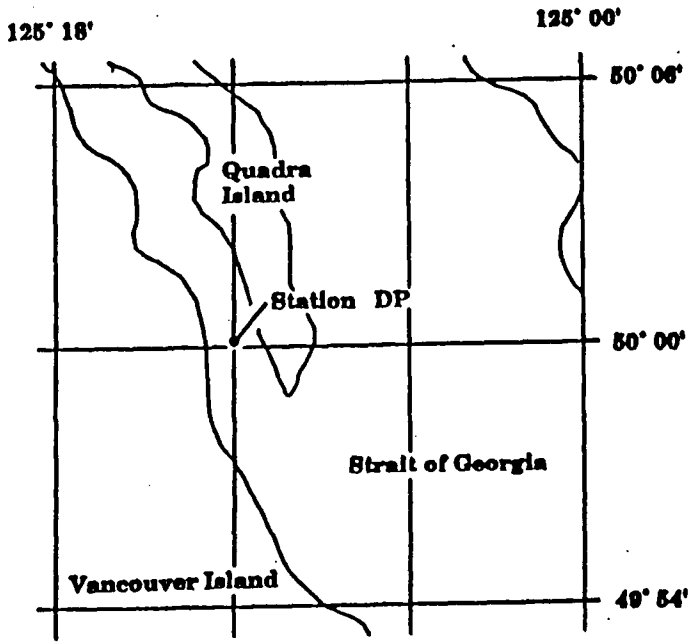

Figure 37. Time-depth contour plot of σ_t for Station DP located at the southern entrance to DP. This station was sampled recursively over the 24 hour period 24–25 June 1986. Contouring interval is 0.5 σ_t. Times of higher high water (HHW) and lower low water (LLW) are shown from which the general duration of the flood and ebb tides may be inferred.

data collected during 26 Nov 1986. Ebb/flood current velocities (directed parallel to the Vancouver Island shore) were obtained from several CTDV casts stationed axially in the jet. The flood currents were clearly not uniform in direction with depth and generally showed an inflow at depth during all phases of the tide. These (unpublished) data at least qualitatively support the existence of a density current emanating from DP. Observations at Station CMS (CTD 100401–412) off Cape Mudge Shoals, are in marked contrast to those for Stations DP, WPT and OP. There is an advance and retreat of the dense bottom waters, but relatively little tidal movement in the upper layer with the exception of the period during the $12 - 15^{th}$ hours corresponding to the change from lower-low water to higher-high water. The negatively buoyant plume is found below 20 m at all four stations.

1.4: T-S Characteristics

Constructing T-S diagrams has proven to be an invaluable aid in identifying source water masses and mixing ratios (Neumann and Pierson, 1966; Tolmazin, 1985). Although variability in the upper layers of the ocean due to direct atmospheric forcing makes identification of a surface layer water mass difficult, T-S curves for all CTD data obtained enabled an envelope of possible surface layer T-S curves to be determined. A reasonable average from within these envelopes was selected and considered as the surface water mass for SG surface (SG_{sfc}), JS surface (JS_{sfc}) and QCST surface ($QCST_{sfc}$) waters.

The T-S curves clearly show the two layer structure of the entire inside passage. Salient features of the physical oceanography are also easily identified. Surface

water becomes progressively colder and more saline seaward; deep lower layer waters become warmer and less saline as they progress up-channel. In addition, the penetration at depth of oceanic waters into the SG is evidence of the major impact continental shelf processes can have on the general estuarine circulation and the ventilation of deep waters throughout the study area (Pickard, 1975; Geyer and Cannon, 1982; Farmer and Freeland, 1983). Differences in the T-S characteristics and two layer structure between the two years were negligible (Figure 38).

Mixing ratios were estimated for the waters of DP, JS and QCST. These estimates are shown in Table 5 as well as T-S characteristics of the source water masses for each area. Mixing ratio estimates were calculated by solving three simultaneous algebraic equations given as:

$$1 = \gamma_1 + \gamma_2 + \gamma_3$$

$$T_\eta = \gamma_1 T_1 + \gamma_2 T_2 + \gamma_3 T_3$$

$$S_\eta = \gamma_1 S_1 + \gamma_2 S_2 + \gamma_3 S_3$$

where T_η and S_η represent the T-S characteristics of a particular water mass, and $\gamma_{1,2,3}$, $T_{1,2,3}$ and $S_{1,2,3}$ represent, respectively, the mixing ratios and T-S characteristics associated with the three source water masses. Errors in $\gamma_{1,2,3}$ are approximately $\pm 10\%$ and arise due to ambiguities in the choices of T and S for specific water masses.

1.5: Rotational Effects

Sloping subsurface isopycnals were a feature of many of the across -channel sections made in both years (Figures 12 and 13, 17–21 and 32-36). When this

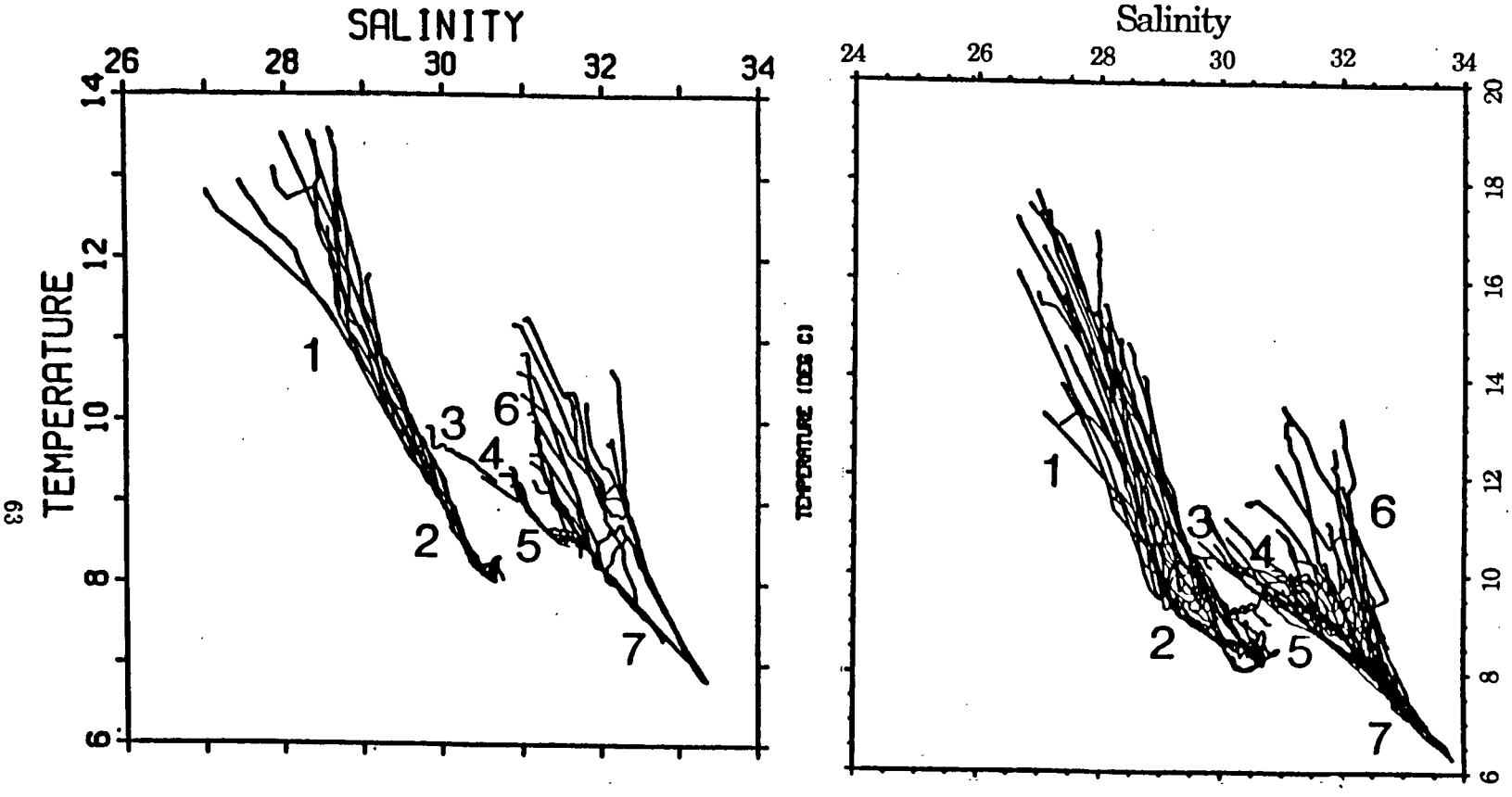

Figure 38. Composite TS curves for the entire study area for both 1985 and 1986. Water masses ($1 = SG_{sfc}$, $2 = SG_{dp}$, $3 = DP$, $4 = JS_{sfc}$, $5 = JS_{dp}$, $6 = QCST_{sfc}$ and $7 = QCST_{dp}$) are shown adjacent to their characteristic TS curves.

Table 5
Parameters and results of the T-S analysis made in §1.5. Summary includes the water mass, source water masses (subscripts 'sfc' and 'dp' refer to surface and deep layers respectively), T-S properties of the source water masses and the derived mixing co-efficients. Mixing co-efficients are approximately ±10%.

Year	Water Mass °C/ppt	Source Water Masses	T-S properties °C/ppt	Mixing ratios %
1985	DP	SG_{sfc}	10.5/29.2	56
	9.8/29.8	SG_{dp}	8.6/30.2	23
		JS_{sfc}	9.0/31.0	21
	JS_{sfc}	DP	9.8/29.8	41
	9.0/31.0	$QCST_{sfc}$	8.8/31.55	49
		$QCST_{dp}$	7.0/33.1	10
1986	DP	SG_{sfc}	11.5/29.0	62
	10.4/29.6	SG_{dp}	8.5/30.5	34
		JS_{sfc}	9.4/31.4	4
	JS_{sfc}	DP	10.4/29.6	42
	9.4/31.4	$QCST_{sfc}$	10.7/32.1	22
		$QCST_{dp}$	7.4/33.1	36

phenomenon is present in space-varying (along-channel) two-dimensional data, such as that presented here, it indicates the presence of three-dimensional processes. Oceanic length and time scales associated with the residual circulation of the inside passage imply that the three-dimensional characteristics of this circulation may be partly associated with rotation. However, in narrow channels, three-dimensional effects may arise due to channel curvature, lateral friction, turbulence, topography or time-dependent effects (Young and Hay, 1987). For the implied motions to be considered geostrophic, the fluid must be assumed to be invisced, time invariant and hydrostatic.

The importance of rotation can be demonstrated by comparing the channel width with the internal Rossby radius of deformation associated with the baroclinic

modes of motion. Given the two layer structure of QCSD, QCST and the SG, the internal Rossby radius, r_2, for a two-layer system is (LeBlond and Mysak, 1978):

$$r_2 = \left(\frac{g\prime}{f^2} \cdot \frac{H_1 H_2}{H_1 + H_2} \right)^{1/2} \qquad (1.1)$$

where $g\prime$, the reduced gravity is:

$$g\prime = g \frac{(\rho_2 - \rho_1)}{\rho_2}. \qquad (1.2)$$

The subscripts 1 and 2 refer to the upper and lower layers respectively, H to the layer depth and ρ to the layer density. Table 6 shows the calculated r_2 for all across-channel sections. In all cases, the local channel width is greater than the local r_2 and rotational effects may be considered of some importance. However, it is dangerous to conclude that the implied motions are strictly geostrophic! Nonetheless, when rotation can be considered important, simple geostrophic calculations can give some, albeit limited, insight into the implied motions.

Geostrophic shear in a two layer model is calculated as:

$$V = \frac{g\prime}{f} \cdot \frac{\partial H_1}{\partial y} \qquad (1.3)$$

where $\partial H_1 / \partial y$ is the across-channel slope of the interfacial isopycnal and the lower layer is considered at rest. Thus, (1.3) gives an estimate of the residual flow in the surface layer if the assumption that lower layer velocities are negligible is reasonable. Table 6 shows the calculated upper layer velocities, V, for across-channel sections with identifiable sloping interfacial isopycnals.

Direct current measurements made within the study area are in reasonable agreement with estimates of V from (1.3). A mooring in the vicinity of section 11 (Figure 17) gave mean currents at 15 m of 13 cm/s seaward (Thomson, 1976),

Table 6
Geostrophic shear calculations using a two layer model. Channel width (km), internal Rossby radius of deformation, r_2 (km), interfacial isopycnal (σ_t) and geostrophic shear ($cm \cdot s^{-1}$) are shown. Only those sections where subsurface isopycnals were obviously sloping across-channel were considered.

Section	Channel Width	r_2	Interfacial isopycnal	V ($cm \cdot s^{-1}$)
6	27.5†	5.7	24.5	18.7
7	16.0‡	5.0	25.5	-18.5
11	17.0	4.2	24.5	12.6
12	17.0	5.5/8.4	24.5/25.5	14.2/-18.7
13	23.0	4.3	24.5	9.8
14	15.0	2.8	24.5	7.2
15	16.0	3.6	24.6	10.5
24	16.0	4.5	23.0	40.0
25	16.0	4.4	22.5	16.1
26	25.0	13.4	22.5	13.4

† This distance represents the length of the section itself as the channel width of QCSD is in the order of hundreds of kms.

‡ The width of the channel in this instance is given by the distance separating the 60 m isobaths.

compared to 12.6 cm/s as per Table 6. Data from section 26 (Figure 34) yielded surface currents of 13.4 cm/s compared to 10 cm/s obtained from drift bottles (Waldichuck, 1957).

It should be noted that the net volume transport is very difficult to quantify as it is subject to large errors (Thomson, 1977; Godin *et al.*, 1981). The upper and lower layer volume transports are neary equal and of opposite sign (LeBlond, 1983). Thus, the net volume transport is small and of the order of the errors associated with the measurements. Furthermore, the residual circulation is sensitive to meteorological conditions and shelf processes thereby introducing errors into residual transport measurements (Frisch *et al.*, 1981; Godin *et al.*, 1981). Calculations of geostrophic shear from single across-channel sections are, therefore, not expected

to portray completely the residual circulation.

1.6: Summary

Data collected during the cruises of the research vessels CSS Vector (26–29 August 1985, 29 May 1986 and 23–25 June 1986) and Parizeau (3 September 1986) were used to compile a general hydrography of the waters lying between Vancouver Island and BC's mainland coast. This hydrography was in turn used in an analysis of the return migration routes of adult homing sockeye salmon (*Oncorhynchus nerka*) through these waters.

Positive estuarine circulation dominates the physical oceanography of this region. Warm, relatively fresh water moves seaward on the surface and cold, saline water intrudes at depth. This circulation was observed to be stronger in spring and early summer, when fresh water input into the system was greater, than in later summer. The four oceanographic regimes identified in Thomson *et al.* (1985) and terHart (1988) remained distinct: the slightly stratified central and northern portions of the SG resulting from a buoyancy layer composed of fresh water run-off principally from the Fraser River, and to a much lesser extent from mainland inlets; the vertically well-mixed waters of DP due to vigorous tidal agitation; the weakly stratified waters of JS; and the less weakly stratified waters of QCST caused by the presence of JS water on the surface and the intrusion of cold, saline Pacific Ocean water at depth. These four regimes are separated by tidally mixed fronts created by vigorous mixing of the entire water column by rapid tidal streams in the shallow and constricted regions of Seymour Narrows, Blackney Pass and Weynton

Passage. Similar fronts were found east and west of Nahwitti Bar. A surface front separating the well mixed water of eastern JS from the weakly stratified water of western JS was observed near Kelsey Bay. A surface estuarine front was observed in northern QCST where the buoyancy layer exiting QCST meets the upwelling enhanced oceanic waters of QCSD. A similar estuarine front was found in the SG where the buoyancy layer formed in Malaspina Strait and enhanced by restricted lateral spreading debouches into the SG. A set of three 24-hour stations in the vicinity of Weynton Passage and a set of four 24-hour stations in the vicinity of Cape Mudge show the strength and tidal variability of the flows and mixing processes over a diurnal tidal cycle. Dense water masses formed in these regions are seen to exude into western JS and northern SG respectively during all phases of the tide. These processes may play an important role in the formation and renewal of intermediate and deep water in both basins. The most dense waters were present during minimal tidal flows and the resultant density currents are expected to be strongest during these periods. T-S diagrams clearly show the two layer structure of the entire inside passage as well as the relative variability in the upper and lower layers. The upper layer is clearly seen to become more saline seaward; similarily, bottom waters become progressively fresher as they progress up-channel. Calculated mixing ratios give rough estimates of the proportions of SG surface and deep water present in JS.

CHAPTER 2

ULTRASONIC TRACKING: HORIZONTAL AND VERTICAL DISTRIBUTIONS

2.1: Introduction

The return migration of Pacific salmon (*Oncorhynchus spp.*) is a complex, fascinating and much debated phenomenon. The return migration of adult sockeye salmon, which may traverse distances as great as 6000 km (French *et al.*, 1976) and ends with remarkable spatial and temporal precision (Royce *et al.*, 1968) in the salmon's natal stream, is a classic example of animal migration. Quite apart from the academic interest associated with this migration, the returning adult sockeye have a tremendous worth as a commercial fishery. Knowing the sockeye's return migration mechanism and understanding its choice of routes is clearly of great value to both the scientific commmunity and the commercial fishery.

The return migration itself may be thought of in three phases: oceanic, coastal or estuarine and riverine. Oceanic migration mechanisms are, as yet, undetermined. Riverine migratory behaviour is generally considered to be directed by olfactory information learned years earlier in freshwater (Johnson and Hasler, 1980; Hasler and Scholz, 1983). The mechanisms responsible for the estuarine phase of the return migration must necessarily be a combination of both the oceanic and riverine mechanisms as estuarine environments represent the interface between oceanic and riverine environments. A persistent, unavoidable large scale change in the sockeye's immediate environment during the return migration must require a similar scale change in guidance mechanisms. Moreover, the returning sockeye begin to undergo

profound changes in morphology, physiology and behaviour that prepare them to enter freshwater and spawn. Given the changing oceanographic conditions and the changing condition of the animal itself, it is not surprising that the coastal phase of the return migration is poorly understood. To further complicate issues, how migrating salmon integrate diverse orientation cues, such as celestial (Groot, 1965; Brannon, 1972) and magnetic (Quinn, 1980; Quinn and Brannon, 1982) is not known. Nonetheless, as migratory cues abound in the salmon's immediate hydrographic environment (Tully *et al.*, 1960; Royal and Tully, 1961; Favorite, 1961; Royce *et al.*, 1968; Leggett, 1977; Mysak *et al.*, 1982; Quinn, 1982; Groot and Quinn, 1986), it is only natural to consider the horizontal and vertical movements during migration to the hydrography.

To this end, oceanic temperatures (Mysak *et al.*, 1982, IPFSC, 1984; Hamilton, 1984; Burgner, 1980; Blackbourn, 1987; Groot and Quinn, 1987) and Fraser River run-off (Favorite, 1961; Wickett, 1977) have been positively correlated with sockeye return migration routes and timings. These correlations, in part, motivated MOIST.

To study the factors guiding migrations in coastal waters, ultra-sonically tagged sockeye were tracked with a directional hydrophone while the physical oceanographic hydrography was specified by recording vertical T and S profiles. Currents, which may significantly affect the fish's horizontal and vertical distribution (Brett, 1983; Arnold and Cook, 1984; Dodson and Dohse, 1984), were measured along the telemetred track by a Lagrangian drifter. The collection of these data was intended to help illustrate the relationship between the migrating salmon's horizontal and vertical movement and distribution and its immediate environment.

2.2: Data Collection and Processing

terHart *et al.* (1987) and terHart and Quinn (1989) provide compilations of the complete data set for 1985 and 1986 respectively. A complete description of the capture and tagging of individual salmon as well as the logic behind the chosen methods is provided in Quinn and terHart (1987). Thus, methodology will not be discussed in detail here.

The ultrasonic tag and receiver/decoder unit were manufactured by Vemco, Ltd., Nova Scotia. The transmitters were 74 mm × 16 mm, weighed 28 grams in air (13 grams in water) and, for fish tracked in 1985, emitted pulses at one of five frequencies (50, 60, 65.5, 69 or 76.8 khz). Interference with commercially available depth sounders operating at a frequency of 50 khz resulted in only one transmitting frequency (76.8 khz) being employed in 1986. The pulse rate was proportional to depth and prior calibration to a depth of 50 m resulted in accuracies of ±1 m.

The Melibe, an 11 m workboat, was used as the tracking vessel and as such, utilized an externally mounted directional hydrophone (Vemco, Ltd.) that could be swung into or out of position approximately 1 m below the water's surface and manually rotated through approximately 300°. The receiver/decoder was mounted inside the cabin of the Melibe and provided a continuous digital readout of depth. Fish depth was recorded manually every minute, provided the unit was receiving, and ship's position, determined by a LORAN C (Raytheon, Ltd.) receiver, was recorded manually every 5 minutes. The LORAN C unit was calibrated periodically using radar fixes and local topographic features. The accuracy of the position finding system was dependent on the location of the vessel and was generally found to be better in open water than in constricted channels. The range of the transmitter

was such that the position of the tracking vessel closely approximated the position of the fish.

The Nitinat Queen, a 12 m self-propelled steel barge, was the platform from which the physical oceanographic measurements were made. The limited manueverability and speed of this vessel, as well as logistic constraints, made this a somewhat less than ideal choice. As a result, the physical oceanography was conducted aboard the Keta, a 14 m converted purse seiner, during 1986.

The same physical oceanographic instrumentation used during the baseline cruises was employed during the salmon tracking. CTD casts were made at 15-45 minute intervals along the fish's track and extended from the surface to 60 m depth or to within 10–15 m of the bottom if the depth was less than 60 m.

The CTD data were despiked and averaged over 1 m depth intervals. Sigma-T (σ_T) was calculated using the International Equation of State, 1980 (Pond and Pickard, 1983). Header data consisting of fish number, consecutive CTD cast number, local time (PDT), date (day, month, year) and position (lat, long) were added for each track. Data that were contaminated by an intermittent failure in the temperature circuitry during 1985 were removed manually. This problem did not occur during 1986.

Current measurements were made using surface drifters with passive window blind drogues. Cross-sectional area of the drogues was approximately 6 m^2. In 1985, these drogues were rigged at depths of 7.5 m and 30.0 m (measured from the surface to the center of the drogue) and deployed or recovered from a 12 ft Zodiac inflatable boat. As many as 4 drifters were deployed at a time and placed so that the fish's most likely track would pass through or at least near the current drifter.

The initial distance separating drifters rigged at the same depth was approximately .2–.5 nautical miles. Drifters were recovered when their position no longer approximated the fish's location or when the distance from the Nitinat Queen precluded an accurate determination of position.

Radar was used to determine the position of the Nitinat Queen and consequently, the current drifters. Thus, to determine a drifter's position, the ship's position would be fixed by taking radar bearings and ranges from the local topography and then a radar range and bearing would be determined from the ship to the drogue. The position of the CTD stations were simply those of the ship. Accuracies in the position of the ship were likely ± 50 –± 100 m, depending on the distance from the shore and the nature of the topography. Accuracies in the drogue's position, then would be of the order ± 50 –± 200 m, depending on the distance from the ship and the care taken to produce the fix.

In 1986, current drifters were rigged for a depth of 7.5 m and deployed in arrays consisting of 3 drifters only. The drifters were deployed from and recovered to the Keta . Drifter positions were established by positioning the ship alongside the drifter and using the ship's LORAN C (Raytheon, Ltd.) receiver. This resulted in greater accuracies in the drifter positions as well as a savings in manpower and increased safety margins during deployment and recovery. CTD station positions were also determined by LORAN C in 1986.

The aerodynamic and hydrodynamic drag on the component parts of the current drifter is negligible compared to that of the drogue (Buckley and Pond, 1976). Thus, the drogue can be said to be experiencing only the current at whatever depth it has been rigged for and is integrating over. There was, therefore, no

correction made to the data for the depth of the drogue.

2.3: Horizontal Movements

2.3.1: General Overview

An analysis of the tagged sockeye's horizontal movements in relation to the observed T, S and currents for the two years of tracking data is presented in Quinn and terHart (1987) and Quinn *et al.* (1989). A brief overview only will be provided here in order that the vertical and horizontal movements may be compared and contrasted.

A total of 33 tracks were obtained during the summers of 1985 and 1986. Twenty-eight sockeye were tracked with fully functioning ultrasonic tags for sufficient time to characterize the fish's vertical and horizontal distributions. CTD data were not collected for 3 fish tracked in 1986 (8607†, 8608 and 8609) due to logistic constraints. Table 7 (adapted from Quinn *et al.*, 1989) summarizes the tracking data for both years.

While correlations of sockeye migratory routes (Groot and Quinn, 1987; Xie and Hsieh, 1989) and timing (Burgner, 1980; Blackbourn, 1987) with oceanographic variables helped motivate MOIST, a relation between horizontal movement and distribution and T and/or S has, to date, proved very elusive. In general, horizontal movements were extremely variable, far more so than the general patterns of vertical movements, and were apparently controlled by different factors. It was clear,

† The convention used throughout when referring to a particular fish track is such that 8607 refers to the 7^{th} fish (07) tracked in 1986 (86). Thus, 8516 refers to the 15^{th} fish tracked in 1985 and so on.

Table 7
Location, duration, direction, speed of movement and depth of travel of adult sockeye salmon tracked in 1985 and 1986. Net direction refers to the compass direction from point of release to the point where the fish was abandoned, lost or recaptured. Net distance travelled is determined in an analogous manner to that of net direction.

Track	Region	Duration (hours)	Net direction	Water Speed†‡ (km/h)	Net distance	Average Depth (meters)
8503	JS	14.83	101°	2.47	13.50	6.1
8504	QCST	9.45	63°	2.85	0.47	9.1
8505	JS	6.02	20°	2.00	2.47	8.6
8507	DP	3.57	136°	2.15	1.50	20.3
8508	DP	2.93	2°	2.66	1.99	19.9
8509	DP	12.33	212°	3.28	1.11	11.8
8510	DP	4.98	195°	1.38	4.43	11.7
8511	SG	7.83	299°	2.13	12.45	18.0
8512	SG	10.00	111°	1.31	1.20	21.3
8513	SG	2.93	125°	1.16	6.42	6.7
8514	SG	9.82	112°	N.A.	13.16	11.3
8515	SG	7.02	110°	3.42	16.15	N.A.
8516	SG	12.50	108°	3.82	34.00	14.9
8517	SG	6.75	274°	N.A.	7.76	N.A.
8601	QCST	21.38	294°	1.84	5.52	14.6
8602	QCST	9.33	127°	3.89	28.04	15.2
8603	QCST	10.00	303°	1.18	10.32	19.9
8604	QCST	6.50	145°	1.52	2.15	9.1
8605	QCST	6.00	277°	1.20	3.61	16.0
8606	QCST	33.00	105°	2.43	43.24	7.5
8607*	JS	8.00	111°	N.A.	16.89	17.8
8608*	QCST	18.00	125°	N.A.	10.98	14.3
8609*	JS	13.08	302°	N.A.	10.83	13.2
8610	SG	13.07	113°	3.69	28.72	11.2
8611	SG	9.25	351°	1.15	5.87	17.8
8612	SG	7.50	128°	2.51	11.95	17.8
8613	SG	22.08	35°	1.78	12.45	19.5
8614	SG	26.05	126°	1.42	24.63	28.6
8615	SG	9.00	102°	2.64	12.57	16.7
8616	SG	8.33	354°	1.87	4.70	13.4

* Concurrent CTD data were not obtained for this track.

† Water speeds are estimated swimming speeds of the fish in the water, derived from ground speeds and estimates of current speeds.

‡ N.A. implies that data were not available.

however, that the coastal phase of the homeward migration was less well oriented than the oceanic phase (Quinn and terHart, 1987). The majority of tracked fish did display a strong directional preference, either southeastward or northwestward, during some parts of the observed track. Exceptional fish displayed apparently random orientation (8509) or almost no movement whatsoever (8612). It is noteworthy that no sockeye made significant progress to the northeast or southwest.

Current data obtained in the vicinity of the telemetred track helped resolve a highly significant, asymmetrical bimodal orientation (SE/NW) in the tracking data. When the sockeye's progress over the ground was considered the resultant of an advecting current and the derived fish's speed and direction, it was shown that the tracked sockeye maintained some directional preference and did not compensate for current displacement. Similar current analysis also showed a weak but non-random fish orientation with respect to the observed currents.

Biased bimodal orientation was evident when southeastward moving fish encountered topography that obstructed the fish's path (8503, 8606, 8610). The obstruction tended to cause the sockeye to swim aimlessly in the near vicinity of the obstruction, then reverse direction and eventually, by swinging around to the north, resume a southeastward heading. Many fish caught and released near obstructions headed to the northwest immediately (8504, 8511, 8613). Biased bimodal orientation has been documented for schools of sockeye smolts (Groot, 1965; 1972), laboratory studies of juvenile sockeye (Groot, 1965; Quinn and Brannon, 1982), Chum salmon (*Oncorhynchus keta*)(Quinn and Groot, 1984b) as well as many other animals (e.g. reptiles: Landoth, 1973; birds: Bingman, 1981).

Analysis of the horizontal movements also showed that there was a much

stronger southeastward bias in fish direction in the SG than in QCST, JS or DP. Given the bimodal orientation of fish tracked in SG, QCST and JS, it is noteworthy that the average speeds were faster in the homeward (southeastward) direction than in the seaward (northwestward) direction. No significant difference in overall average swimming speed was found in different oceanographic regimes.

In summary, it appeared that the increased stratification in the SG may have aided orientation towards the Fraser River and that a general asymmetrical bimodal orientation (southeastward/northwestward) in QCST, JS, and DP gave way to a unimodal southeastward orientation in the SG. At some point, olfactory stimuli and rheotactic responses characteristic of upriver migration (Johnson and Hasler, 1980) must supercede the mechanism responsible for the observed orientation in these data. Although near surface waters, especially in the southern SG, contain relatively large volumes of water originating from the Fraser River, no clear evidence of this change in migratory mechanisms was observed.

2.4: Vertical Movements

2.4.1: General Overview

Vertical distribution of sockeye tagged in 1985 is discussed in Quinn and terHart (1987). A brief summary of vertical distribution for both the 1985 and 1986 tagging studies is presented in Quinn *et al.* (1989). Both studies deal quantitatively with the sockeye's depth distribution but only qualitatively with the relation between depth and T or S. In order for subsequent, more quantitative observations of the sockeye's depth distribution to be made with respect to the vertical oceanographic structure, the results obtained in Quinn and terHart, (1987) and Quinn *et*

al. (1989) must be introduced.

In comparison, patterns of vertical movement for 1985 and 1986 in all 4 oceanographic regimes were similar and much less complicated than the corresponding horizontal patterns of movement. In general, many salmon dived abruptly immediately upon release, stayed at considerable depths (30–60 m) for periods up to 80 minutes and then ascended to the surface. Of those sockeye that made deep initial dives, subsequent vertical movement differed substantially and was easily distinguishable from this initial dive. This type of initial vertical distribution was observed more often in QCST, JS and DP than in the SG. Subsequent patterns of vertical movement were characterized by long periods spent within a narrow range of depths, interspersed with brief, shallow dives or ascents. Only a few sockeye repeatedly dove and ascended and only one, 8511 did so continuously.

Diel patterns of movement were obtained for 5 fish tracked in 1986. Estimated swimming speeds were generally slower during the night than during the day and during certain night-time periods, the fish were apparently drifting (LORAN C positions indicated that the tracking boat was moving but no propulsive power was required to keep within range of the transmitter). In addition, diel patterns of vertical distribution showed that during night-time periods, tracked fish were observed at depths significantly closer to the surface than during day-time periods (Quinn *et al.*, 1989).

Qualitative observations suggested that orientation and depth distribution were related. A disoriented fish is defined as one that did not make significant progress homeward (in all cases assumed to be the Fraser River). Invariably, frequent large amplitude vertical excursions were associated with disoriented horizon-

tal movements. The term disoriented shall be used to refer to either poor horizontal orientation or vertical distributions characterized by frequent large amplitude excursions. The term oriented shall be used to refer to fish that made significant progress homeward during all or part of their track or to vertical distributions characterized by infrequent small amplitude vertical excursions. Figure 39 (from Quinn and terHart, 1987) clearly shows this difference in oriented versus disoriented behaviour.

Sockeye tracking conducted in the vertically and horizontally well-mixed waters of DP was considered the experimental control. The absence of even weak vertical structure leaves the fish with very limited choices of T or S and virtually no choice of T or S gradient. The fish's vertical distribution in this type of oceanographic regime can therefore be considered independent of a preferred T or S or gradient. Tracking observations in DP and eastern JS clearly showed a general preference for near surface waters (Figure 40).

Sockeye tracked in the northern regime (QCST, JS and DP) spent significantly more time within 10 m of the surface than did sockeye in the SG. Fish in the north also displayed a greater tendency to dive not only immediately after release, but also throughout the duration of the track. The fish in this region were rarely observed at depths greater than 30 m and as the thermoclines and haloclines extended to depths of 20–30 m (Figure 41), sockeye occupied depths in the vicinity of the largest gradients in T and S.

The more complex T and S stratification in the SG seemed to elicit more complex patterns of vertical distribution and movement. Minute by minute analysis of the depth data revealed that sockeye tracked in the SG spent less time in the

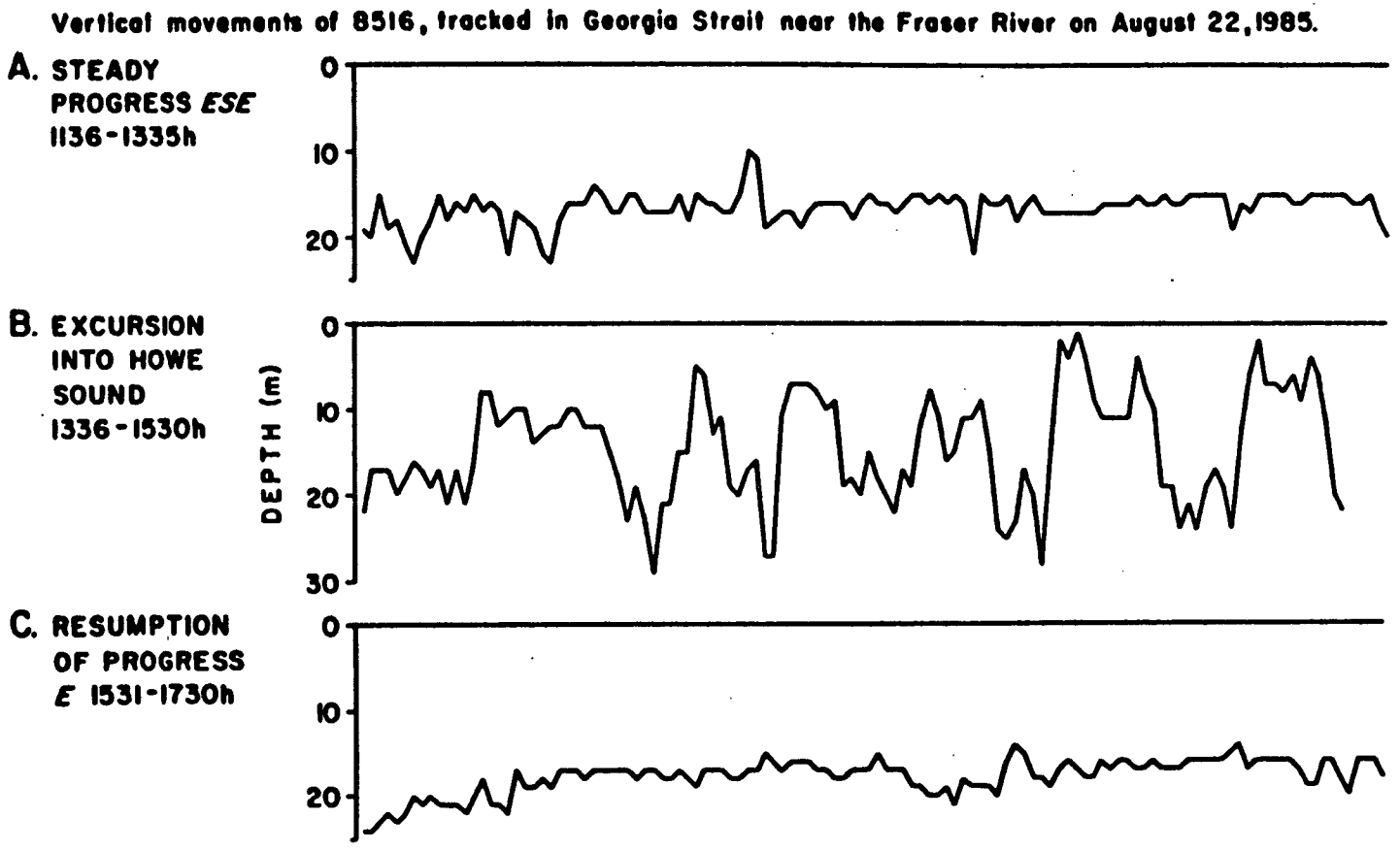

Figure 39. Oriented and disoriented vertical movements for 8516. Depth is shown on the y-axis and time on the x-axis.

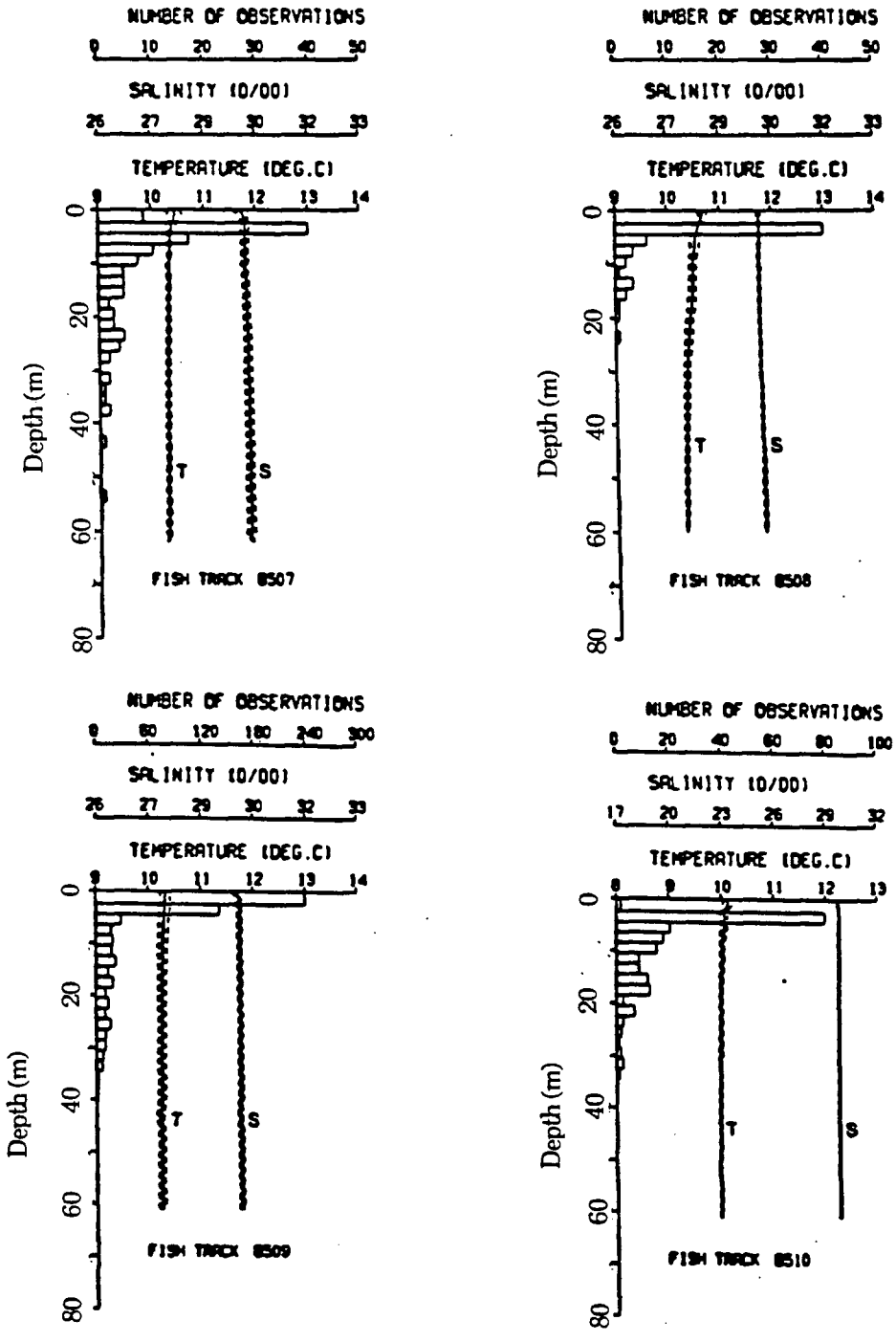

Figure 40 . Composite fish depth histogram and T and S profiles for 8507, 8508, 8509 and 8510. Tracks were conducted in the homogeneous waters of eastern JS and DP.

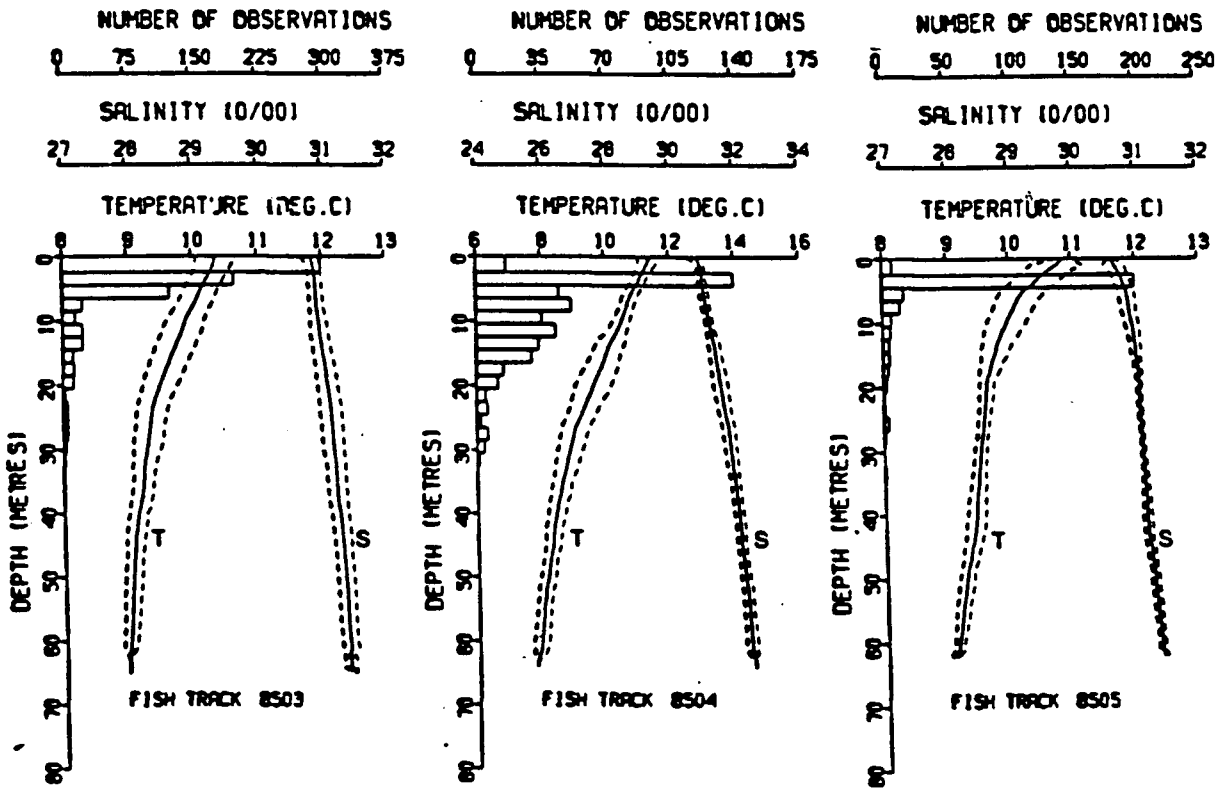

Figure 41 . Composite fish depth histogram and T and S profiles for 8503, 8504 and 8505. Tracks were conducted in the slightly stratified waters of QCST and western JS.

top 10 m of the water column than did their northern counterparts even though the average depth of travel did not statistically differ. This result is explained by the frequent deep dives and ascents made by sockeye tracked in the north which served to increase the average depths of several fish tracked for short periods of time. Sockeye tracked in the SG tended to avoid the warmer, less saline ($\leq$ 27 ppt) near surface waters (Thomson *et al.*,1986) and preferred depths directly above or below the maximum gradients. Although there was a general avoidance of near surface waters, frequent, brief excursions (tens of minutes) were made into these waters. The only fish that spent a significant portion of time in waters $\geq$ 16°C did so as part of a sequence of 28 dives and ascents. It should be noted that in this case, salinities in the surface mixed layer were $\geq$ 27 ppt.

In general, vertical profiles of T and S in the SG were characterized by thin thermo/haloclines and relatively strong T and S gradients (Figure 42). There were several exceptions, however, and the vertical distribution of sockeye tracked in these exceptional regimes within the SG resembled the vertical distribution of sockeye tracked in QCST and JS in that there was a relatively broad range of observed depths that extended throughout the thermo- and haloclines. The overall results generally supported Westerberg (1982; 1984) and Ichihara and Nakamura (1982) who proposed that vertical distribution and movement was related to a well defined T and S gradient.

The near surface orientation of sockeye tracked in 1985 in all oceanographic regimes was not as evident in 1986. T and S structure was essentially similar for both years and was not likely the cause for this difference (Figure 42). It has been proposed (T.P. Quinn personal communication) that the genetic differences inherent

in sockeye returning to different river systems may be responsible for the observed differences in depth of travel.

2.4.2: Ambient Oceanographic Variables

The remainder of this study will deal with those tracks for which concurrent CTD data were obtained. Twenty-five of the 28 tracks considered by Quinn and terHart (1987) and Quinn *et al.* (1989) meet this criteria (Table 7). In addition, data from 8614, 8615 and 8616 were not considered. Hence, the remaining analysis is based on data from 22 separate fish tracks.

The following discussion briefly addresses the importance, possible use and mechanism whereby the physical oceanographic structure may aid orientation by homeward migrating sockeye. As such, it will also serve to motivate the remainder of this analysis.

Orientation requires that the fish observe some directional quantity in its environment. The hydrography can provide directional cues through horizontal gradients of scalar properties sensible to the fish. Some of the hydrographic dependent orientation mechanisms that have been proposed are (Brannon, 1982):

i) Optimization of physiological conditions;

ii) Population specific pheromones;

iii) Selective tidal-stream transport;

iv) Olfaction-mediated tidal rheotaxis; and

v) Olfaction at stratified depths.

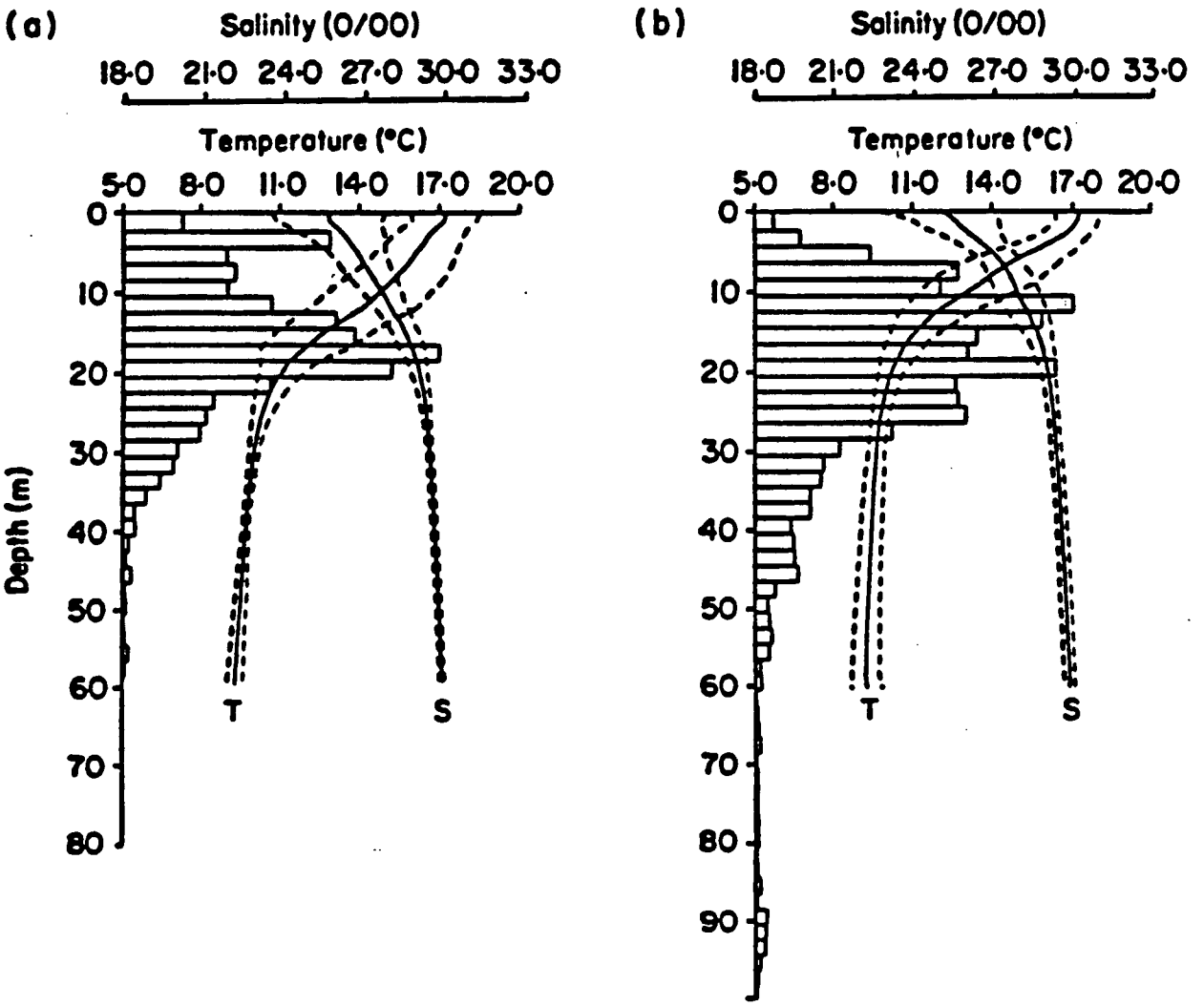

Figure 42 . Composite fish depth histogram and T and S profiles for fish tracked in 1985 and 1986 ((a) and (b) respectively) in QCST/JS and the SG. Dashed lines represent ± 1 standard deviation. There were 3,175 (7,414) observations of fish depth and 128(74) CTD casts in 1985(1986) .

Detailed, quantitave analysis of the relationship between T, S and D and the tracked sockeye is necessary in order to determine how the hydrographic structure affects orientation and, ultimately, migration.

The large horizontal scale and long time scale hydrographic features that are of the same order of magnitude as the length and time scales of the complete return migration cannot, of course, be directly sensed by the migrating sockeye. In fact, the hydrographic near field of the fish is dominated by fine- and micro-structure features that are at least an order of magnitude larger than the mean vertical gradients, which are themselves at least an order magnitude of greater than the mean horizontal gradients. In many cases, vertical profiles of hydrographic parameters, such as T and S, contain 'steps': nearly homogeneous layers are separated by large gradients (Muench *et al.*, 1990). the distribution of other solutes, and in particular directional olfactants, are concomitant to that of temperature and/or salinity (Westerberg, 1984). The magnitude of the solute gradient at a particular T or S step need not necessarily be related to the magnitude of the T or S gradient. Moreover, as solutes diffuse more slowly than heat, olfactant micro-structure can be present after the temperature structure has diffused to homogeneity.

Vertical variability in the ocean's upper layers is the result of a large number of complex processes. Near surface irreversible fine- and micro-structure can be related to atmospheric forcing, shear-induced turbulence and double-diffusive salt-fingering and layering. Reversible fine- and micro-structure, associated with the modulation of the density field by internal wave fields, is always present in an externally and/or internally forced stratified fluid (LeBlond and Mysak, 1978).

A well known feature of the world's oceans is the aspect ratio of hydrographic

features; the horizontal extent of these features are $\gg$ than their vertical extent (Gill, 1982). Gravity and stratification are resposible for greatly extending some oceanographic phenomeon, such as specific water masses, in the horizontal and compressing them in the vertical. Hence, surfaces of equal density and other properties tend to be almost horizontal. In many cases, the thinness of these layers relative to their horizontal extent is such that the vertical stratification can mirror the horizontal distribution of hydrographic parameters. In particular, a single dive can take a fish through hydrographic regimes corresponding to a basin-wide horizontal distribution.

The spreading and diffusion of a passive tracer in the oceans is also strongly affected by the presence of fine- and micro-structure features (Ewart and Bendiner, 1981). Tracer diffusion experiments show that a point source in a homogeneous layer is initially spread by weak turbulence in the layer. Spreading within fine- and micro-structure gradients above and below the homogeneous layer is by slow vertical diffusion and shear dispersion. Filaments of the tracer trail down-shear with intermittent turbulence leaking the tracer into other homogeneous regions. A complex regime develops with several levels delineated by the tracer. The net result is that the extent of the trailing filaments is much larger than the bulk of the tracer. The analogous oceanic aspect ratio is preserved. The vertical distribution of odour from a large-scale, diffuse and continuous source, like the Fraser River, results in homogeneous layers that are filled with odour of differing concentrations. The vertical distribution is concomitant with that of T and S.

Vertical current shear has been observed to be concentrated in the density gradient layers (Woods, 1968; Simpson, 1975 ; Van Leer and Rooth, 1975) and

therefore strongly affects fine- and micro-structure features present there. Any horizontal variation in the layer will be stretched in the direction of the shear. This effect is integrated in time so that even a weak shear will have a noticeable effect in elongating these structures in the down-stream direction. Similarily, vertical variations within the gradient layers will be tilted and elongated in the horizontal. Hence, vertical gradients can become part of the horizontal fine- and micro-structure.

In estuarine oceanographic regimes, the residual estuarine circulation may indirectly provide orientation cues. A homeward migrating salmon could orient to the river mouth by swimming aainst the shear as mirrored in fine- and micro-structure gradient layers. The detection of these structures could be by olfaction or by directly sensing the temperature field. However, it is not clear how the sign of the shear, or more directly, the T, S or odour source, can be determined. In a two-layer estuarine model, which is appropriate for most of the southern inside passage, the thermo- and haloclines as well as the greatest shear in the residual circulation are co-incident. Hence, fine- and micro-structure features within the thermocline should have a good correlation to the direction of the source. In addition, the buoyancy layer in the SG contains a greater percentage of Fraser River water by volume than other surface layers within the study area. Thus, the concentration of home stream odors is enhanced in conjunction with increased stratification; orientation by olfaction or T sensing in shear modulated fine- and micro-structure may be more easily observed in this regime than others. In addition, the differing oceanographic regimes within the southern inside passage may ellicit different orientation mechanisms. In this way, the role of the general oceanography on orientation and migration may be determined.

During the tracking itself and the subsequent qualitative analysis, the depth time series of the fish appeared periodic in nature (Figure 43). Observations of fish depth at 1 min. intervals for periods up to 33 hours provided detailed time series of depth and these data suggested an underlying periodicity to the fish's vertical movements regardless of the T or S structure. Therefore, I undertook to quantify this apparent pattern and to use that information to help determine if the fish sought or avoided a particular value of T or S or a particular gradient of T or S. The premise was that knowing the fish's inherent depth distribution independent of the vertical structure in the water column and that this distribution would be manifested in other oceanographic regimes, one could filter the two depth distributions and be left with the fish's preferred choice of T or S or their gradients. Bull (1936) and Bardach and Björklund (1957) found conditioned responses in fishes to T changes as little as .03–.05°C. Westerberg (1982; 1984) gave evidence supporting the hypothesis that Atlantic salmon were orienting to microstructure T gradients. Thus, it is not considered unreasonable that fish tracked in this study were sensitive and would react to small changes in T and S.

The vertical and horizontal homogeneity of the water masses in DP and eastern JS provided depth time series data independent of relatively large variations in T and S. Thus, any depth preference would be most obvious in these oceanographic regimes. Fourier analysis might resolve the frequency components in the JS and DP depth data and therefore provide an appropriate filter to determine if a relationship between the fish and T or S existed.

To this end, the CTD data obtained during the fish tracking program was combined with the fish depth time series data to produce an "ambient" oceano-

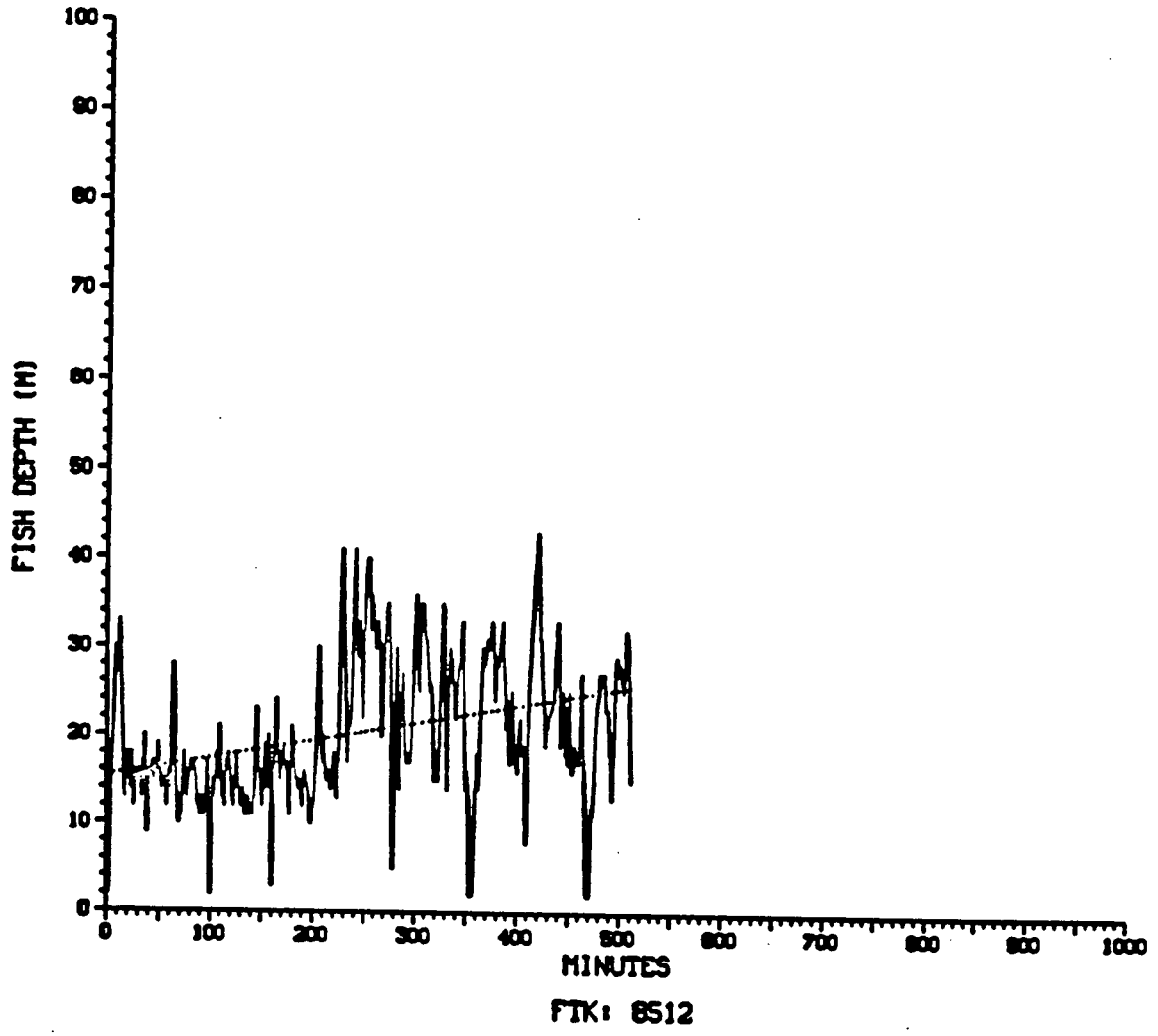

Figure 43 . Depth time series AOV data for 8512 tracked in the SG near the northern tip of Texada Island. The dashed line represents the least-squares estimate of the linear trend.

graphic variable (AOV) dataset. It is considered "ambient" in the sense that the time series produced is a mathematical representation of the T and S that the fish actually experienced at any specific time during the track (Thomson *et al.*, 1986).

The AOV's were determined by a simple algorithm that assumes that:

$$\frac{\partial T}{\partial Z}, \frac{\partial S}{\partial Z} >> \frac{\partial T}{\partial X}, \frac{\partial T}{\partial Y}, \frac{\partial S}{\partial X}, \frac{\partial S}{\partial Y}. \tag{2.1}$$

This is to say that the vertical gradients of T and S are much greater than the horizontal slopes of the isotherms or isohalines. This is considered a reasonable assumption as:

$$\begin{aligned} \frac{\partial T}{\partial Z} &\approx O(4.0 \times 10^{-2})\ ^{\circ}\mathrm{C} \cdot \mathrm{m}^{-1}, \\ \frac{\partial T}{\partial X}, \frac{\partial T}{\partial Y} &\approx O(5.0 \times 10^{-5})\ ^{\circ}\mathrm{C} \cdot \mathrm{m}^{-1}, \\ \frac{\partial S}{\partial Z} &\approx O(2.0 \times 10^{-2})\ \mathrm{ppt} \cdot \mathrm{m}^{-1}, \\ \frac{\partial S}{\partial X}, \frac{\partial S}{\partial Y} &\approx O(2.5 \times 10^{-5})\ \mathrm{ppt} \cdot \mathrm{m}^{-1}. \end{aligned}$$

This assumption breaks down in two regions of concern. Firstly, in the vicinity of strong hybrid tidally mixed fronts, like those observed at Cape Mudge in the Strait of Georgia, and Blackney and Weynton Passages in Johnstone Strait, the horizontal and vertical gradients may well be of the same order of magnitude. However, no successful tracks were completed in the vicinity of these features and there is therefore no AOV data computed for these regions. Secondly, the water masses present in Discovery Passage and eastern Johnstone Strait were vertically and horizontally very well-mixed and observations showed that the vertical and horizontal gradients, though weak, were of the same order of magnitude. Although the assumption (2.1) breaks down, this poses no problem insofar as the analysis is concerned as T and S are very nearly constant in both the vertical and horizontal directions and the salmon therefore has but one choice of T and/or S.

Ambient T(S) was calculated by linearly interpolating the T(S) provided by the CTD casts immediately before and after observation of fish depth at a given time. The ambient depth is simply the observed depth of the fish.

Thomson *et al.* (1986) provides a sampling of AOV data products for fish tracked during 1985. The work presented in this manuscript is a graphical representation of the frequency distributions and correlations of the AOV's. Other than stating that the fish tended to avoid water with salinities $\leq$ 27 ppt, no attempt was made by the authors to interpret their results.

In order to determine the possible existence of a preferred T or S, the extremely strong cross-correlation between depth (D), T and S in the AOV data due to purely physical constraints must be considered. Figure 44 shows the coherence and phase for T and S. The strength of this and other cross-correlations (ie. T/D or S/D) would clearly mask any significantly weaker cross-correlations, like those assumed to exist between the fish's depth of migration and T or S. Thus, filtering out the strong cross-correlation in T/D and S/D in the raw data due solely to the physical oceanography of the region is necessary to reveal any other weaker correlations between these variables and the fish. However, the nature of the relationships between T, S or D and the sockeye is not known and any form of filtering may, in fact, remove the sought after signal. An acceptable form for this type of filter was not found. Considering this weakness, cross-correlations between the T(S) and D time series due to the tracked sockeye's response to its ambient environment cannot be determined with any degree of certainty. A simple algorithm was used to smooth the T and S time series AOV data to reduce time dependent effects. The CTD cast data was moving-averaged in time over a period (approximately 3 hours) in which

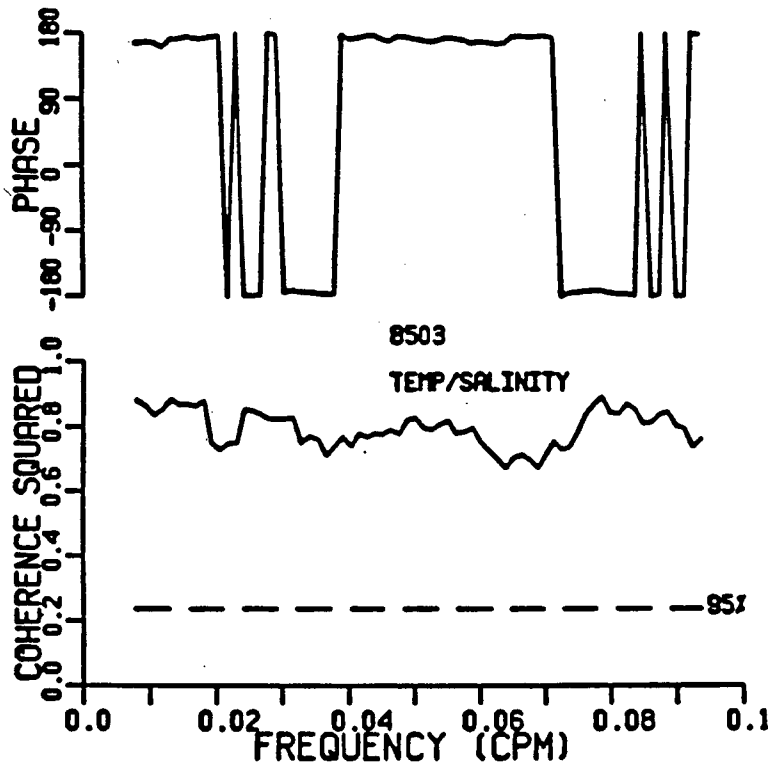

Figure 44. Coherence and phase differences for raw T/S AOV data for fish 8503 tracked in the western extremity of JS. The time series are highly coherent and virtually 180^0 out of phase at all times.

the tides did not dramatically alter the vertical structure of the water column. The fish's observed depth and interpolated (AOV) T(S) at that depth and time was subtracted from the mean state created by the moving average. Thus, we have:

$$x_{\mathrm{anom}_{i,k}}\big|_{z_{obs}} = x_{\mathrm{aov}_{i,k}}\big|_{z_{obs}} - \bar{x}_k\big|_{z_{obs}} \tag{2.2}$$

where

$$\bar{x}_k(z) = \frac{1}{M}\sum_{j=1}^{M} x_j(z) \tag{2.3}$$

and

$$i = 1,2,3,\cdots N$$

$$j = 1,2,3,\cdots M$$

$$k = 1,2,3,\cdots P$$

Note that N represents the total number of observations, M represents the weight of the moving average and P represents the total number of weighted averages formed. Note that for the majority of $\bar{x}_k(z)$, $M = 4$ except in cases where there were fewer than 4 casts made.

Once x_{anom_i} had been calculated from the AOV T and S data, some pre-processing and qualification procedures were carried out to ensure that the correct analytical techniques and therefore accurate results would be obtained.

Pre-processing included the removal or correction of obvious outliers in the data, caused by errors in the recording or processing of the original tracking and CTD data, and trend removal. Trend removal, required so as not to mask low frequency spectral content in the data and to unduly distort the processing of correlation quantities (Bendat and Piersol, 1971), was carried out by fitting a least-squares linear curve to the data. In fact, the linear trend may actually be a low-

frequency component in the data. No evidence was found to indicate that the calculated linear trend was actually a true trend in the data. The linear fit, $\hat{x}_{\mathrm{anom}_i}$ to x_{anom_i} is given as:

$$\hat{x}_{\mathrm{anom}_i} = ai + b \qquad i = 1, 2, 3, \cdots N$$

where

$$a = \frac{12 \sum_{n=1}^{N} n x_{\mathrm{anom}_i} - 6(N+1) \sum_{n=1}^{N} x_{\mathrm{anom}_i}}{hN(N-1)(N+1)}$$

$$b = \frac{2(2N+1) \sum_{n+1}^{N} x_{\mathrm{anom}_i} - 6 \sum_{n=1}^{N} n x_{\mathrm{anom}_i}}{N(N-1)}.$$

N is the total number of observations and h, the sampling interval is 1 min. De-trended time series were then calculated as:

$$\tilde{x}_{\mathrm{anom}_i} = x_{\mathrm{anom}_i}\big|_{z_{\mathrm{obs}}} - \hat{x}_{\mathrm{anom}_i} \qquad i = 1, 2, 3, \cdots N$$

for T(S) and

$$\tilde{z}_{\mathrm{anom}_i} = z_{\mathrm{obs}_i} - \hat{z}_{\mathrm{anom}_i} \qquad i = 1, 2, 3, \cdots N$$

for D.

Lastly, to simplify later calculations, the de-trended time series were transformed so that the arithmetic means of the transformed time series were equal to zero. The zero-mean, de-trended T(S) and depth anomaly time series were trivially calculated as:

$$\alpha_i = \tilde{x}_{\mathrm{anom}_i} - \frac{1}{N} \sum_{n=1}^{N} \tilde{x}_{\mathrm{anom}_i} \qquad i = 1, 2, 3, \cdots N \tag{2.4}$$

for T(S) and

$$\gamma_i = \tilde{z}_i - \frac{1}{N} \sum_{n=1}^{N} \tilde{z}_i \qquad i = 1, 2, 3, \cdots N \tag{2.5}$$

for depth.

Qualification of the data included tests for stationarity and a search for periodicity. Determination of stationarity is vital as the analytical procedures for stationary and non- stationary data are different. Stationarity implies that the statistical properties of the time series are independent of time. A minimum requirement for this to be true is that the probability density function be time invariant and hence a constant mean and variance exists (Jenkins and Watts, 1968). An estimate of the probability density function for the raw depth time series data is provided by the depth histograms for each fish (Figures 40 and 41). The unimodal distribution of the majority of the data suggests that an assumption of stationarity is not unreasonable. However, as the physical processes which were responsible for the raw AOV data were not time invariant, a more rigorous test of stationarity is necessary.†

If stationarity is to be determined, it must be assumed that any given sample record will properly reflect the non-stationary character of the process in question and that the sample record itself is long enough to differentiate random fluctuations from non-stationary trends. A simple, non-parametric procedure which does not

† Note that the time series derived herein do not contain data from observations made in darkness. Quinn *et al.* (1989) shows that the vertical distributions and movement patterns for sockeye tracked during darkness are substantially different from those tracked during the day. Thus, stationarity cannot be assumed for time series combining tracking data acquired during day and night. Similarily, time series produced by combining data from different oceanographic regimes cannot be considered stationary.

require a knowledge of the sampling distributions of any data parameter (ie. if they are normally distributed or otherwise), is the run test. Consider a sequence of observations where each observed value may be classified into one of two mutually exclusive categories: either a '+' observation or a '−' observation. A 'run' is defined as a sequence of observations in one category that is preceded and followed by a sequence of observations in the other category. The number of runs in the complete dataset is an indication as to whether or not the results are independent observations of the sample parameter chosen. The existence of a trend can be determined by hypothesizing that no trend exists and hence a sequence of N observations are independent realizations of the same random variable. Any population estimator, or parameter, will work equally well (Bendat and Piersol, 1971).

To test for stationarity in α_i and γ_i, values of standard deviation, σ, calculated as:

$$\sigma = \left[\sum_{i=1}^{M} \frac{(\chi_i)^2}{M-1}\right]^{1/2} \qquad i = 1, 2, 3, \cdots M$$

for $\chi_i = \alpha_i$ and γ_i were computed from consecutive 20 min. segments ($M = 20$) for the entire record length. The consecutive σ values were then categorized as either greater than (ie. a '+' observation) or less than (ie. a '−' observation) the median value. Figure 45 is a representative result of this test. The data can be considered stationary with 95% confidence if the number of runs in the sequence of σ relative to the median value was ≥ 6 but ≤ 15 (Bendat and Piersol, 1971). Table 8 shows that the majority of derived time series can be considered stationary at the 95% confidence level.

Tests for periodicity in α_i and γ_i were conducted for the DP data (8507, 8508, 8509 and 8510) first to determine if an intrinsic depth distribution independent

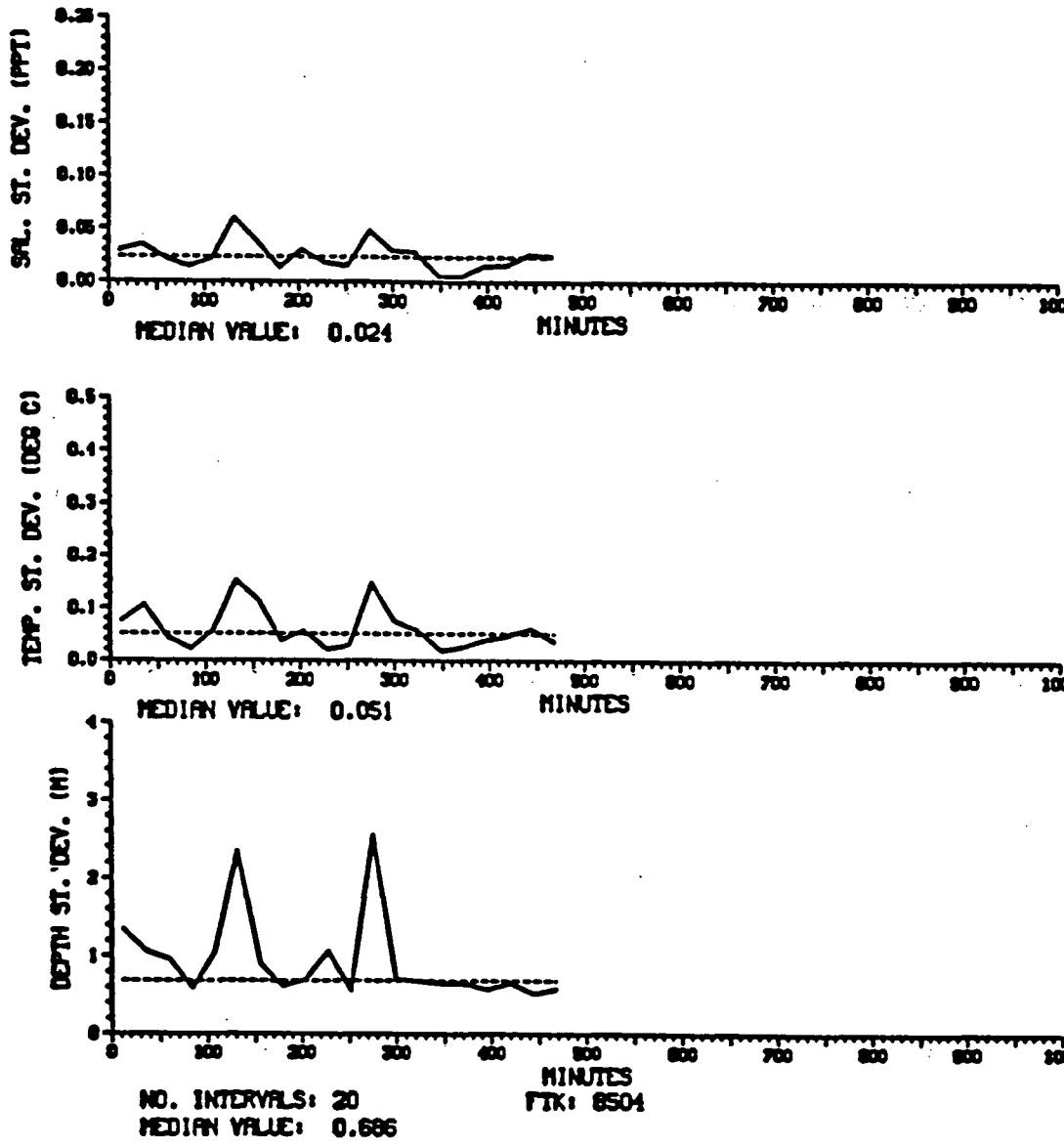

Figure 45 . Run test of standard deviation (σ_{20}) for consecutive intervals of 20 observations about the median for all intervals. A single run consists of a sequence of consecutive observations of σ_{20} either greater or less than the median value. Data is for 8504 tracked in QCST near Malcolm Island.

Table 8
Results of the run test performed on the α_i and γ_i time series data for each fish. The number of runs of σ_{20_i} (the standard deviation of sequential 20 minute segments of the track) about σ_{med} (the median standard deviation of all the σ_{20_i}) is given for D, T and S. The number of runs is shown as N_{run}. Stationarity may be assumed at the 95% significance level if the number of runs, N_{run} satisfies $6 \leq N_{run} \leq 15$. Note that ♠ and ♡ imply, respectively, that stationarity can or can not be assumed.

Fish	σ_{med} D/T/S	N_{run}	Stationarity D/T/S
8503	.291/.045/.016	7/ 6/ 4	♠/♠/♡
8504	.686/.051/.024	8/10/ 9	♠/♠/♠
8505	.532/.043/.021	4/ 8/ 8	♡/♠/♠
8509	1.090/.010/.018	9/ 3/ 6	♠/♡/♠
8510	1.299/.003/.002	3/ 2/ 2	♡/♡/♡
8511	2.045/.172/.095	6/ 9/ 3	♠/♠/♡
8512	1.009/.116/.057	5/ 2/ 5	♡/♡/♡
8514	1.187/.306/.235	5/10/10	♡/♠/♠
8516	.395/.072/.022	7/ 6/ 7	♠/♠/♠
8601	1.907/.023/.003	7/ 6/ 8	♠/♠/♠
8602	1.450/.072/.028	6/ 8/ 7	♠/♠/♠
8603	1.548/.027/.015	4/ 7/ 7	♡/♠/♠
8604	.743/.026/.019	10/ 4/ 8	♠/♡/♠
8605	1.227/.050/.403	5/ 6/	♡/♠/
8606	.525/.270/.015	3/ 7/ 3	♡/♠/♡
8610	.492/.026/.037	10/ 6/ 8	♠/♠/♠
8611	.944/.099/.020	12/ 7/11	♠/♠/♠
8612	1.318/.135/.404	5/ 2/	♡/♡/
8613	1.251/.160/.050	8/ 6/ 6	♠/♠/♠

of T(S) or T(S) gradients existed. Estimates of the normalized autocorrelation function, R_{η_r}, given by:

$$R^{\alpha}_{\eta_r} = \frac{\sum_{i=1}^{N-r} \alpha_i \alpha_{i+r}}{(N-r)\sigma^2} \qquad r = 1, 2, 3, \cdots m \tag{2.6}$$

for T(S) and, when α_i is replaced by γ_i, D. N is the total number of observations of α_i or γ_i. The lag number, r, corresponds to the time displacement and the maximum lag number, m=100, was chosen as larger values produced negligible differences in the results.

$R^{\alpha}_{\eta_r}$ and $R^{\gamma}_{\eta_r}$ (hereafter defined as $R^{\alpha,\gamma}_{\eta_r}$ for convenience) results show much greater correlations between the T and S time series than between the T(S) and depth time series. The form of $R^{\alpha,\gamma}_{\eta_r}$ shown in Figure 46 suggests that periodicity is not a feature of these data. $R^{\gamma}_{\eta_r}$ for 8510, though different in appearance from $R^{\gamma}_{\eta_r}$ for 8509, is not statistically different given the 95% confidence interval. The general form of $R^{\gamma}_{\eta_r}$ indicates that γ_i corresponds to a $O(1)$ auto-regressive process (Jenkins and Watts, 1968). This result is in agreement with the qualitative observation that fish tracked in homogeneous regimes were unimodally surface oriented. A quantitative estimate of this behaviour could be obtained according to:

$$\chi_i = \alpha\chi_{i-1} + \mu(1-\alpha) \qquad 0 \leq \alpha \leq 1$$

where χ_i is the predicted depth, μ is the observed mean depth and α is an empirically determined parameterization of the $O(1)$ process. However, the error associated with a predictive estimate of depth using this type of process and these data would be large enough to render the exercise meaningless.

As no periodicity was found in γ_i or α_i for DP, $R^{\alpha,\gamma}_{\eta_r}$ estimates for all regimes were calculated without filtering for the hypothesized intrinsic depth distribution. The general form of $R^{\alpha,\gamma}_{\eta_r}$ for all time series data was not sufficiently similar to conclude that $R^{\alpha,\gamma}_{\eta_r}$ was independent of vertical T(S) structure. The general form of $R^{\alpha,\gamma}_{\eta}$ for data in stratified regimes was such that periodicity appeared to be characteristic of these data.

One notable exception, 8511, in the $R^{\gamma}_{\eta_r}$ data was found. In this instance, periodicity was clearly present. There is a statistically significant cycle of approximately 18 lags evident in the autocorrelogram (Figure 47). This translates into a period of approximately 18 minutes in γ_i. In fact, 8511 is the only fish that continu-

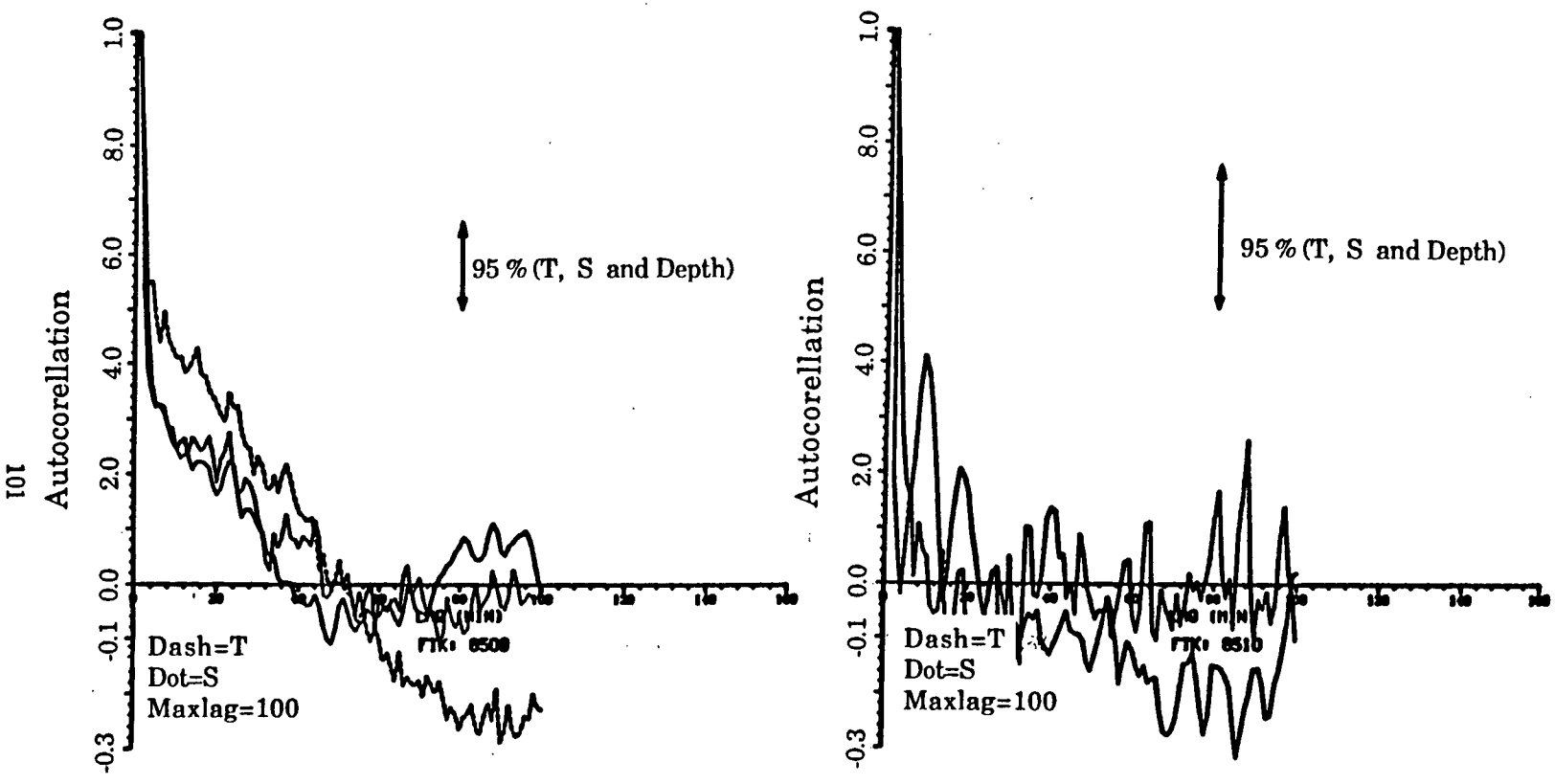

Figure 46. Autocorrelation $R_{\eta_r}^{\alpha,\gamma}$ vs lag for 8509 and 8510 tracked in the homogeneous water of DP.

ously dove and ascended throughout the duration of its track. It made a series of 28 dives and ascents during the 7.83 hour track duration. Considering one cycle to be a dive or ascent, we have approximately .28 hrs/cycle or about 17 mins/cycle. This agrees reasonably well with the results obtained via the $R^{\gamma}_{\eta_r}$ analysis and served to motivate additional analysis of the time series datas.

Based on the $R^{\gamma}_{\eta_r}$ result that some evidence of periodicity was present, estimates of the autospectrum, $G^{\alpha,\gamma}$ were calculated using an FFT algorithm available in UBC's computing library (UBC FOURT, 1986). Specific data pre-processing for the calculation of the FFT consisted of applying a cosine taper to the first and last 10% of the record to be analyzed to reduce the effect of side-lobe leakage inherent in finite length records (Bendat and Piersol, 1971). The cosine taper, C_T, was of the form:

$$C_{T_n} = \cos\left(\frac{90.0^{\circ} n}{N}\right) \qquad n = 1, 2, 3, \cdots N$$

where N equals 10% of the total record length.

Raw estimates of $G^{\alpha,\gamma}$ were smoothed by band averaging. The choice for the number of bands, N_B, to smooth over was determined by inspection. N_B = 12 provided the best resolution with reasonable confidence intervals. The 95% confidence interval was calculated using Bendat and Piersol, (1971). The effective resolution bandwidth, B_e, was calculated as (Bendat and Piersol, 1971):

$$B_e = \frac{\nu}{N}. \qquad \nu = 2N_B,\ N = \text{total record length}$$

For a constant $\nu = 2N_B = 24$, B_e varies as the inverse of the record length. Most fish tracked in both years provided N large enough to yield acceptable confidence intervals and resolution, B_e.

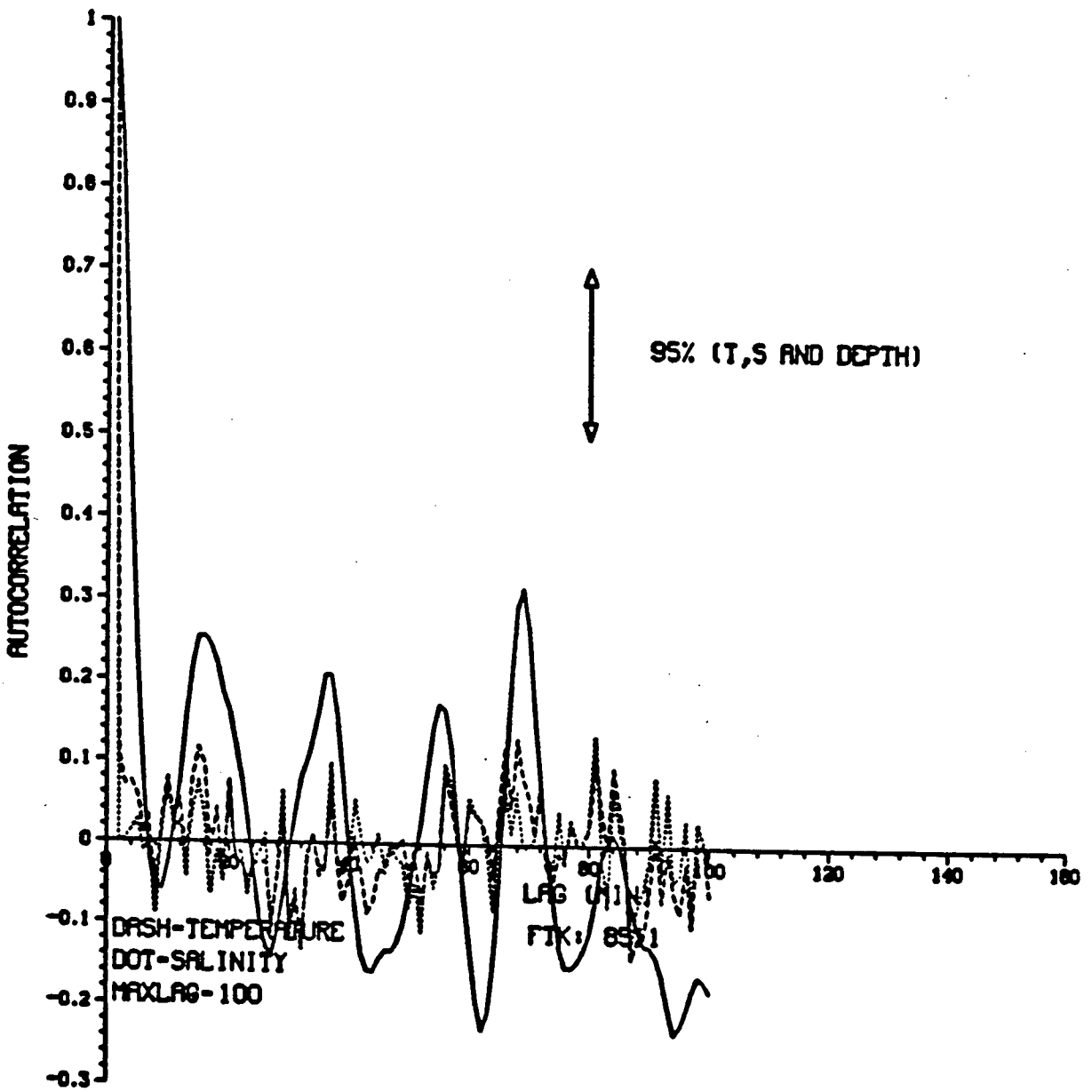

Figure 47 . Autocorrelation $R_{\eta_r}^{\alpha,\gamma}$ vs lag for 8511 tracked in the SG near the northern tip of Texada Island. Periodicity is implied by statistically significant zero-crossings.

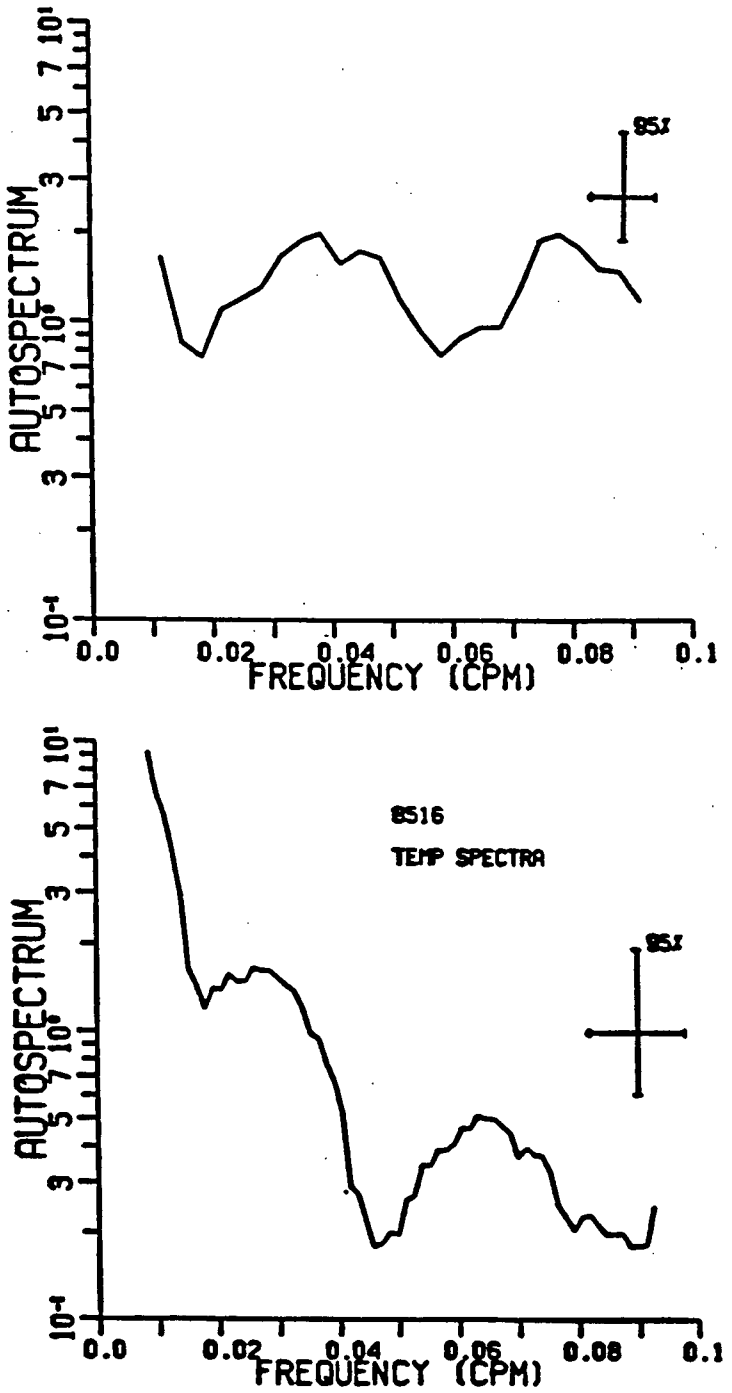

Figure 48 . Autospectrum G^{γ} for all fish tracked in both years (upper frame). G^{α} (T data) for 8516 (tracked in the SG) is shown in the lower frame.

$G^{\alpha,\gamma}$ results are in general agreement with those derived from $R^{\alpha,\gamma}_{\eta_r}$. There are no spectral peaks evident in α_i or γ_i for fish tracked in DP. The 18 min. cycle that was detected in $R^{\gamma}_{\eta_r}$ for 8511 is evident in $G^{\alpha,\gamma}$ for the majority of fish tracked in stratified regimes as a $.07 \pm .01$ cycles/min peak (period$\approx$ 15 min). Figure 48 shows a plot of a calculation of G^{α} for 8516 and G^{γ} for all fish tracked in both years. Note that there is evidence of an additional peak at approximately $.03 \pm .01$ cycles/min, corresponding to a period of$\approx$ 33 mins., in both (a) and (b) of Figure 48. This peak was observed in fish tracked in stratified regimes in the majority of T, S and D data. These results were verified by calculating variance preserving forms of $G^{\alpha,\gamma}$. However, large variances at low frequencies did indicate the existence of trends in α_i and γ_i. Similarily, Table 8 shows that trends exist in some of the linearly de-trended data. Thus, this form of trend removal was not successful in all cases. However, in cases where linear de-trending was appropriate significant spectral contributions are evident at the same frequencies as those cases where trend removal was not completely successful. Thus, trend removal was not necessary to resolve these peaks.

Given that 95% confidence implies that noise alone will produce a similar result in 1 out of 20 records and that the peaks in $G^{\alpha,\gamma}$ are not large compared to the error bars, these periodicities are considered significant for two physical reasons:

1.) Spectral peaks in the tracking data for the QCST/JS and SG oceanographic regimes could arise due to the internal scales of motion inherent in the density structure. The internal wave cut-off frequency (the Brunt-Vaisala frequency, N^2) in these regimes is at least an order of magnitude greater than the observed fre-

quencies in the tracking data. In the homogeneous waters of DP, N^2 is of the same order of magnitude as the observed frequencies and may therefore explain why no spectral contributions were detected in this regime. However, it is extremely unlikely that the moving platform from which the CTD measurements were made could resolve the same frequencies in different density stratification. Moreover, it is not known what external or internal forcing would produce motions at these periods. The conclusion, then, is that these frequencies do not arise due to purely dynamic oceanographic causes.

2.) They occur in fish that appeared both oriented and disoriented. 8511 and 8603 were disoriented (swam continuously northwestward away from the Fraser River) throughout the duration of their tracks. 8514, 8516, 8606, 8611, and 8613 all displayed portions of oriented (swam southeastward towards the Fraser River) and disoriented behaviour.

It is somewhat co-incedental that one frequency is twice the other. If the diving velocity (depth/min) were constant for oriented and disoriented fish, and the depth of successive dives was different, it would appear to the FFT algorithm that there are two separate frequencies when, in fact, there is only one. However, the diving velocity, as is discussed in §2.4.4: (f), is not the same for oriented and disoriented fish and the FFT algorithm does resolve two true, distinct peaks.

It is hypothesized that the two spectral peaks correspond to two distinct modes of behaviour in stratified regimes. The higher frequency (ca. .07 cyles/min)

corresponds to searching behaviour (Westerberg, 1982; 1985; Døving *et al.*, 1985) in disoriented fish. The lower of two frequencies (ca. .03 cycles/min) represents depth distributions associated with oriented fish. These fish were observed to swim at relatively constant depths and to make infrequent but periodic sudden vertical excursions. Time series data for completely disoriented fish (ie. 8511 and 8512) do not have significant spectral contributions at this lower frequency while data for fish displaying oriented and disoriented swimming behaviour (ie. 8516) contain both spectral peaks.

Composite spectrums were produced in order to decrease the 95% limits and more completely resolve the observed frequencies. G^{γ} is shown in Figure 48 for all fish tracked in 1985 and 1986 in QCST, JS and the SG. Although the 95% confidence interval is reduced, the peaks remain only marginally significant.

2.4.3: Energy Expenditure

Periodicity in the data deduced from spectral analysis did not directly reveal any relations between the physical oceanography and the fish's vertical distribution. Periods of approximately 15 and 33 minutes were found in oriented and disoriented fish tracked in QCST, JS and the SG but not in DP. These periods were also more apparent in fish tracked in regions where the T gradients were larger (SG and QCST). As an intrinsic depth distribution was not apparent and the calculated frequencies, in general, appeared related to searching for migratory cues, a more direct approach to determining any relationship between the hydrography and the fish was considered.

It was observed that sockeye swimming in regions of little or no stratification

frequently made a series of steep dives and ascents. Moreover, it was also observed, at least qualitatively, that sockeye swimming in the homeward direction usually swam within a relatively narrow range of depths as opposed to those fish who appeared disoriented. A quantitative estimate of this behaviour was considered in terms of the energy expended swimming vertically and horizontally.

The energy expended by migration over long distances dictates that economical choices be made between foraging for food, searching for migratory cues and clues, swimming speed and direction (M^{c}Keown, 1984; Weihs, 1987). Energy budgets for fishes have evolved to the generally accepted form (Brafield, 1985):

$$C = P + R + U + F \tag{2.7}$$

where C is the energy input (ingested food), P is the energy accumulated as growth of the somatic and reproductive tissues, U + F is the energy lost as waste (urine and feces respectively) and not available for growth or metabolism, R. Metabolism, R, reflects the energy lost as heat. This heat loss is composed of the fish's basal metabolism, the energy expended in a resting, non-stressed 'basic' state, and the energy expended in specialized activities such as swimming, feeding, aggression, migration, spawning, etc. The vast majority of energy requirements for fish are incurred in these specialized activities (M^{c}Keown, 1984). Brett (1983) concludes that for sockeye migrating in offshore waters, 44% of the total available energy is required for metabolic purposes and that up to 75% of the total available energy is required for riverine migration.

As a considerable portion of the energy budget for migrating sockeye is expended swimming, a quantitative estimate of the role the ambient density gradient may play in the vertical distribution of these fishes was attempted.

The basic premise is that, as in all of physics, there is a finite amount of energy available. Furthermore, as in all of nature, any animal must optimize energy expended in order to survive. In this case, the migrating salmon must reach its natal stream with sufficient energy reserves to spawn and thereby ensure the survival of the species. Considering the relationship between vertical and horizontal swimming, it is reasonable to expect that an excess of energy spent swimming vertically, for whatever purpose, will leave insufficient energy available for horizontal movement and vice versa. Both types of swimming behaviour are necessary; vertical movements may provide migratory clues (Brannon, 1982), orientation information (Westerberg, 1982; 1984; Døving, 1985), danger avoidance and access to food while horizontal movement, at the very least, is required to successfully complete the migration.

An approximation of R was attempted by assuming that all the energy lost as heat was expended by swimming and that $R \gg P + U + F$ at least for the duration of any particular track. Thus, R can be estimated by the work done by the fish against the fluid by swimming horizontally and vertically and the work done against the buoyancy force by swimming vertically. Energy expended swimming in the vertical is clearly related to the vertical density gradient and therefore, environmental factors may impose some form of control on the fish's vertical distribution.

To calculate the rate of work (the energy expended) by a fish swimming vertically, we first consider the vertical buoyancy force F_i. It is given as:

$$F_i = \left| \sum_{i=2}^{N} g(\rho_f - \rho_i) \times \mathrm{VOL} \right|$$

where g is the acceleration due to gravity, N is the number of observations made during all or part of a track(s), ρ_f is the density of the fish, ρ_i is the ambient

density and VOL is the approximate volume of the fish, estimated as .012 m^3. Thus, if $\rho_f \neq \rho_i$, F > 0 and the tracked sockeye must expent energy to compensate for this additional force if constant depth is to be maintained.

Sockeye salmon are capable of maintaining neutral buoyancy (ie. $\rho_f = \rho_i \Rightarrow F \equiv 0$) in the water column by means of a swim bladder connected to the esophagus (Gee, 1983). The fish's density can be matched to the ambient density by forcing gases into or extracting gases from the swim bladder either directly by gulping or eructing gases , or directly by osmosis (Gee, 1983). The time lag between change of depth and achieving neutral buoyancy by the above mentioned means is not precisely known. In addition, numerous fishes have been observed to compensate for non-neutral buoyancy by coupling swimming speed and angle of attack (the longitudinal angle of the fish relative to the horizontal). An increase or decrease in hydrodynamic lift can therefore be generated (Magnuson, 1978; Webb and Weihs, 1983) to compensate for the hydrostatic buoyancy forces. For simplicity, it was assumed that the change in depth of the fish and the resulting change in the buoyancy force was compensated for immediately at each new depth by utilizing the swim bladder and/or changing swimming speed and angle of attack. Thus, $\rho_f \equiv \rho_i$ and the vertical buoyancy force $F^V_{B_i}$ is given as:

$$F^V_{B_i} = \left| \sum_{i=2}^{N} g(\rho_i - \rho_{i-1}) \times \mathrm{VOL} \right| \tag{2.8}$$

The energy expended to achieve neutral buoyancy was assumed to exactly balance the change in buoyancy forces between observed depths. (2.8) implies that if $\rho_i = \rho_{i-1}$, then $F^V_{B_i} \equiv 0$. Hence, no energy is expended by the fish compensating for non-neutral buoyancy within vertically homogeneous density fields.

The rate of doing work against the buoyancy force $W^V_{B_i}$, was calculated as

(Webb, 1978):

$$W^V_{B_i} = F^V_{B_i} \times V^V_i \qquad i = 2,3\cdots N-1 \tag{2.9}$$

where the absolute value of vertical velocity, V^V_i, was calculated using a centered second order finite difference scheme. This is given by:

$$V^V_i = \left| \frac{(D_{i+1} - D_{i-1})}{2 \times 60} \right|. \qquad i = 2,3,\cdots N-1. \tag{2.10}$$

V^V_i has units of ms^{-1} as observations of depth, D, were made every minute.

The rate of work done by a swimming fish against a fluid is related to the hydrodynamic drag, DR_i (Webb, 1978) where:

$$\mathbf{DR}_i = .5 \times CD_i \times |\bar{\rho}_i| \times S \times |\mathbf{V}_i| \times \mathbf{V}_i \tag{2.11}$$

Some simplifications of (2.11) are possible as:

$$|\mathbf{V}_i|^2 = (V^H_i)^2 + (V^V_i)^2. \tag{2.12}$$

where V^H_i is the horizontal velocity and $V^H_i \gg V^V_i$. (2.12) may be re-written as:

$$|\mathbf{V}_i|^2 \approx (V^H_i)^2. \tag{2.13}$$

The vertical DR^V_i, and horizontal, DR^H_i, components of (2.11) using (2.13) are:

$$DR^V_i = .5CD^V_i |\bar{\rho}_i| S V^H_i V^V_i; \tag{2.14}$$

$$DR^H_i = .5CD^H_i |\bar{\rho}_i| S (V^H_i)^2. \tag{2.15}$$

S, the wetted surface area of the fish, is taken to be 0.10 m^2. In (2.14), the mean density, $\bar{\rho}$, is simply:

$$\bar{\rho} = (\rho_i + \rho_{i-1})/2 \qquad i = 1,2,3\cdots N$$

and in (2.15), $\bar{\rho}$ is taken to be the average ambient density of the entire track. Thus, for (2.15), we have:

$$\bar{\rho} = \frac{1}{N}\sum_{i=1}^{N}\rho_i.$$

The vertical drag co-efficient, CD_i^V, may be expressed as a function of the vertical Reynolds number, R_i^V. For laminar boundary layer flow, CD_i^V is calculated as:

$$CD_i^V = (4.2)(1.33)\left(R_i^V\right)^{-1/2} \tag{2.16}$$

The factor 4.2 arises as a result of a correction for pressure drag (Bainbridge, 1961) and for the undulatory motion associated with propulsion (Lighthill, 1971). The average swimming speed for all fish was calculated to be approximately 1.0 m/s (Quinn *et al*, 1989). At these velocities, the boundary layer may be expected to be laminar (Webb, 1975; Blake, 1983). However, (2.16) is recognized as a simplification and will only give reasonable estimates of the drag co-efficient for streamlined bodies at small flow speeds. At higher flow speeds, (2.16) underestimates the the drag co-efficient. R_i^V defined as:

$$R_i^V = \frac{V_i^V L}{\nu_i}$$

where L, defined as the characteristic fish length, is taken to be .60 m.

Variations in temperature can cause significant variations in the kinematic viscosity , ν, and therefore R_i^V (Webb and Weihs, 1983). Considering these variations, ν_i was calculated from the empirical formula (Weast, 1974):

$$\nu_i = \frac{10^{a_i}}{\bar{\rho}}; \tag{2.17}$$

$$a_i = \left[\frac{1301}{998.333 + 8.1855(T_i - 20) + 0.00585(T_i - 20)^2} - 3.30233\right] \times 10^{-1}.$$

The rate of work done by the fish swimming vertically against the fluid is calculated as (Webb, 1978):

$$W^V_{F_i} = DR^V_i \times V^V_i. \tag{2.18}$$

Finally, the total rate of work done by the fish swimming vertically, W^V_T, can now be calculated using (2.10) and (2.17). We have:

$$W^V_T = \sum_{i=2}^{N} (W^V_{B_i} + W^V_{F_i}). \tag{2.19}$$

It now remains to estimate the work done by the fish swimming horizontally. The reader will recall that we have considered horizontal gradients of density negligible in the regions where tracking was carried out. This assumption in conjunction with those used to construct the estimate for R imply that we need only consider the work expended by swimming against the fluid. The horizontal drag co-efficient, CD^H_i is analogous to (2.16) and is given as:

$$CD^H_i = (4.2)(1.33)\left(R^H_i\right)^{-1/2}$$

and R^H_i, the horizontal Reynolds Number is taken as:

$$R^H_i = \frac{V^H_i L}{\nu_i}.$$

The total work expended by swimming horizontally is analogous to eq.(2.19) and written as:

$$W^H_T = \sum_{i=2}^{N} (DR^H_i \times V^H_i). \tag{2.20}$$

A representative plot of the total work rates vs time is shown in Figure 49 for 8516 and 8603. It can be seen that intermittency is common to all these figures.

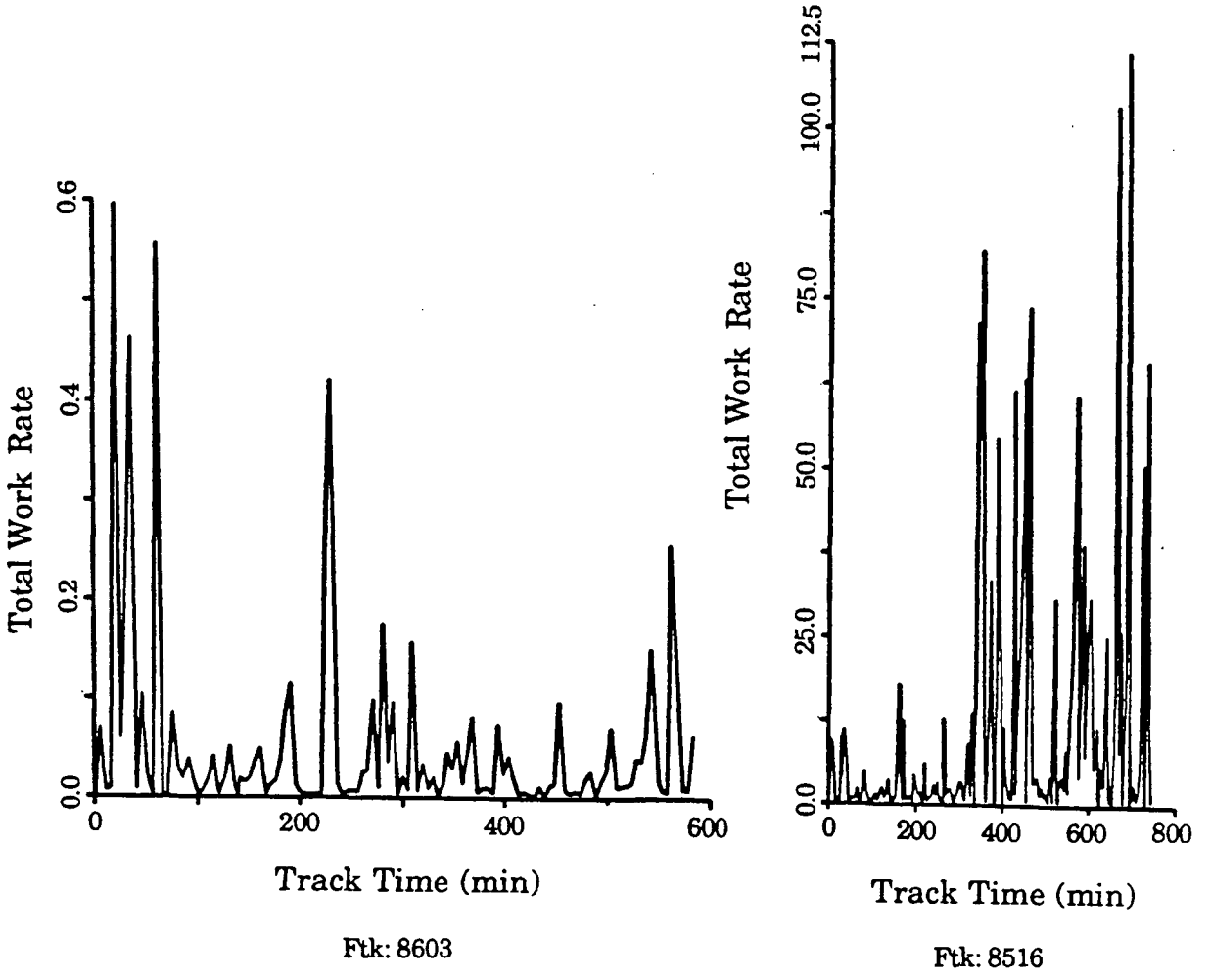

Figure 49 . Total work rate considering rate of energy expenditure by swimming vertically and horizontally. Units of work rate are $Joules \cdot min^{-1}$. Elapsed track time is shown on the x-axis. Normalized area represents the average work rate over the entire track in $Joules \cdot min^{-1}$. 8516 was tracked in the central SG and 8603 central QCST.

Although it appeared during tracking that most of the fish were generally swimming in a steady fashion, calculations of work rate show that energy expended swimming varied a great deal over the duration of the track. Laboratory studies on sockeye metabolic rates (Brett, 1963) give estimates of energy expenditure of approximately 45 cal/kg/day for fish migrating in riverine conditions. Considering a 3 kg fish and Brett's (1983) figure of 44% of total energy required for metabolic processes in offshore waters, approximately 79.2 cal/day are expended metabolically. The area under the curve shown in Figure 49 was numerically determined and this calculation represents the total energy expended by the fish swimming vertically and horizontally. The total energy expended divided by the track duration gives an average rate of energy expenditure. Table 9 gives the average energy expenditure (Joules $\cdot$ min^{-1}) for individual fish.

The extreme variability in the total work rate cannot be completely accounted for. Calculations of horizontal swimming velocity are not corrected for advection by near surface currents and this error does account for some of the observed variability. 8510 was tracked just north of Seymour Narrows when tidal currents were approaching a maximum. In this instance, advection accounts for the very large rate of energy expenditure shown in Table 9.

The variability in the total rate of work implies that different fish proportioned differing amounts of energy to swimming. This is in general agreement with Brett (1983) in that only 44% of available energy is used for migratory swimming and therefore the majority of energy available is being used in other parts of the energy budget. Table 9 also shows that the rate of work done against the buoyancy force is much less than that expended against the fluid alone. Considering the disparity

Table 9
The average work rate calculated for a complete track. Units are Joules · min^{-1}. The rate of energy expenditure swimming horizontally, the total rate considering vertical and horizontal swimming and the standard error associated with the total work rate are given for each fish.

Fish	Horizontal Work Rate	Total Work Rate	Standard Error (±)
8503	0.125	0.127	.004
8504	3.070	3.153	.103
8505	0.043	0.043	.002
8507	0.046	0.046	.002
8508	0.115	0.120	.006
8509	0.634	0.640	.006
8510	10.374	11.618	.284
8511	0.034	0.038	.002
8512	0.022	0.022	.001
8513	0.010	0.013	.005
8514	0.018	0.018	.003
8516	11.582	11.530	.175
8601	0.066	0.066	.001
8602	3.430	3.385	.045
8603	0.050	0.051	.002
8604	0.039	0.039	.002
8605	0.075	0.077	.003
8606	0.156	0.155	.014
8610	1.235	1.264	.003
8611	0.195	0.204	.003
8612	0.106	0.104	.003
8613	0.195	0.204	.005

in these work rates, it appears that the vertical difference in buoyancy force, and therefore the T and S gradients, do not inhibit the fish's vertical excursions.

The aspect ratio, AR, of a particular track is calculated as:

$$AR = \frac{DIST^H}{DIST^V}$$

where $DIST^H$ and $DIST^V$ represent the horizontal and vertical distances travelled. The aspect ratio gives a general indication of the fish's overall energy expenditure† with regards to either vertical or horizontal swimming as well as a measure of

† It should be noted that overall distance travelled gives no indication of the

orientation (Quinn and terHart, 1987). It is necessary, however, to determine some numeric standard that relates orientation and AR. The choice, while not completely arbitrary, is somewhat subjective. The choices made for the purposes of selecting an 'oriented' and 'disoriented' AR follow Quinn and terHart (1987), and are:

i.) The entire track of 8512 is representative of an extremely disoriented fish as very little progress over the the ground was made as well as frequent deep vertical excursions. The AR for this track was the minimum observed for both years and as such, was chosen as AR_{min}.

ii.) The portion of 8516 between 1531 hrs and 1730 hrs represents a very well oriented fish. In this case, the AR for this portion of this track was considered to be AR_{max}.

As $AR_{min} = 9.765$ and $AR_{max} = 75.141$, the calculated AR's for each track were normalized as:

$$AR_{\eta} = \frac{AR - AR_{min}}{AR_{max} - AR_{min}} \qquad 0 \leq AR_{\eta} \leq 1.$$

The normalized aspect ratio, AR_{η}, represents the relative degree of southeastward orientation where $AR_{\eta} = 1$ implies 'perfect' homeward orientation and $AR_{\eta} = 0$ implies complete disorientation.

---

acceleration. Swimming at maximum velocity (burst speed) incurs significant energy expenditures (Soofiani and Hawkins, 1985). Brett and Groves (1979) state that the metabolic cost of 20 seconds at bursting speeds equals 15 minutes of active metabolism (approximately 1–2 body lengths/sec for adults) or 3 hours of basal metabolism.

Table 10 gives both AR and AR_η. Clearly, orientation varies considerabley and is poor overall, but similar for all fish in all regimes. The parameter AR_η, when compared to the actual horizontal track of the tagged fish, yields a reasonable quantitative estimate of the relative degree of homeward orientation.

Table 10
Normalized aspect ratios, AR_η, for each fish. Total distances travelled (m) in the vertical and the horizontal as well as the raw aspect ratio, AR, is given.

Regime	Fish	Vertical distance travelled	Horizontal distance travelled	AR	AR_η
QCST/JS	8503	816.00	24599.50	30.146	0.312
	8504	846.00	18654.50	22.050	0.188
	8505	526.00	8573.41	16.299	0.100
DP	8507	624.00	8486.52	13.600	0.059
	8508	218.00	5594.66	25.664	0.243
	8509	2232.00	65348.06	29.278	0.298
	8510	760.00	15319.98	20.158	0.159
SG	8511	1163.00	11886.15	10.220	0.007
	8512	1330.00	12987.63	9.765	0.000
	8513	479.00	6989.42	14.592	0.074
	8514	1839.00	36883.71	20.056	0.157
	8516	1278.00	47996.96	37.556	0.425
QCST/JS	8601	1220.00	16283.64	13.347	0.055
	8602	699.00	30006.11	42.927	0.507
	8603	1197.00	19400.81	16.208	0.099
	8604	566.00	9999.15	17.666	0.121
	8605	596.00	14075.13	23.616	0.212
	8606	1015.00	51329.75	50.571	0.624
SG	8610	1034.00	54890.05	53.085	0.663
	8611	1237.00	23269.78	18.811	0.138
	8612	588.00	20948.08	35.626	0.396
	8613	743.00	16198.73	21.802	0.184

2.4.4: Swimming Velocity and AOV Relationships

As spectral analysis and AR_η gave some evidence for a possible relation between vertical/horizontal distribution and the sockeye's physical environment, a number of hypotheses were tested in an attempt to further quantify the results of previous sections.

AR_η implied that vertical and horizontal swimming velocities are negatively correlated as oriented and disoriented behaviour could be characterized by the depth and frequency of vertical excursions.

Without an acceptable model for relating vertical and horizontal swimming behaviour, or swimming behaviour and physical environment, scatter plots of several hypothesized relations for individual and composite fish tracks were produced. These plots were then examined for any discernable relations between the chosen variables. The intent here was to sacrifice detailed causal knowledge for general relationships.

Where applicable, all data were normalized using the following transformation:

$$x_\eta = \frac{x_n - x_{\min}}{x_{\max} - x_{\min}}, \qquad 0 \leq x_\eta \leq 1; \tag{2.21}$$

where x_n represents the n^{th} data point. This transformation provided a convenient scale with which to compare the different data subsets.

(a) Horizontal and Vertical Velocity

Figure 50 is an example of the scatter plot produced in an attempt to relate horizontal and vertical velocity. No correlation between horizontal and vertical velocity was evident in any of the scatter plots produced. The tendency for the

data values to lie against either axis is an artifact of the normalization procedure when a relatively large maximum value exists in the non-normalized data.

Fish tracked in the same oceanographic regimes were grouped together in order to reduce the statistical error inherent in small data sets. The resulting plots showed no clear evidence of any correlation. There is also no clear evidence indicating that fish tracked in a particular oceanographic regime were better oriented than in others. It was clear, however, that most data points were concentrated near the origin and that there is less chance of finding data points near the maximum in the horizontal or vertical swimming velocities. It is also interesting to note that the maximum swimming speed observed is well above the anaerobic threshold for sockeye salmon ($\geq$ 3 body lengths/sec or $\approx$ 1.8 m/sec; Brett, 1983).

(b) Depth Anomaly and Normalized Vertical Velocity

As for horizontal and vertical velocities, simple correlations were sought between depth and vertical velocity. Given a statistically significant mean depth of travel and the qualitative observation that well oriented fish tended to swim with infrequent shallow vertical excursions, the data were analysed to see if a tendency to return to a preferred depth (the mean) would manifest itself as an increase in vertical velocity the greater the deviation from the mean. If this were true, a positive correlation between depth and vertical velocity would exist.

Representative scatter plots of depth anomaly, D_{anom_i}, calculated as:

$$D_{anom_i} = \left| D_i - \frac{1}{N} \sum_{i=1}^{N} D_i \right|$$

and normalized vertical velocity, V_η^V are shown in Figure 51. It was evident from these calculations for all tracks in both years that D_{amom_i} and V_η^V for fish tracked

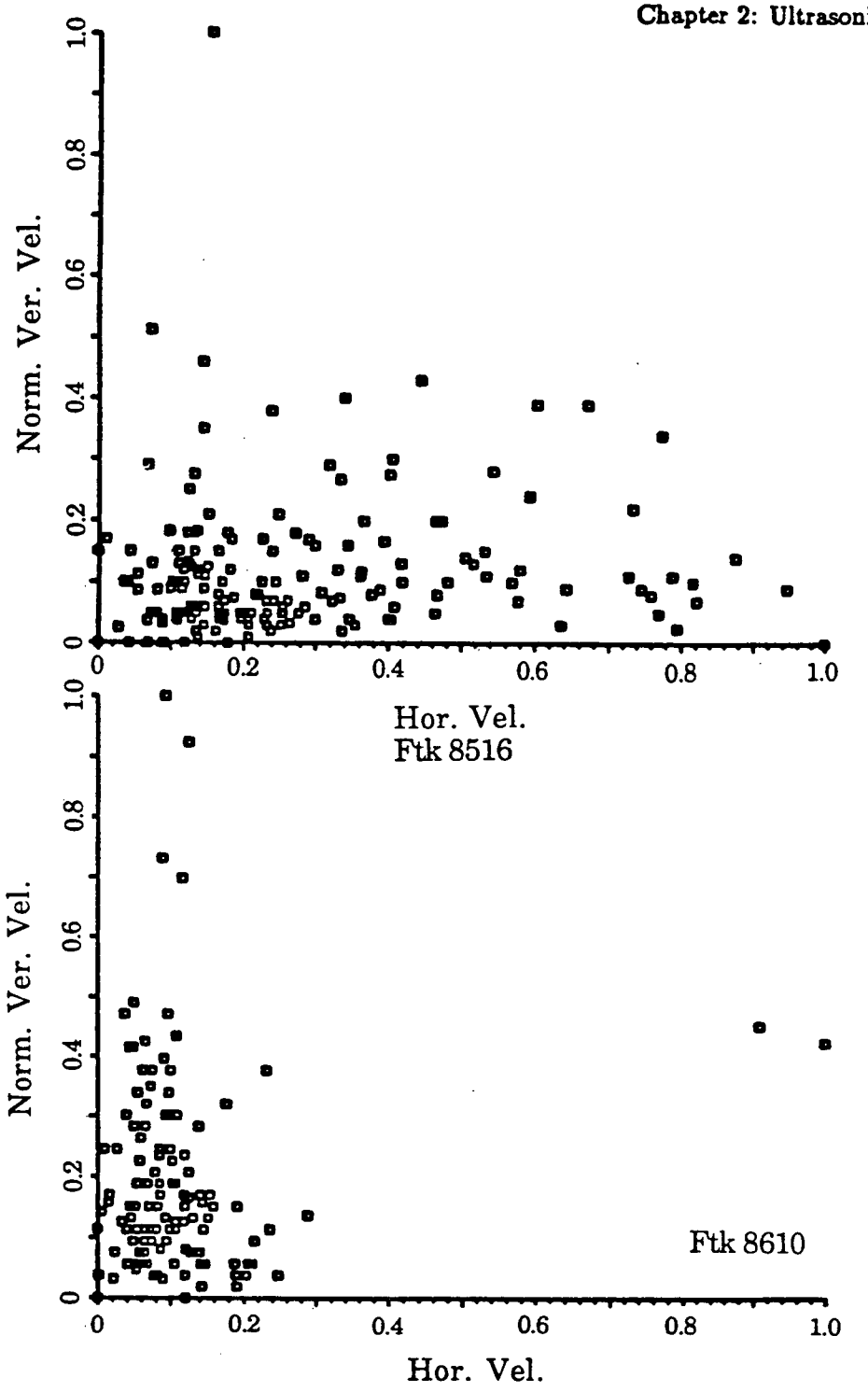

Figure 50 . Scatter plots of horizontal and vertical velocities for 8516, tracked in central SG near the BC mainland coast, and 8610, tracked in northern SG south of Cape Mudge.

in JS, QCST and DP were more positively correlated than those tracked in the SG for both years. Correlations in the SG were, in general, slightly negative while those for QCST, JS and DP were never negative.

(c) Depth and Normalized Vertical Velocity

Correlations bewteen D_{anom_i} and V_η^V suggested that the mean and therefore D_{anom_i} did not accurately represent the sockeye's depth distribution. Thus, unfiltered observations of depth and V_η^V were considered. Scatter plots of depth and normalized vertical velocity generally show a weak positive correlation. Given the scatter of the data, it is probably more appropriate to conclude that there is no clear evidence of a negative correlation. Nonetheless, there are several conclusions that can be made based on these plots.

Firstly, the mean depth is easily seen to be different for each oceanographic regime and for different years in the same regime. Secondly, as vertical velocity and depth are positively correlated, the greater the depth, the greater the vertical velocity. This correlation is stronger in the less stratified regimes of JS, QCST and DP than in the more strongly stratified SG (cf. Figures 52 and 53). The two tracking years, 1985 and 1986, are similar in that weaker stratification implied a stronger positive correlation between depth and vertical velocity.

In terms of orientation, the observation that well oriented fish tended to swim at a specific depth for relatively long periods of time is partially evidenced in these plots. Well oriented fish exhibited stronger positive correlations than those fish which were poorly oriented. Without prior knowledge of the fish's actual track, however, the difference in correlation coefficients alone is not sufficient to differentiate oriented from disoriented fish.

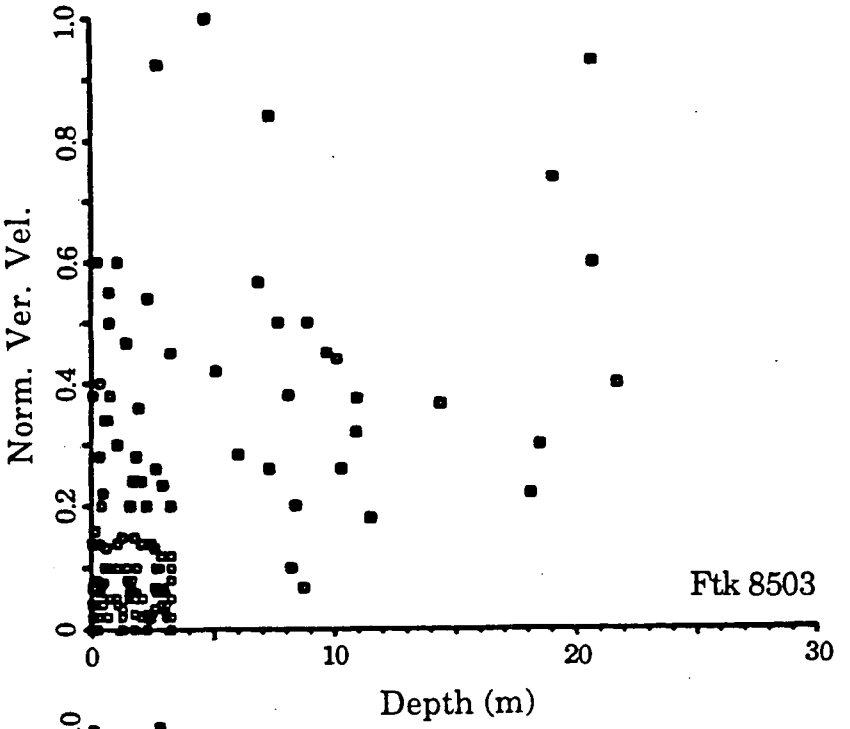

Ver. Vel. Max.=0.083
Ver. Vel. Min.=0.000
Lin. Cor. Cof.=0.418

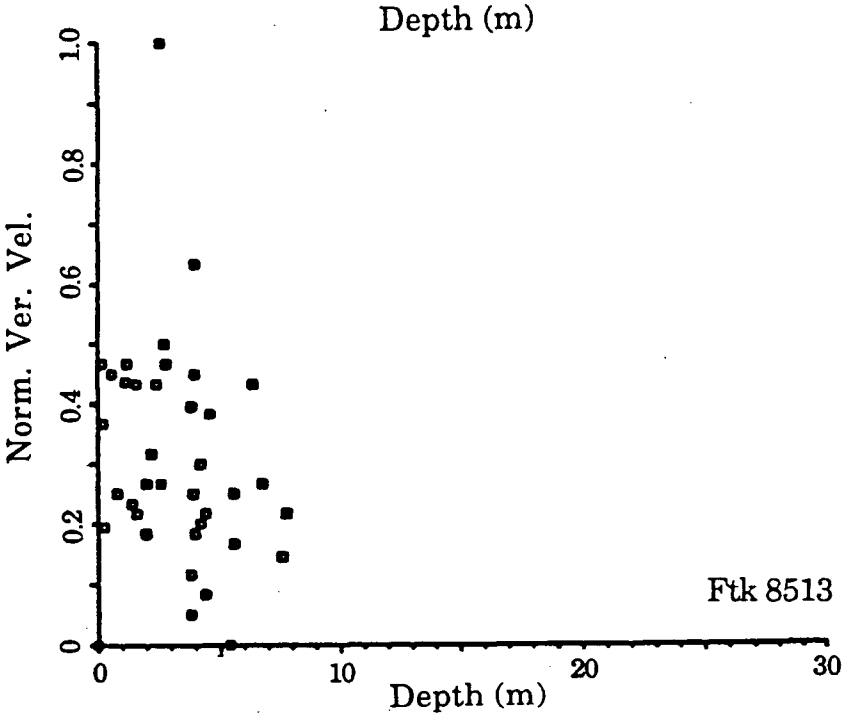

Ver. Vel. Max.=0.100
Ver. Vel. Min.=0.000
Lin. Cor. Cof.=-0.352

Figure 51 . Scatter plots of depth anomaly and normalized vertical velocity for 8503, tracked in the western extremity of JS, and 8513, tracked in the SG near the southern entrance to Sabine Channel. The depth anomaly represents the absolute value of the distance away from the mean depth.

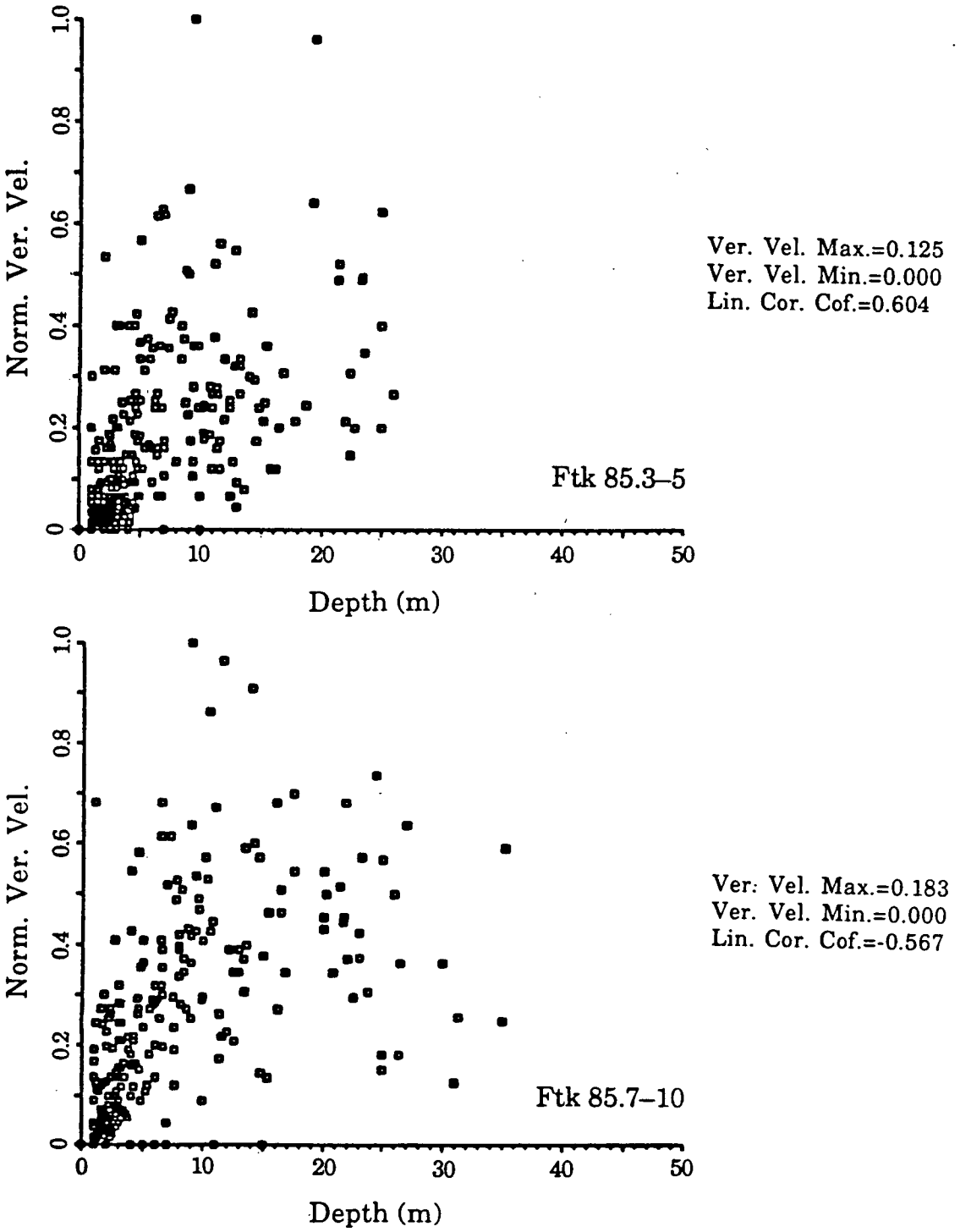

Figure 52 . Scatter plots of depth and normalized vertical velocity for the composite data 85.3–5 (fish tracked in QCST/JS) and 85.7–10 (fish tracked in the SG).

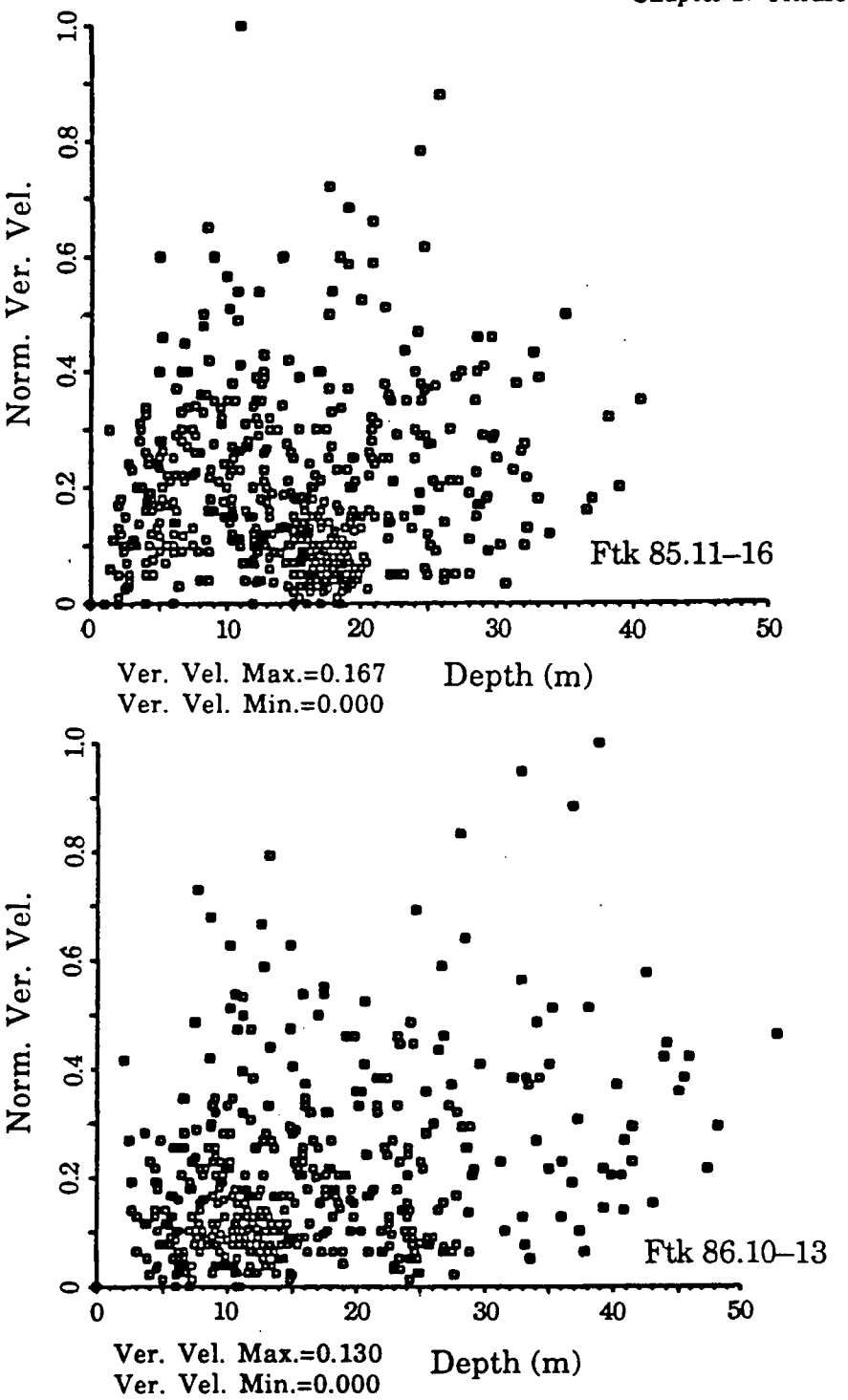

Figure 53 . Scatter plots of depth and normalized vertical velocity for the composite data 85.11–16 and 86.10 –13. These data are for all fish tracked in the SG for both years.

(d) Depth and Normalized T Gradient

Quinn *et al.* (1987) and Quinn and terHart (1988) could neither conclusively support nor refute, at least qualitatively, Westerberg (1982; 1984) and Døving (1985) who concluded that migrating Atlantic salmon used microscale temperature gradients as a migratory clue. It is well documented that salmonids possess highly sensitive olfactory systems (Bertmar and Toft, 1969; Døving, 1985) capable of differentiating fine and micro-scale hydrographic features. Specifically, the olfactory ability of many salmonids to differentiate water masses of different origins, as well as different pheromones, has been observed (Brannon, 1982). It does seem reasonable, then, to assume that such a highly evolved faculty has some specialized purpose. T gradients demark transitions from one T regime to another and within BC's inside passage, as the thermoclines and haloclines are coincidental, they demark different water masses of different origins. Given these abilities, the most efficient way to gather T or olfactory information is to remain in or near the region of maximum gradients in T or S. Thus, very little energy is expended in detecting the greatest possible difference.

Scatter plots of normalized T gradient $(\partial \mathrm{T}/\partial z)_\eta$ and depth showed that fish tracked in this study tended to occupy depths associated with the weakest T gradients. There were clearly more data points in the vicinity of the minimum gradient for the majority of fish tracked. In addition, sockeye that were, in general, well oriented had greater concentrations of data points in the region of the weakest T gradient. In fact, where CTD vertical profiles of T and S showed a thin distinct thermocline and halocline, there is a bifurcation of the data showing a concentration of data points corresponding to different relatively well-mixed layers separated by

the strong T and S gradients. Figure 54, showing a 8511 and 8514 tracked in the SG clearly illustrates this bifurcation.

In regions of little or no stratification (eastern JS and DP), individual scatter plots showed little tendency towards this phenomenen. Similarily, in the presence of a weak T gradient encompassing the observed range of fish depths, data points were equally distributed throughout the observed values for the T gradient.

Considering the T derivative and depth scatter plots, 8514 (Figure 54) provides an interesting composite of both types of observed behaviour. The CTD data shows a strong tidal influence present in the surface waters of the central SG. Warm, less saline water from Howe Sound and the Fraser River is seen to be advected by a strong flood tide into the region where 8514 was tracked . The presence of a surface mixed layer and a strong thermocline is eradicated by the advancing warm, comparatively fresh water originating in the south-central SG. The time evolution of the CTD data clearly shows the gradual weakening and deepening of the thermocline and the displacement of the surface mixed layer (terHart and Quinn, 1989). In conjunction with the above mentioned observations, 8514 does not exhibit any tendency toward the minimum T gradient when there are weak T gradients extending throughout the observed range of depths, as there were during the latter portions of the track. During the early portions of the track, when a thin thermocline and strong T gradients existed, 8514 exhibited a tendency toward the well-mixed regions separated by the thermocline and there was a bifurcation of the data points. The scatter plot of depth and $(\partial T/\partial z)_\eta$(Figure 54) is the sum of these behaviours; there is no clear tendency towards the maximum gradient and there is a bifurcation of the data points.

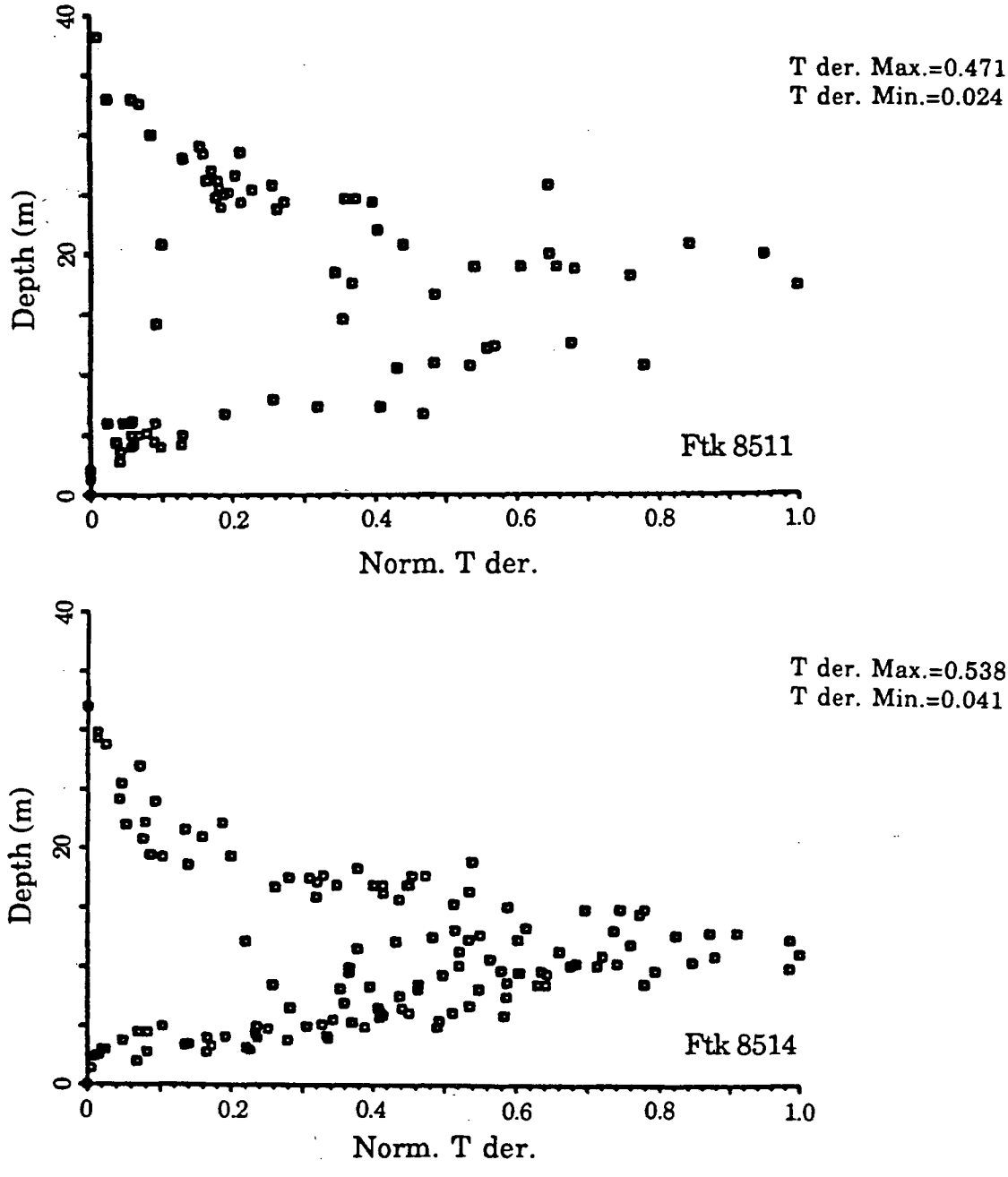

Figure 54 . Scatter plots of normalized temperature derivative, $(\partial T/\partial z)_\eta$ and depth for 8511, tracked in the SG near the northern tip of Texada Island, and 8514, tracked in cenral SG near the entrance to Sabine Channel.

(e) $(\partial T/\partial z)_\eta$ and V_η^V

Scatter plots of $(\partial T/\partial z)_\eta$ and V_η^V were produced in an attempt to further elucidate the relationship between T gradient and depth. $(\partial T/\partial z)_\eta$ and V_η were generally weakly correlated. Frequent, slow dives/ascents of short duration will produce plots similar to that of Figure 54 and discussed in §(d) above. Thus, observed depth and V_η^V will not relate to the maximums in $(\partial T/\partial z)_\eta$. The conclusion, then, is that sockeye did not remain within the greatest gradient, but frequently swam through it. Scatter plots of $(\partial T/\partial z)_\eta$ and D support this observation. This conclusion is in concert with those made by Westerberg (1984).

(f) Dive/Ascent Characteristics

Considering the time between successive dives/ascents and depth, Figures 55 and 56 show that these data correspond to two distinct modes of behaviour: frequent deep diving and infrequent deep, but frequent shallow dives and long durations at nearly constant depths. Disoriented fish (Figure 55: 8511) do not display the latter grouping of data points while oriented fish (Figure 55: 8516 and Figure 56: 8603, 8606), even if only for a portion of their track do.

Dive characteristics were further examined by considering dive duration. Figures 57 and 58 show dive depth and dive duration for disoriented (Figure 57: 8511, 8512) and oriented (Figure 58: 8516, 8610) fish in the SG. There is a tendency in oriented fish to make infrequent deep dives of long duration and frequent shallow dives of short duration. Hence, the depth distribution of an oriented fish will be characterized by relatively long periods spent within a narrow range of depths. Conversely, disoriented fish tended to make frequent, deep dives of short duration and

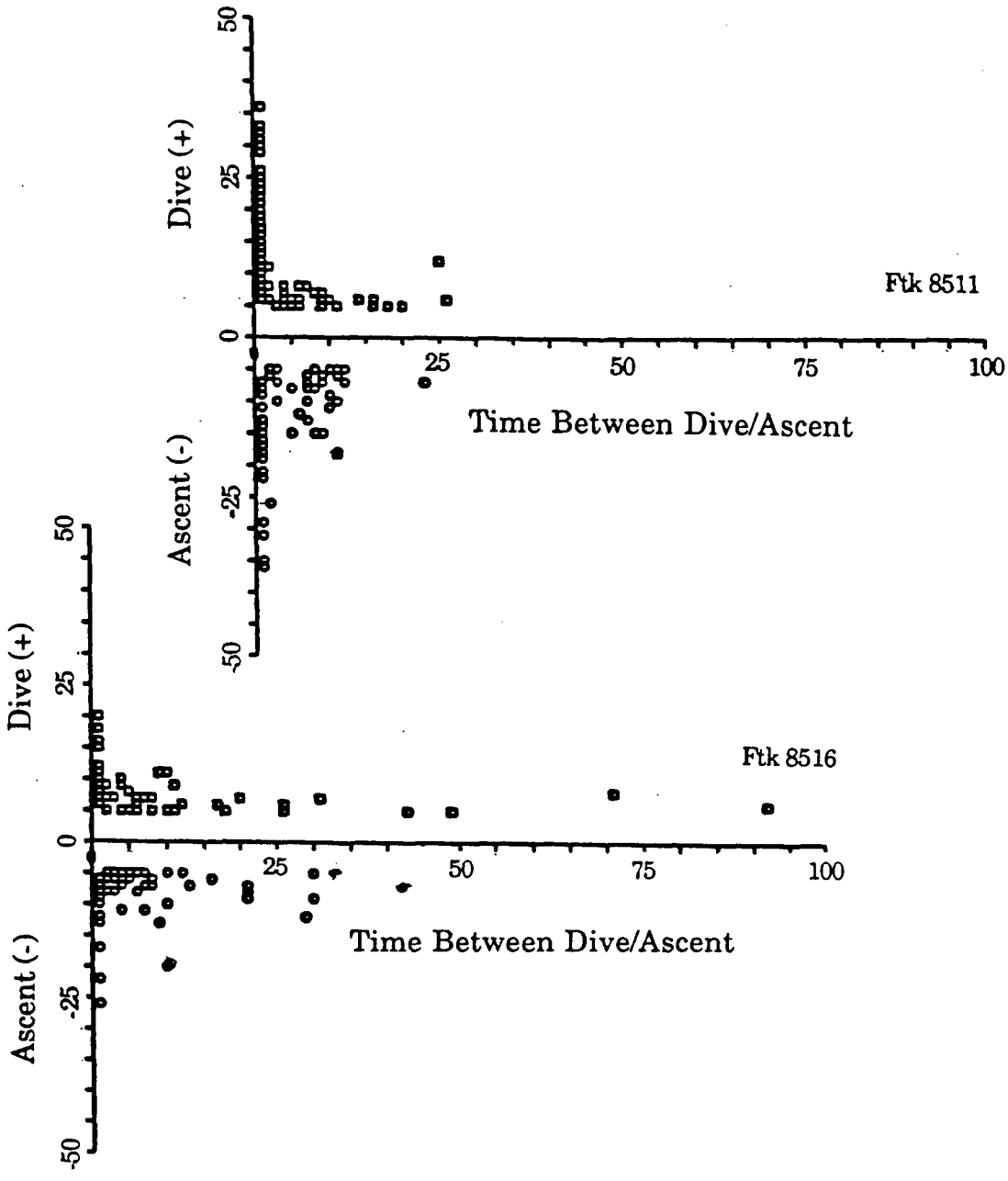

Figure 55 . Time between successive dives/ascents (min) versus depth of dive/ascent (m) for 8511, tracked in the SG near the northern tip of Texada Island, and 8516, tracked in central SG near the BC mainland coast. Data shown for 8511 is characteristic of disoriented fish; there are frequent deep dives and no periods of relatively constant depth. These data are in sharp contrast to those for oriented fish represented here by 8516.

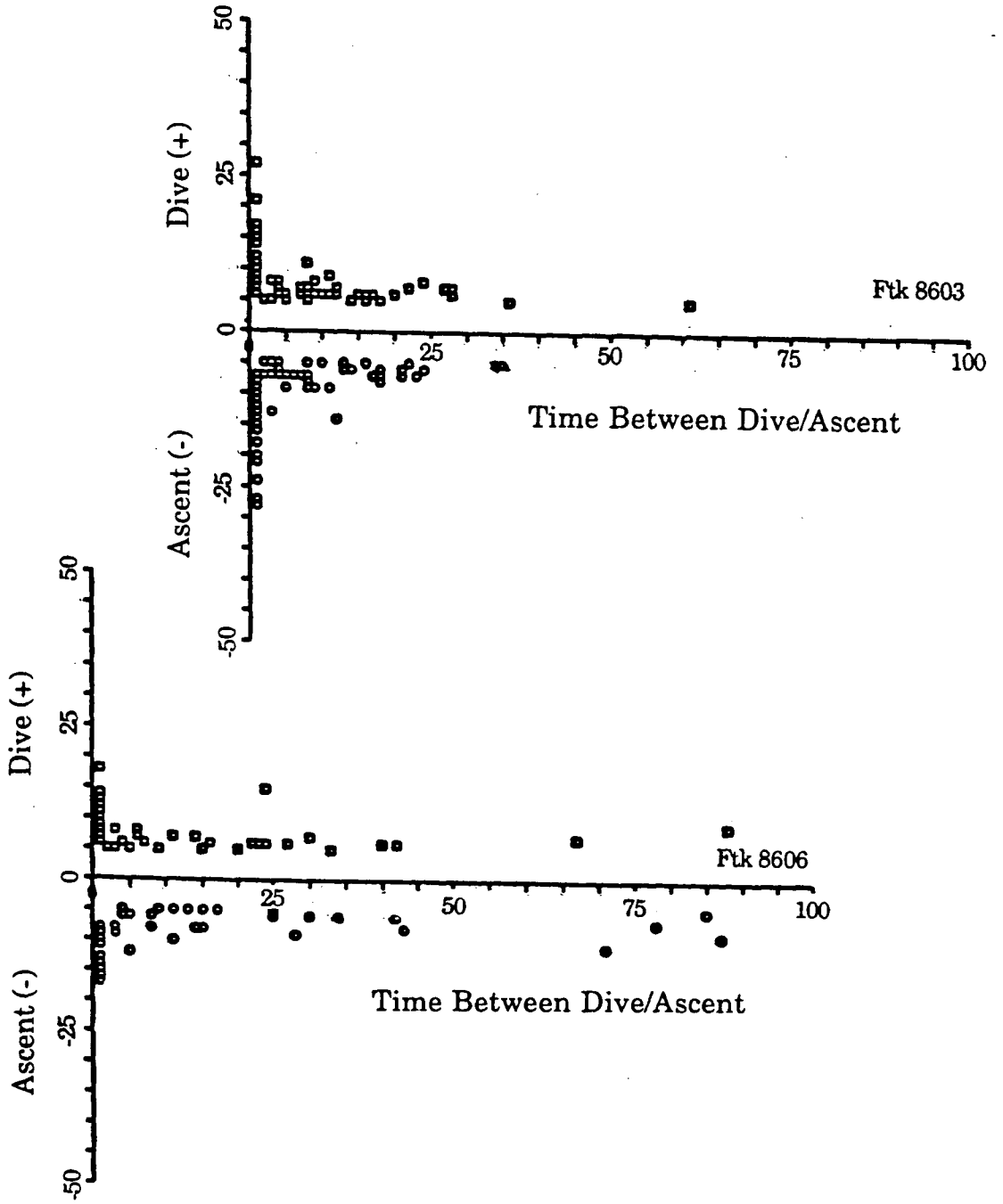

Figure 56 . Time between successive dives/ascents (min) versus depth of dive/ascent (m) for 8603 and 8606 (both tracked in QCST). These data are characteristic of oriented fish in that there are relatively infrequent dives and long periods spent at constant depths.

spent little time at relatively constant depths. These results are in good agreement with qualitative observations of depth distributions made earlier.

Table 11 shows the least-squares linear fit to the dive and duration data for each fish. The slopes of the linear fit to these data are different for oriented and disoriented fish in different oceanographic regimes (cf. fish tracked in DP where all fish were disoriented and those tracked in any other regime) implying the diving characteristics for oriented and disoriented fish differ depending on stratification. Note that the mean slopes for these lines are different for different years in the same regimes. In addition, the magnitude of the slope is inversely proportional to orientation.

2.4.5: Dimensional Analysis

Investigators have had success correlating physical variables such as freshwater run-off, sea-surface T , S, sea-surface height, etc (Favorite, 1961; Wickett, 1977; Burgner, 1980; Mysak *et al.*, 1982; IPSFC, 1984; Hamilton, 1984; Blackbourn, 1987; Groot and Quinn, 1987, Xie and Hsieh, 1989) with run timing and/or horizontal distribution. It must be remembered, however, that correlation is not a necessary or sufficient condition for cause. To date, a significant correlation between some physical parameter and a salmon's vertical distribution has not been found, let alone a causal relationship. In an effort to identify any possible relationship between the salmon's physical environment and its vertical distribution, dimensional analysis was employed.

Dimensional analysis techniques allow one to determine the functional relationship between groups of variables (Binder, 1973) without exactly knowing the

Table 11
Linear least squares fit to the dive duration data for each fish. Intercept, b, and slope, m, are shown for each fish. The standard error is given for b and m. Fish order is by orientation by regime and year. Oriented and disoriented fish are represented by the subscripts 'o' and 'd' respectively

Fish	Regime	b	(±)	m	(±)
8503_o	JS(w)	2.96	0.82	2.56	0.34
8504_d	QCST	3.14	0.59	2.08	0.15
8505_d	JS(w)	4.01	2.35	4.29	1.19
				$\bar{m} = 2.98 \pm .42$	
8507_d	DP	1.70	1.88	6.99	0.96
8509_d	DP	6.17	1.04	3.44	0.49
8508_d	DP	4.86	2.06	2.46	0.86
8510_d	DP	4.05	1.32	4.14	0.58
				$\bar{m} = 4.26 \pm .38$	
8516_o	SG	5.40	0.85	1.21	0.34
8513_o	SG	5.19	1.06	1.29	0.50
8514_o	SG	2.30	0.78	3.09	0.28
8511_d	SG	0.75	1.25	4.11	0.35
8512_d	SG	2.67	0.66	2.53	0.17
				$\bar{m} = 2.47 \pm .15$	
8602_o	QCST	3.45	1.31	2.17	0.53
8606_o	QCST	2.69	0.58	2.56	0.26
8603_d	QCST	2.45	0.84	2.25	0.28
8605_d	QCST	7.19	1.35	0.26	0.55
8604_d	QCST	3.92	1.65	1.36	0.65
8601_d	QCST	5.55	0.71	1.07	0.28
				$\bar{m} = 1.61 \pm .18$	
8612_o	SG	4.44	1.04	0.91	0.39
8610_o	SG	6.96	1.30	0.68	0.66
8613_d	SG	6.38	1.19	0.81	0.36
8611_d	SG	2.83	0.73	2.57	0.20
				$\bar{m} = 1.24 \pm .22$	

underlying physics. The functional form of the relationship is provided at the expense of the detail.

The fish's vertical distribution may be represented by the absolute value of its vertical velocity, V. If V is large, the fish's vertical distribution is characterized

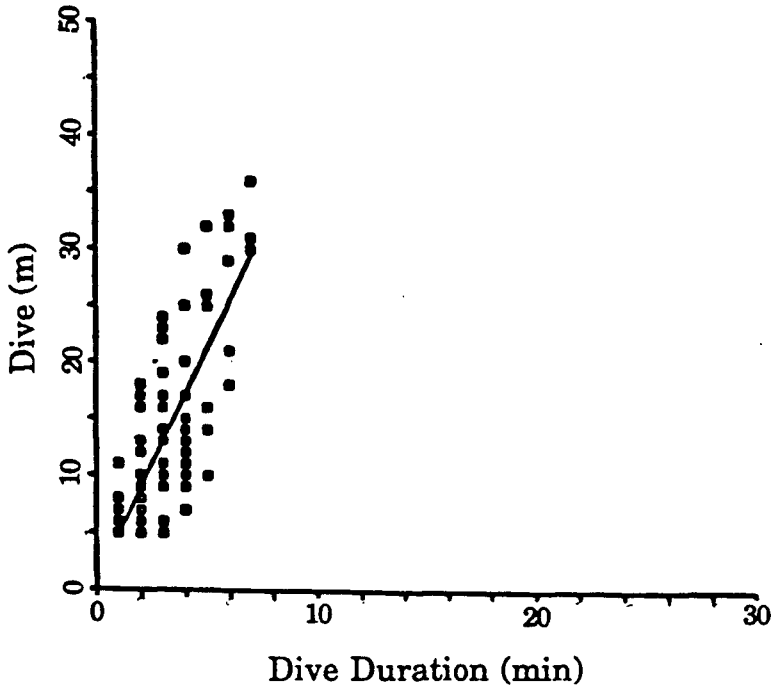

Ftk 8511
Slope: 4.11
Intcpt: 0.75

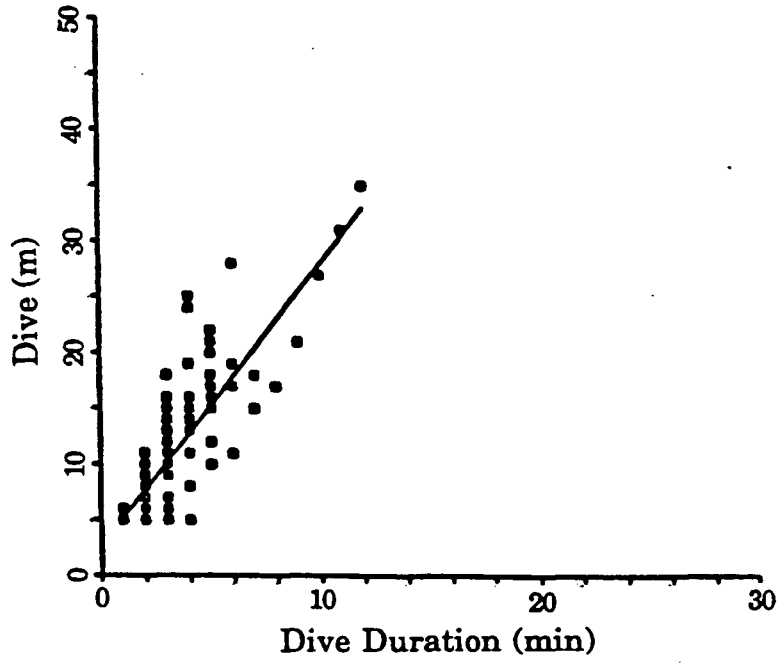

Ftk 8512
Slope: 2.53
Intcpt: 2.67

Figure 57 . Dive duration (min) vs depth of dive (m) for 8511 and 8512. Linear, least-squares best fit estimates are shown as solid straight lines through the data. Both fish were tracked in the SG near the northern tip of Texada Island and were considered disoriented.

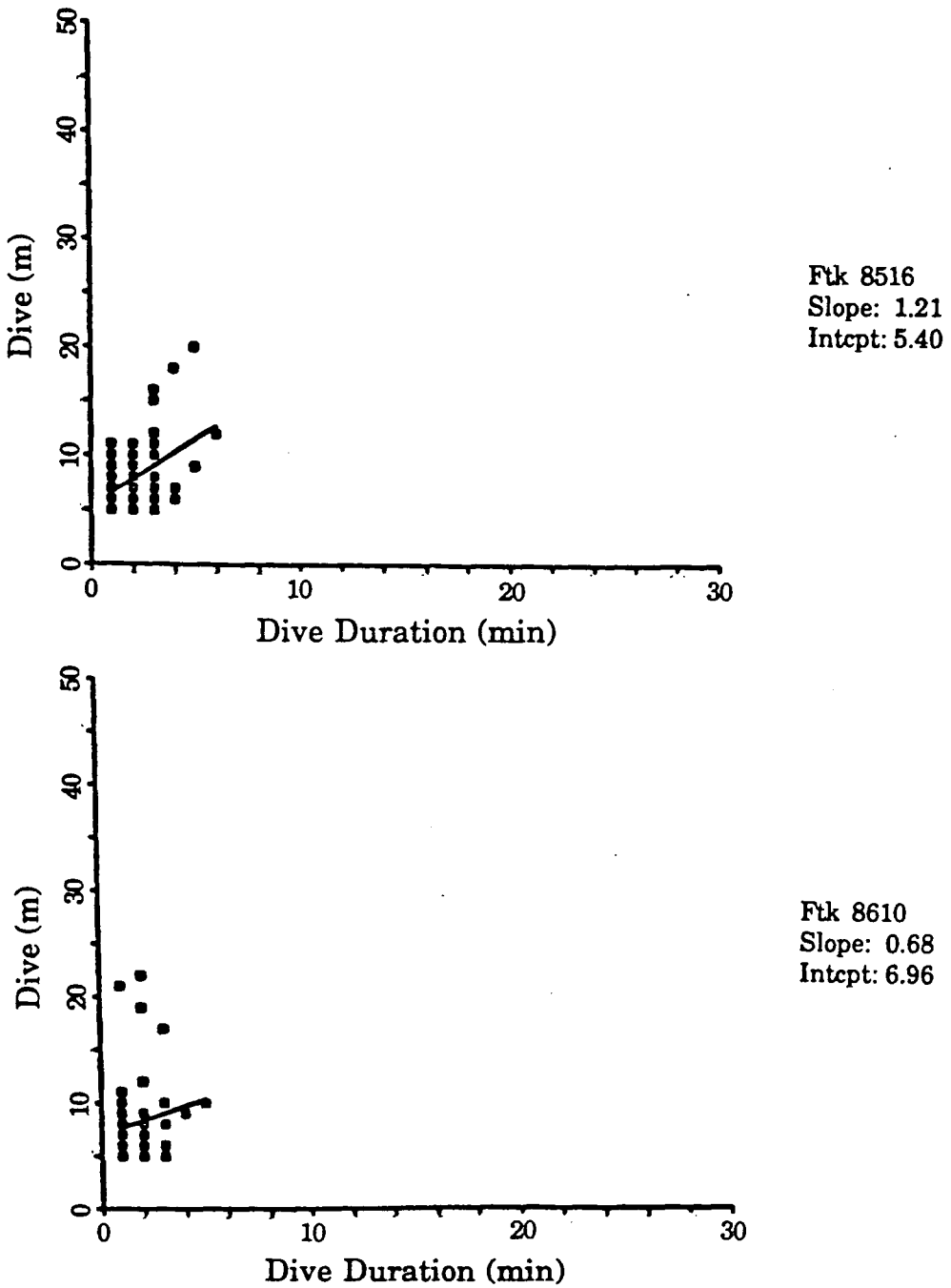

Figure 58 . Dive duration (min) vs depth of dive (m) for 8516, tracked in central SG near the BC mainland coast, and 8610, tracked in northern SG south of Cape Mudge. Linear, least-squares best fit estimates are shown as solid straight lines through the data. Both tracks are considered characteristic of oriented fish.

by frequent, large amplitude ascents and/or descents. If V is small, then depth changes tend to be infrequent and of small amplitude. Relevant physical variables were taken to be the temperature dependent fluid viscosity, ν, the fish's mass, M, the earth's gravitational force, G, and the buoyancy force, B, due to vertical density changes in the water column.

In terms of their dimensions, V, ν, B, G and M are:

$$V = \frac{L}{T},\ \nu = \frac{L^2}{T},\ G = \frac{L}{T^2},\ B = \frac{ML}{T^2} \text{ and } M = M$$

where L, M and T are the dimensions of length, mass and time respectively. We seek a dimensionally homogeneous relationship of the form:

$$V = f(B, M, \nu, G), \tag{2.21}$$

In terms of the appropriate dimensions, we have:

$$\frac{L}{T} \propto \left(\frac{ML}{T^2}\right)^a (M)^b \left(\frac{L^2}{T}\right)^c \left(\frac{L}{T^2}\right)^d \tag{2.22}$$

Equation (2.22) yields three equations for the four variables a, b, c and d. These three equations may be solved to give a, c and d in terms of b. The choice (2.21) yields the relationship:

$$V \propto B^{-b} M^b \nu^{1/3} G^{b+1/3}$$

which is re-written in dimensional form as:

$$V \propto (\nu G)^{1/3} f(\frac{MG}{B}). \tag{2.23}$$

Re-writing (2.23) will give a convenient set of non-dimensional coordinates:

$$\frac{V}{(\nu G)^{1/3}} \propto f(\frac{MG}{B}). \tag{2.24}$$

The choice (2.21) is not unique in that other equally valid relationships may be determined depending on the choice of variables. To test other possible solutions for any evidence of functional dependence, the following relations were also considered:

$$V = f(M, \nu, G, \partial\rho/\partial z) \tag{2.25}$$

and

$$V = f(M, \nu, \partial\rho/\partial z) \tag{2.26}$$

which yielded, respectively, the non-dimensional co-ordinates:

$$\frac{V}{(\nu G)^{1/3}} \propto \frac{(\partial\rho/\partial z)\nu^{8/3}}{MG^{4/3}} \tag{2.27}$$

$$\frac{V}{\nu} \propto \left(\frac{\partial\rho/\partial z}{M}\right)^{1/4} \tag{2.28}$$

Provided an appropriate choice of variables has been made, scatter plots of (2.24), (2.27) and (2.28) will reveal the form of the functional relationship between the non-dimensional variables. Figures 59 and 60 are representative plots of (2.24) and (2.27) and (2.28) respectively for one fish. Although all possible variables were not tested, the most reasonable choices were. These results suggest that physical variables alone are not sufficient to specify the sockeye's vertical distribution. Other undetermined behavioural factors, such as physiological requirements, may play an important role in motivating the fish's vertical movements.

2.5: Summary

Physical oceanographic influences on the estuarine phase of the return migration of sockeye salmon (*Oncorhynchus nerka*) were examined using data col-

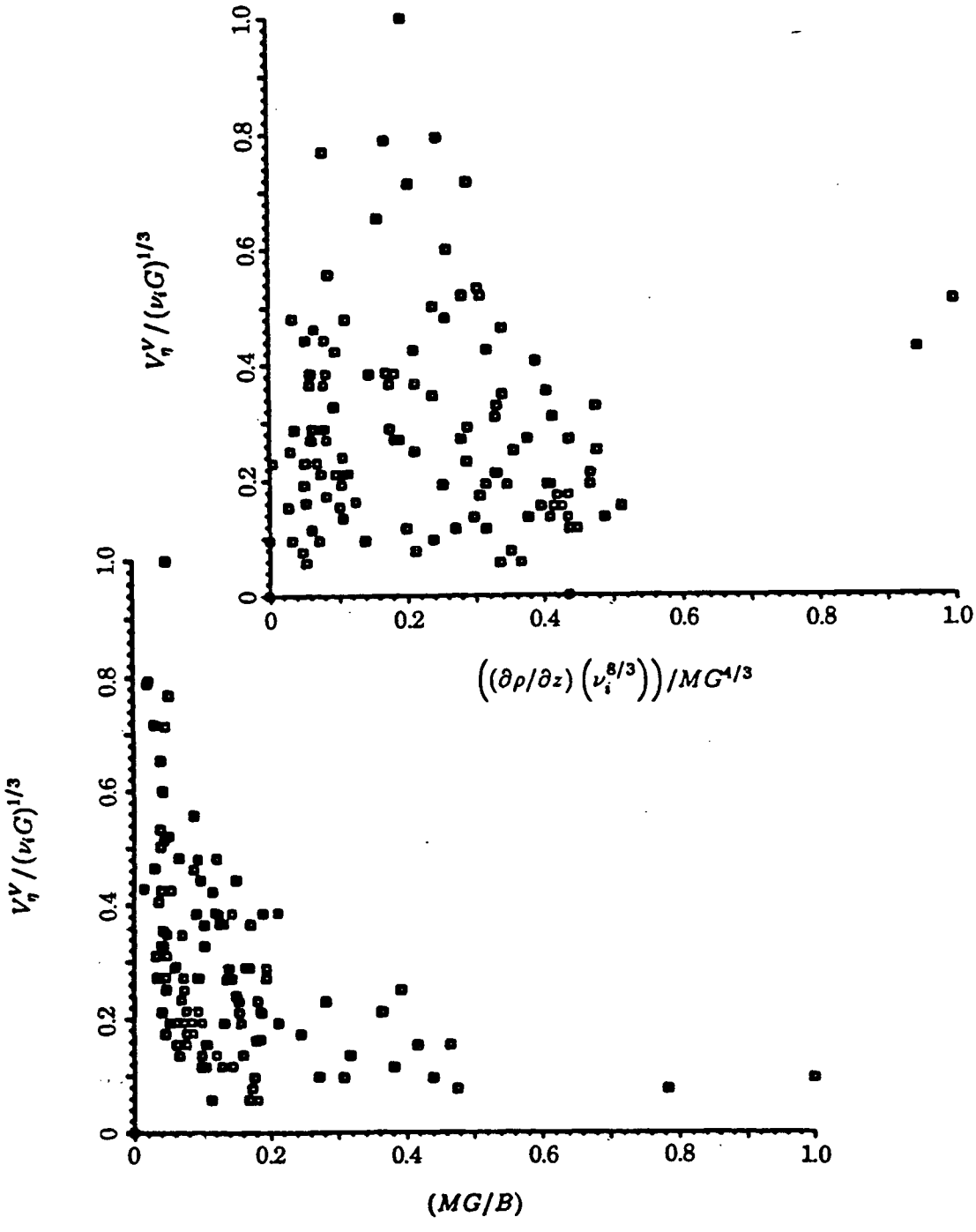

Figure 59 . Scatter plots of non-dimensional parameterization of ultrasonically telemetred fish tracking and physical oceanographic data. Data shown is for 8603 which was tracked in central QCST.

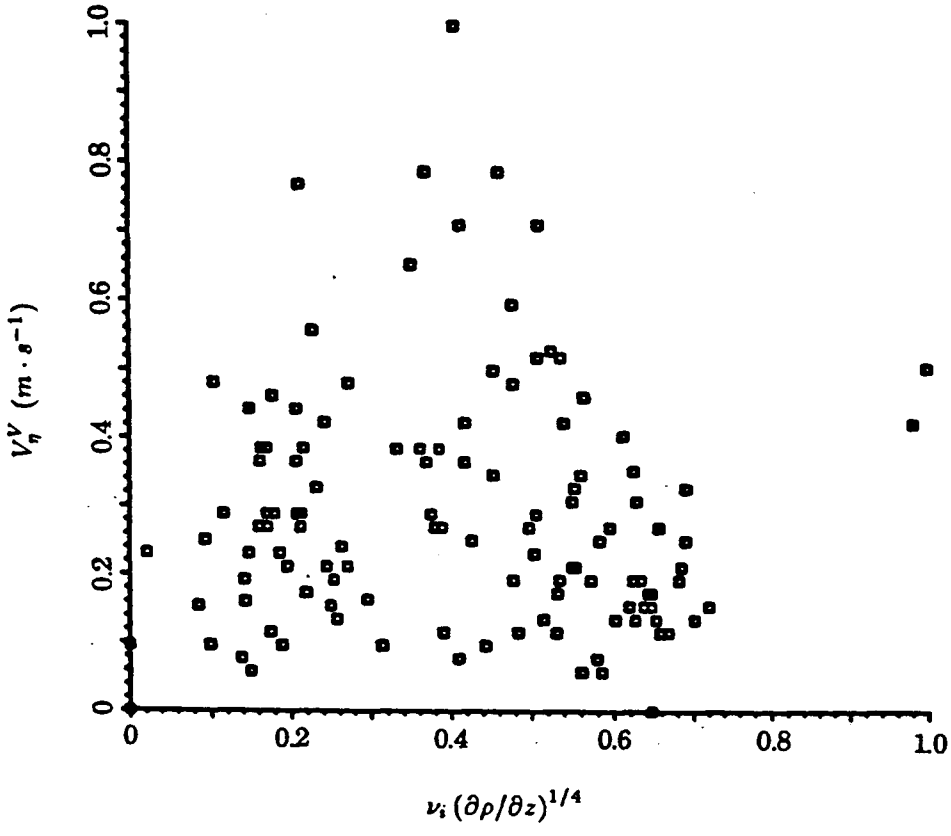

Figure 60 . Scatter plot of dimensional relationships determined by parameterization of ultrasonically telemetred fish tracking and physical oceanographic data for 8603. This fish was tracked in central QCST.

lected during two summers of ultrasonic telemetry and concurrent conductivity-temperature-depth casts. Twenty-two separate tracks were examined and an attempt to quantify the environmental factors influencing vertical and horizontal distribution was made.

The well-mixed, nearly homogeneous water of Discovery Passage was considered an experimental control in that sockeye tracked in this oceanographic regime must necessarily exhibit a depth distribution independent of a preferred temperature/salinity or temperature/salinity gradient. Although frequent vertical excursions qualitatively appeared to be a characteristic feature of fish tracked in vertically well-mixed waters, spectral analysis revealed no periodicity in the tracking data for Discovery Passage. Similar analysis of tracking data collected in oceanographic regimes with varying degrees of stratification showed statistically significant periodic vertical excursions of approximately 15.4 and 33.3 mins./cycle. Periodic movements quantitatively distinguished oriented or disoriented tracks, or portions thereof, in stratified regimes. The nature of cyclical vertical excursions is believed to be an orientation mechanism whereby disoriented fish 'sample' the available water column for orientation clues. This type of behaviour has been observed for other salmonids (Ichihara and Nakamura, 1982; Westerberg, 1982, 1984).

Calculations of work rate considering vertical and horizontal swimming and vertical density gradients show that energy expenditure was highly intermittent for all fish tracked. The high degree of variability in energy expenditure is partially caused by time varying swimming speeds and frequent burst swimming. Horizontal work rate was several orders of magnitude greater than the vertical work rate. Work done against vertical buoyancy differences was negligible compared to the work done

against the hydrodynamic drag. Thus, stratification did not limit or inhibit vertical excursions. Calculations of average energy expenditure (cal/track) also agree favourably with Brett (1983). However, several tracks show caloric expenditures beyond what may reasonably be assumed to be available.

The normalized aspect ratio, a linear transformation of the non-dimensional ratio of horizontal to vertical distance travelled, gave a clear indication of homeward orientation. However, scatter plots for individual and composite fish tracks revealed no relation between horizontal and vertical velocity.

Scatter plots of depth and normalized vertical velocity, V_η^V, were more positively correlated in regimes that were more weakly stratified. This result is in concert with the qualitative observation of the near-surface depth distribution of fish tracked in Discovery Passage and eastern Johnstone Strait. Depth and V_η were more strongly correlated in oriented than disoriented fish and this is an indication that well oriented fish remain at relatively constant depths for extended periods of time.

Observations of depth and normalized T gradient, $(\partial T/\partial z)_\eta$ showed that sockeye were more often observed at depths associated with the minimum in $(\partial T/\partial z)_\eta$, especially in regimes characterized by strong stratification. In regimes of weak or nearly uniform vertical gradients, observations of fish depth spanned the range of observed $(\partial T/\partial z)_\eta$. Vertical distribution relative to $(\partial T/\partial z)_\eta$ was similar in different oceanographic regimes regardless of the magnitude of the the gradients if the form of the stratification was similar. Scatter plots of $(\partial T/\partial z)_\eta$ and V_η^V were very weakly correlated and a consistent conclusion regarding depth, V_η and $(\partial T/\partial z)_\eta$is such that sockeye did not remain at depths associated with the

maximum gradients, but frequently swam through them.

Dive/ascent characteristics revealed two distinct modes of vertical movements. This result is in concert with those obtained from the spectral analysis. Time between successive dives showed that disoriented fish made frequent, relatively deep dives and rarely remained at constant depth while oriented fish made infrequent deep, but frequent shallow dives and often remained at constant depths. The slope of the least-squares linear fit to dive duration versus depth data shows that the rate of change of depth is, in general, greater for disoriented fish in all oceanographic regimes. In addition, the rate of change of depth for oriented fish is greater in regimes that are more weakly stratified.

Future field work in this area should be implemented so that the vertical, horizontal and spatial resolution of the physical oceanographic measurements and the vertical resolution of the tracking data be improved. The vertical and horizontal scales associated with the hydrographic parameters measured in this study were in the order of one and hundreds of meters respectively. In the future, measurements of these parameters and current shears should be made at scales as close as possible to the estimated sensing capabilities of the fish. Free-falling instrumentation and multiple vessels could provide the much more highly resolved data required. These data would not only provide a far more complete qualitative description of the tracked fish's vertical distribution, but also temperature, salinity and depth at scales commensurate with those of hydrographically borne orientation cues. Complete quantification of the relationship between the physical oceanography and the tracked sockeye's vertical distributinon must await improved field and theoretical studies.

As no clear quantitative relationship was found between physical oceanographic variables and vertical distributions, dimensional analysis was employed in an attempt to reveal the functional form of any relationship that might exist in the data. This attempt was unsuccessful and it can be concluded that physical variables alone were insufficient to specify the vertical distribution of the tracked sockeye. The numerous other attempts discussed previously would seem to support this generalization. An effective quantification of the sockeye's vertical distribution must somehow include the physiological and motivational state of the fish.

References

Arnold, G.P. and P.H. Cook, 1984: Fich migration by selective tidal stream transport: first results with a computer simulation model for the European continental shelf. In: McCleave, J.D., G.P. Arnold, J.J. Dodson and W.H. Neill (eds.), *Mechanisms of Migration in Fishes.* Plenum Press, New York, New York. p227–261.

Bainbridge, R., 1961: Problems of fish locomotion. Vertebrate Locomotion Symposium of the Zoological Society of London. 5: 13–32.

Bardach, J.E. and R.G. Björklund, 1957: The temperature sensitivity of some American freshwater fishes. *American naturalist*, 91: 233–251.

Blake, R.W., 1983: *Fish Locomotion.* University Press, Cambridge, England. 203pp.

Bendat, J.J and A.G. Piersol, 1971: *Random Data: Analysis and Measurement Procedures.* Wiley Interscience, New York, New York. 407pp.

Benjamin, T.P., 1968: Gravity currents and related phenomena. *J. Fluid Mech.*, 31: 209–248.

Binder, R., 1973: *Fluid Mechanics.* Prentice-Hall, Inc. Englewood cliffs, N.J.. 401pp.

Bertmar, G. and R. Toft, 1969: Sensory mechanisms of homing in salmonid fish. I. Introductory experiments on the olfactory sense in grilse of Baltic salmon (*Salmo salar*). *Behaviour*, 35: 235–241.

Bingman, C., M.D. Godfrey and J.W. Tukey, 1967: Modern techniques of power spectral analysis. *Trans. IEEE Audio and Electroacoustics*, AU–15.

Bingman, V.P., 1981: Savannah sparrows have a magnetic compass. *Anim. Behav.*, 29: 962–963.

Blackbourn, D.J., 1987: Sea surface temperature and preseason prediction of return timing in Fraser River sockeye salmon *Oncorhynchus nerka. Can. Sp. Publ. Fish. Aquat. Sci.*, 96: 296–306.

Bowman, M.J. and W.E. Essais, (eds), 1978: *Oceanic Fronts in Coastal Processes.* Proceedings of a Workshop Held at the Marine Sciences Research Center, May 25–27, 1977. Springer-Verlag, Berlin Heidelberg New York. 114pp.

Brafield, A.E., 1985: Laboratory studies of energy budgets. In: Tytler, P. and P. Callow (eds.), *Fish Energetics.* John Hopkins University Press. Baltimore, Maryland. p283–307.

Brannon, E.L., 1972: Mechanisms controlling migration of sockeye salmon fry. *Int. Pacific Salmon Fish. Comm. Bull.*, 21: 1–86.

Brannon, E.L., 1982: Orientation mechanisms of homing salmonids. In: Brannon, E.L. and E.M. Salo (eds.), *Proceedings of the Salmon and Trout Migratory Behaviour Symosium.* School of Fisheries, University of Washington, Seattle, Wa.. p219–227.

Brett, J.R., 1965: The swimming energetics of salmon. *Scientific American*, 213: 80–85.

Brett, J.R., 1983: Life energetics of sockeye salmon *Oncorhynchus nerka.* In: Osprey, W.P. and S.I. Lustick (eds.), *Behavioural Energetics: The cost of Survival in Vertebrates.* Ohio State University Press, Columbia, Ohio. p29–63.

Brett, J.R. and N.R. Glass, 1973: Metabolic rates and critical swimming speed of sockeye salmon *Oncorhynchus nerka* in relation to size and temperature. *J. Fish. Res. Board Can.*, 30: 379–387.

Brett, J.R. and T.P. Groves, 1979: Physiological energetics. In: Hoar, W.P., D.J. Randall and J.R. Brett (eds.), *Fish Physiology, Vol. VIII.* New York Academic Press, New York, New York. p279–352.

Buckley, J.P. and S. Pond, 1976: Wind and surface circulation of a fjord. *J. Fish. Res. Bd. Can.*, 10: 2265–2271.

Bull, H.D., 1936: Studies on conditined responses in fishes. Part VII. Temperature perception in teleosts. *Journal of the Marine Biological Association of the United Kingdom*, 21: 1–27.

Burgner, R.L., 1980: Some features of ocean migrations and timing of Pacific salmon. In: McNeill, W.J. and D.C. Himsworth (eds.). *Salmonid Ecosystems of the North Pacific.* Oregon State University Prees, Corvallis, Oregon. p153–164.

Daniel, F.N., 1985: Summer circulation of the waters in Queen Charlotte Sound. *Atmos. Ocean*, 23: 393–413.

Dodimead, A.J. 1980: A general review of the oceanography of the Queen Charlotte Sound–Hectate Strait–Dixon Entrance region. *Can. Manuscr. Rep. Fish. Aquat. Sci. No. 1574.* Dep. Fish. and Oceans, Pac. Biol. Stn., Nanaimo, B.C.. 248pp.

Dodson, J.J. and L.A. Dohse, 1984: A model of olfactory mediated conditining of directional bias in fish migrating in reversing tidal currents based on the homing migratino of American Shad (*Alosa sapidisisima*). In: M^{c}Cleave, J.D., G.P. Arnold and W.H. Neill (eds.). *Mechanisms of Migration in Fishes.* Plenum Press, New York, New York. p263–281.

Døving, K.B., H. Westerberg and P.B. Johnson, 1985: Role of olfaction in the behavioral and neuronal responses of Atlantic salmon, *Salmo salar*, to hydrographic stratification. *Can. J. Fish. Aqua. Sci.*, 42: 1658–1667.

Farmer, D.M. and H.J. Freeland, 1983: The physical oceanorgraphy of fjords. *Progress in Oceanography*, 12: 147–219.

Ewart, T.E. and W.P. Bendiner, 1981: An observation of the horizontal and vertical diffusion of a passive tracer in the deep ocean. *JPO*, 5: 95–107.

Favorite, F., 1961: Surface temperatures and salinity off the Washington and British Columbia coast, August 1958 and 1959. *J. Fish. Res. Bd. Can.*, 18: 311–319.

French, R., H. Bilton, M. Osako and A. Hartt, 1976: Distribution and origin of sockeye salmon (*Oncorhynchus nerka*) in offshore waters of the North Pacific Ocean. *IPSFC Bull. 34*, 113p.

Frisch, A.S., J. Holbrook and A.B. Ages, 1981: Observations of a summertime reversal in the circulation in the Strait of Juan de Fuca. *J. Geophys. Res.*, 86: 2044–2048.

Gee, J.H., 1983: Ecologic implications of buoyancy control in fish. In: Webb, P. and D. Weihs (eds.), *Fish Biomechanics.* Praeger, New York, New York. 398pp.

Geyer, W.R. and G.A. Cannon, 1982: Sill processes related to deep water renewal in a fjord, *J. Geo. Res.*, 87: 7985–7996.

Gill, A.E., 1982: *Atmosphere-Ocean Dynamics.* Academic Press, Inc., New York, New York. 661pp.

Godin, G.J., J. Candelar and R. de-la-Paz-Vela, 1981: On the feasability of detecting net transports in and out of Georgia Strait with an array of current meters. *Atmos. Ocean*, 19: 148–157.

Groot, C., 1965: Onthe orientation of young sockeye salmon (*Oncorhynchus nerka*) during their migration out of lakes. *Behav. Suppl.*, 14: 1–198.

Groot, C., 1972: Migration of yearling sockeye salmon (*Oncorhynchus nerka*)as determined by time-lapse photography of sonar observations. *J. Fish. Res. Bd. Can.*, 29: 1431–1444.

Groot, C. and T.P. Quinn, 1987: The homing migration of sockeye salmon, *Oncorhynchus nerka*, to the Fraser River. *Fish. Bull.*, 85: 455–469.

Hamilton, K., 1985: A study of the variability of the return migration route of Fraser River sockeye salmon (*Oncorhynchus nerka*). *Can. J. Zool.*, 63: 1930–1943.

Hasler, A.D. and A.T. Scholz, 1983: Olfactory Imprinting and Homing in Salmon. Springer-Verlag, Berlin. 134pp.

Ichihara, T. and A. Nakamura, 1982: Vertical movement of mature chum salmon contributing to the improvement of net structure on the Hokkaido coast. In: Melteff, B.R. and R.A. Neve (eds.), *Proceedings of the North Pacific aquaculture symposium.* Alaska Sea Grant, Fairbanks, AK. p39–49.

International Pacific Salmon Fisheries Commission (IPFSC), 1984: Annual Report, 1983. New Westminister, B.C..

Jenkins, G.M. and D.G. Watts, 1968: *Spectral Analysis and its Applications.* Holden-Day, San Francisco, Ca. 525pp.

Johnson, P.B. and A.D. Hasler, 1980: The use of chemical cues in the upstream migration of coho salmon, *Oncorhynchus kisutch*, Walbaum. *J. Fish. Biol.*, 17: 67–73.

Landreth, J.F., 1973: Orientation and behaviour of the rattlesnake, *Crotalus atrox. Copeia*, 1973: 26–31.

LeBlond, P.H., 1983: The Strait of Georgia: functional anatomy of a coastal sea. *Can. J. Fish. Aq. Sci.*, 40: 1033–1063.

LeBlond, P.H. and L.A. Mysak, 1978: *Waves in the Ocean.* Elsevier Scientific Publishing Co., Amsterdam. 602pp.

Leggett, W.C., 1977: The ecology of fish migrations. *A. Rev. Ecol. Syst.*, 8: 285–308.

Lighthill, M.J., 1971: Large-amplitude elongated body theory of fish locomotion. *Proc. Roy. Soc. (B)*, 179: 125–138.

Magnuson, J.J., 1978: Locomtion by scombroid fishes: Hydromechanics, morphology and behaviour. *Fish Physiology*, 7: 239–313.

M^{c}Keown, B.A., 1984: *Fish Migration.* Finiker Press, Beaverton, MC. 217pp.

Muench, R.D., H.J.S. Fernando and G.R. Stegen, 1990: Temperature and salinity staircases in the northwestern Weddell Sea. *JPO*, 20: 295–306.

Moore, C., 1986: Discrete Fourier Transforms with Application to Fourier Series and Convolution Integrals. UBC Computing Services Publication .

Mysak, L.A., C. Groot and K. Hamilton: 1986: A study of climate and fisheries: Interannual variability of the northeast Pacific ocean and its influence o homing migration routes of sockeye salmon. *Climatological Bulletin*, 20: 26–35.

Mysak, L.A., H.Hsieh and T. Parsons, 1982: On the relationship between interannual baroclinic waves and fish populations in the northeast Pacific. *Biological Oceanography*, 2: 63–103.

Neumann, G. and W.J. Pierson: 1966. Principles of Physical Oceanography. Prentice-Hall, Inc. Englewood Cliffs, N.J.. 544pp.

Pickard, G.L., 1975: Annual and longterm variations of deepwater properties in the coastal waters of southern British Columbia. *J. Fish. Res. Bd. Can.*, 9: 1561–1587.

Pond, G.S. and G.L. Pickard, 1983: Introductory Dynamic Oceanography. 2nd ed.. Pergammon Press, Oxford. 329pp.

Prandtl, L. and O.C. Tietjen, 1957: *Applied Hydro and Aeromechanics* (2nd ed.). Dover Press, New York, New York.

Quinn, T.P., 1980: Evidence for celestial and magnetic compass orientation in lake migrating sockeye salmon fry. *J. comp. Physiol.*, 137: 243–248.

Quinn, T.P., 1982: A model for salmon navigation on the high seas. In: Brannon, E.L. and E.O. Salo (eds.), *Proceedings of the salmon and trout migratory behaviour symosium.* College of Fisheries, University of Washington, Seattle, Wa. p229–237.

Quinn, T.P. and E.L. Brannon, 1982: The use of celestial and magnetic cues by orienting sockeye slamon smolts. *J. comp. Physiol.*, 147: 547–552.

Quinn, T.P. and B. terHart, 1987 Movements of adult sockeye salmon (*Oncorhynchus nerka*) in British Columbia coastal waters in relation to temperature and salinity stratification: Ultrasonic telemetry results. *Can. Spec. Pub. Fish. Aquat. Sci. 96*, p61–77.

Quinn, T.P. and C. Groot, 1984: The effect of water flow rate onbimodal orientation of juvenile chum salmon, *Oncorhynchus keta. Anim. Behav.*, 32: 628–629.

Quinn, T.P., B. terHart and C. Groot, 1989: Migratory orientation and vertical movements of homing adult sockeye salmon, *Oncorhynchus nerka*, in coastal waters. *Anim. Behav.*, 37: 587–599.

Royal, L.A. and J.P. Tully, 1961: Relationship of variable oceanographic factors to migration and survival of Fraser River salmon. *Cal. Coop. Ocean Fish. Invest. Rep.*, 8: 65–68.

Royce, W.F., L.S. Smith and A.C. Hartt, 1968: Models of oceanic migrations of Pacific salmon and comments on guidance mechanisms. *Fish. Bull.*, 66: 441–462.

Royer, L. and W.J. Emery, 1982: Variations of the Fraser River plume and their relationship to forcing by tide, wind and discharge. *Atmos. Ocean*, 20: 357–372.

Schumacher, J.D., C.D. Perason, R.L. Charnell and N.P. Laird, 1978: Regional response to forcing in southern Strait of Georgia. *Est. Coast. Mar. Sci.*, 7: 79–91.

Simpson, J.H., 1975: Observations of small scale vertical shear in the ocean. *Deep-Sea Research*, 22: 619–627.

Soofiani, N.M. and A.D. Hawkins, 1985: Field studies of energy budgets. In: Tytler, P. and P. Callow (eds.), *Fish Energetics*, John Hopkins University Press, Baltimore, Maryland. p283–307.

terHart, B.A., 1988: A multi-year hydrography of British Columbia's inside passage. *Dep. of Ocean. UBC Manuscr. Rep.*. No. 55

terHart, B.A., A.T. Weaver and T.P. Quinn, 1987: Vertical and horizontal distributions of homeward migrating sockeye salmon in relation to temperature, salinity and current observations in coastal waters: Moist 1985. *Dep. of Ocean. UBC Manuscr. Rep.*. No. 49.

terHart, B.A.and T.P. Quinn, 1989: Vertical and horizontal distributions of homeward migrating sockeye salmon in relation to temperature, salinity and current observations in coastal waters: Moist 1986. *Dep. of Ocean. UBC Manuscr. Rep.*. No. 56.

Thomson, K.P., B.A. terHart and P. Welch, 1985: A CTD survey of the inside passage of British Columbia 24–28 June 1985. *Dept. of Ocean. UBC Manuscr. Rep.*. No. 45.

Thomson, K.P., B.A. terHart and T.P. Quinn, 1986: Ambient oceanographic variables of *Oncorhynchus nerka* (MOIST 1985). *Dept. of Ocean. UBC Manuscr. Rep.*. No. 50.

Thomson, R.E., 1976: Tidal currents and estuarine circulation in Johnstone Strait, British Columbia. *J. Fish. Res. Board Can.*, 33: 2242–2264.

Thomson, R.E., 1977: Currents in Johnstone Strait, British Columbia: supplement data on the Vancouver Island site. *J. Fish. Res. Board Can.*, 34: 697–703.

Thomson, R.E., 1981: Oceanography of the British Columbia coast. *Can. Spec. Pub. Fish. Aquat. Sci. 56.* 291p.

Tolmazin, D., 1985: *Elements of Dynamic Oceanography.* Allen & Gunnison, Inc., Winchester, Mass. 181pp.

Tully, J.P., A.J. Dodimead and S. Tabata, 1960: An anomalous increase of temperature in the ocean off the Pacific coast of Canada through 1957 and 1958. *J. Fish. Res. Bd. Can.*, 17: 61–80.

Van Leer, J.C. and C.G. Rooth, 1975: Shear observations in the deep thermocline. *Deep-Sea Research*, 22: 831–836.

Weast, R.C. (ed.), 1974: Handbook of Chemistry and Physics. CRC Press, Cleveland, Ohio.

Webb, P.W., 1978: Hydromechanics: Non-scombroid fish. *Fish Physiology*, 3: 189–237.

Webb, P.W. and D. Weihs, 1983: *Fish Biomechanics.* Praeger, New York, New York. 381pp.

Weihs, D., 1987: Hydromechanics of fish migration in variable environments. *American Fisheries Symposium*, p254–261.

Westerberg, H., 1982: Ultrasonic tracking of Atlantic Salmon (*Salmon Salar L.*) II. Swimming depth and temperature stratification. *Inst. Freshwater Res. Drottningholm. Rep.*, 60: 102–120.

Westerberg, H., 1984: The orientation of fish and the vertical stratification at fine and microstructure scales. In: M^{c}Cleave, J.D., G.I. Arnold and J.J. Dodson (eds.), *Mechanisms of Migration in Fishes.* Plenum Press, New York, New York. p179–203.

Wickett, W.P., 1975: Relationship of coastal oceanographic factors to the migration of Fraser River sockeye salmon (*Oncorhynchus nerka*). *Int. Comm. Explor. Sea. Cm.*, 1977/M.26: p18.

Woods, J.D., 1968: Wave-induced shear instability in the summer thermocline. *JFM*, 32: 791–800.

Xie, l. and W.W. Hsieh, 1989: Predicting the return migration routes of the Fraser River sockeye salmon (*Oncorhynchus nerka*). *Cdn. J. Fish. Aqua. Sci.*, 46: 1287–1292.

Young, B. and A.E. Hay. 1987: Density current flow into Fortune Bay, Newfoundland. *J.P.O.*, 17: 1066–1071.